Proteomic analysis of the *Mycobacterium avium*-containing phagosome membrane

by

Ray-Dean Donovan Pietersen
(PTRRAY003)

SUBMITTED TO THE UNIVERSITY OF CAPE TOWN
In fulfilment of the requirements for the degree

M.Sc (MED) in Medical Biochemistry

Faculty of Health Sciences
UNIVERSITY OF CAPE TOWN

August 2010

Supervisor:
Dr. Lutz Thilo,
Division of Medical Biochemistry,
University of Cape Town

DECLARATION

I, ……, hereby declare that the work on which this dissertation/thesis is based is my original work (except where acknowledgements indicate otherwise) and that neither the whole work nor any part of it has been, is being, or is to be submitted for another degree in this or any other university.

I empower the university to reproduce for the purpose of research either the whole or any portion of the contents in any manner whatsoever.

Signature: .. Signed by candidate

Date: 5 November 2010

ACKNOWLEDGEMENTS

I will ever be grateful to the following people:

Prof. Lutz Thilo for being my main mentor and for engagement that goes beyond the call of duty.

Dr. Chantal de Chastellier (Marseilles) for help and advice with techniques, donation of mycobacterial stocks, provision and analysis of electron microscopy pictures and being a mentor at times.

Various persons in the Division of Immunology (UCT) (Dr Gordon Brown and others) for donating L-929 cells.

Dr Georg Plum (Cologne) for performing protein sequencing.

UCT animal Unit for provision of animals.

My laboratory colleagues Roshan Ebrahim, Maurice Itoe and Alon Gordon for help and friendship.

Members of the Division of Lipidology (UCT) for laboratory space and kindness.

Funders of bursaries: NRF, MRC and Benfara

My family and friends for abundant support in various forms.

Abstract

The worldwide disease of tuberculosis (TB) is caused by the organism *Mycobacterium tuberculosis* (M.tb) and although TB is curable, almost 3 million deaths are reported annually. Pathogenic mycobacteria, like M.tb and *Mycobacterium avium* (M.av), reside intracellularly in phagosomes where they are able to survive, because they block the process of phagosome maturation. Several studies by de Chastellier and Thilo in mouse bone marrow-derived macrophages show that pathogenic mycobacteria maintain a close interaction with the phagosome membrane, probably resulting in the impairment of phagosome maturation processes. Focus has been placed on uncovering the molecular mechanisms that underlie the maturation block. An approach of characterizing M.av-containing phagosomes in terms of cell surface-derived glycoconjugates, revealed that these phagosomes show a 3- to 4-fold depletion of these glycoconjugates as compared to early endosomes with which the phagosomes continuously fuse and exchange membrane molecules (de Chastellier et al., 1995; de Chastellier and Thilo, 2002). The same authors proposed that this depletion might be selective. The aim of this study is to identify the depleted / possibly enriched cell surface-derived glycoproteins on the phagosome membrane of M.av- containing phagosomes, because they might play a role in mycobacteria's intracellular survival.

In the current study, phagosomes were analysed in terms of cell surface-derived glycoconjugates that had been radioactively labelled on the cell-surface. Phagosomes were compared to other endocytic organelles that also carried radioactive label, making it necessary to establish a phagosome purification method. 27% Percoll gradients gave good separation between phagosomes and plasma membrane (PM) / endosomes, but could not remove lysosomes from the phagosomes. Radioactively labelled cell surface-derived glycoconjugates were analysed in terms of radioactivity profiles after separation by SDS-PAGE. For the

plasma membrane, these radioactivity profiles showed that cell surface-derived glycoproteins increased (over the molecular weight of 116 to 205 kDa) after infecting cells with *M. avium*. Radioactivity profiles compared between M.av-containing phagosomes and the cell-surface revealed both depletion (over about 150 to 250 kDa) as well as enrichment (over about 40 to 66 kDa). A similar result was obtained when comparing M.av-containing phagosomes to phagosomes containing hydrophobic magnetic latex beads. Cell surface-derived glycoproteins were enriched (over about 40 to 66 kDa) and depleted (over about 150 to 350 kDa) on mycobacterium-containing phagosomes. Phagosomes containing hydrophobic magnetic latex beads are immature for only several hours and were specifically analysed while still immature. Differences between these two types of phagosomes were therefore due to what mycobacteria do actively. Gel fractions from the generally depleted and enriched molecular weight ranges were selected for protein identification. Having used only half of the SDS-PAGE lane to generate radioactivity profiles, the remaining half was used for protein identification. From the total lists of identified proteins, only cell surface-derived glycoproteins have been listed. A select number of these proteins are referred to as proteins of interest and have functions, among others, in lipid homeostasis (like Niemann Pick type C1) and immune functions (like DC-HIL and CD45). Their possible involvement in mycobacteria's intracellular survival is discussed. This study shows that mycobacteria influence the abundance of cell surface-derived glycoproteins on the phagosomes in a selective manner.

CONTENTS

Abbreviations

µm	micrometre
BMDM	bone marrow-derived macrophages
cm	centimetre
CMC	critical micellar concentration
Da	dalton
dpm	disintegrations per minute
eEn	early endosomes
EM	electron microscopy
En	endosomes
h	hour(s)
HB	homogenisation buffer
IEF	isoelectric focussing
IPG	immobilized pH gradient
kDa	kilodalton
kVh	kilovolt hours
LB	latex beads (non-magnetic)
LM	lysosomal material
Ly	lysosomes
M.av	*Mycobacterium avium*
M.av-LB	*Mycobacterium avium* to which latex beads have been coupled
M.av-Ph	*Mycobacterium avium*-containing phagosomes
mLB	magnetic latex beads
mLB-Ph	magnetic latex beads-containing phagosomes
mm	millimetre
MS/MS	tandem mass spectrometry
MW	molecular weight
NAGA	N-acetyl glucosaminidase
O-β-G	n-octyl β-$_D$-glucopyranoside
p.i.	post-infection
PAGE	polyacrylamide gel electrophoresis
Ph	phagosomes
PhLy	phagolysosomes
pI	isolelectric point
PM	plasma membrane
PNS	postnuclear supernatant
SDS	sodium dodecyl sulphate
WB	Western blot

An overview of tuberculosis

The worldwide disease of tuberculosis (TB) is caused predominantly by the organism *Mycobacterium tuberculosis* (M.tb). Approximately one third of the global human population is infected with M.tb (WHO TB fact sheet at http://www.who.int). It is estimated that 5 – 10% of infected individuals will likely become symptomatic at some time and that the risk of developing clinical manifestations is much higher for individuals who are co-infected with human immunodeficiency virus (HIV) (Harries and Dye, 2006; WHO TB fact sheet at http://www.who.int).

TB is a progressive disease, primarily involving the lungs, but can disseminate to other organs (Sharma et al., 2005). Several *Mycobacterium* species can cause progressive lung disease (Collins, 1989), but only M.tb, *M. africanum* and *M. avium* (M.av) are regularly reported to infect humans. M.av is an opportunistic pathogen that is frequently isolated from HIV patients (Falkinham, 2003) while *M. africanum,* although reported as being variably prevalent in different parts of Africa, has been found to contribute up to 60% of clinical isolates from patients with pulmonary TB (Niemann et al., 2002).

TB is a curable disease (Dye and Williams, 2008), but fatality numbers are still very high (WHO TB report 2009). The current anti-tuberculosis drug regimen is around 40 years old and requires a six to nine months treatment period (Rivers and Mancera, 2008). The emergence of drug resistance, together with HIV co-infection, means that new anti-tuberculosis drugs are urgently required (Rivers and Mancera, 2008). To create new drugs, an understanding of the molecular mechanisms involved in mycobacteria's pathogenesis must be obtained (Glickman and Jacobs, 2001).

Pathogenic mycobacteria commonly gain access to a host through inhalation into the lungs where the bacteria mostly encounter alveolar macrophages which are localised at the air tissue interface (Valdivia-Arenas et al., 2007). Macrophages are responsible for scavenging and destroying invading pathogens. Inside the macrophage, invading pathogens and foreign particles are contained inside phagosomes. Normally, a phagosome will fuse with lysosomes, resulting in the digestion of the phagosome's contents, but virulent pathogenic mycobacteria have a mechanism that causes the phagosome to resist fusion with lysosomes (Armstrong and Hart, 1971). This resistance of phagosome-lysosome fusion is correlated with the survival of pathogenic mycobacteria inside macrophages (Clemens and Horwitz, 1995; de Chastellier et al., 1995; Via et al., 1997). However, phagosome-lysosome fusion has been reported to have varied and conflicting outcomes. For example, after phagosome-lysosome fusion, bacterial viability gradually declines in activated macrophages (Schaible et al., 1998); bacterial growth is arrested in macrophages with functional natural resistance associated macrophage protein 1 (Frehel et al., 2002) and bacteria can rescue themselves from phagolysosomes to reside in immature phagosomes where they multiply normally, even if the rescue process occurs over several days (de Chastellier and Thilo, 2006; de Chastellier et al., 2009). Nonetheless, there seem to be consensus in the literature that resistance to phagosome-lysosome fusion forms mycobacterium's main survival strategy (reviewed in Vieira et al., 2002; Russell et al., 2002; Thilo and de Chastellier, 2004).

Entry into macrophages

The alveolar macrophage is seen as the niche for pathogenic mycobacteria's intracellular survival. A variety of macrophage receptors have been implicated in the phagocytosis of mycobacteria (Ernst, 1998).

In the case of complement receptors (CRs), M.tb is phagocytosed through CR1, CR3 and CR4 on macrophages (Schlesinger et al., 1990; Hirsch et al., 1994). Both direct and opsonic binding of M.tb to CR3 have been described: about 40-50% is direct and 50-60% is opsonic (Melo et al., 2000). Direct binding to CR3 is through M.tb's capsular polysaccharides (Cywes et al., 1997). Complement enhances M.tb's binding to mononuclear phagocytes about three fold (Schlesinger et al., 1990), while the absence of CR3 leads to decreased binding and phagocytosis of M.tb (Rooyakkers and Stokes, 2005). These reports indicate the importance of CRs in the entry of M.tb into its intracellular environment. M.tb can also be phagocytosed through the mannose receptor (MR) which recognizes lipoaribinomannan (LAM) on the surface of virulent M.tb (Schlesinger, 1993; Schlesinger et al., 1994). Polystyrene beads coated with the mannose-capped form of LAM, ManLAM, bound to macrophages three times more than beads coated with AraLAM (not mannose capped) or lipomannan (LM) (Schlesinger et al., 1994). Mannose receptors bind mannosyl and fucosyl residues on the surface of microorganisms (Stahl and Ezekowitz, 1998) through their carbohydrate recognition domains (Mullin et al., 1997). Pre-incubating M.tb with antibodies against LAM reduced the binding of M.tb to macrophages up to 49% (Schlesinger et al., 1994). For human macrophages, the primary receptors for ingesting M.tb are MRs and CRs (Schlesinger, 1993). Several other receptors partake in the phagocytosis of pathogenic mycobacteria. Among these are Fc-gamma receptors (Indik et al., 1995), scavenger receptors and CD14 (Ernst, 1998).

Surfactant protein A (SP-A) and SP-D, also referred to as collectins, have been reported to influence the uptake of mycobacteria by alveolar macrophages (Ernst, 1998; Lopez et al., 2003). Collectins are C-type lectins in which lectin domains are associated with collagenous structures (van de Wetering et al., 2004). The C-terminal lectin is also referred to as a carbohydrate-recognition domain and the function of the collectins is calcium dependent (Cambi et al., 2005). SP-A and SP-D are secreted into the alveolar fluid and can act as

opsonins, coating the surface of pathogens like M.tb, by binding preferentially to mannose type monosaccharides (van de Wetering et al., 2004). These surfactant proteins can also bind directly to macrophages through the MRs (Crouch and Wright, 2001) and have been reported to bind to M.tb through interaction with mycobacteria's LAM molecules (van de Wetering et al., 2004), but SP-A also require fatty acids to bind (Sidobre et al., 2002). SP-A mediates an increase in phagocytosis (Tino and Wright, 1996; Beharka et al., 2002) while SP-D inhibits phagocytosis (Ferguson et al., 1999; Ferguson et al., 2002). Reports were also made of SP-D increasing phagocytosis (Valdivia-Arenas et al., 2007). Increasing phagocytosis will result in the clearing of an infection, while restricting phagocytosis could be related to the control of inflammation and tissue damage (Valdivia-Arenas et al., 2007).

In contrast to earlier thinking, the intracellular fate of pathogenic mycobacteria does not seem to be connected to individual receptors, because blocking specific receptors does not significantly influence mycobacteria's survival (Zimmerli et al., 1996; Ernst, 1998). An exception to this finding is observed for the phagocytosis of M.tb that is opsonised with antibodies, because the resulting majority of phagosomes fuse with lysosomes. However, the mycobateria in the phagolysosomes remain intact and are able to multiply (Armstrong and Hart, 1975).

The phagosome: home and subject of manipulation for mycobacteria

Phagosomes as part of the endocytic pathway

Phagosomes (Ph), after formation, become part of and interact with the organelles of the endocytic pathway (de Chastellier et al., 1995; Mellman, 1996; de Chastellier and Thilo, 1997) and are subjected to the same processes as endosomes (En) (Vieira et al., 2002; Thilo and de Chastellier, 2004). Like newly formed En, namely early En, which exist briefly because they rapidly undergo maturation and fuse with lysosomes (Ly), Ph also mature within

minutes (Pitt et al., 1992; de Chastellier et al., 1995; Oh and Swanson, 1996). Maturation is a process of changing the organelle's constituents through recycling and additions of components (Gruenberg and Maxfield, 1995). Component changes distinguish the maturation stage of an organelle. For instance, Rab5 and transferrin receptors are expected only on early En, while the presence of Rab7 and lysosomal-associated membrane protein 1 (LAMP1) are limited to late En and Ly (Clemens and Horwitz, 1995; Via et al., 1997). The maturation stage of an organelle also dictates its fusogenic character: early En will fuse with one another as well as with immature Ph and intermingle contents and membrane constituents, but not fuse with late En or Ly before they have matured (de Chastellier et al., 1995; de Chastellier and Thilo, 1997; de Chastellier and Thilo, 1999). Although Ph are subjected to the same processes as En, Ph that specifically contain pathogenic mycobacteria are not processed to the point where they can fuse with Ly (reviewed in de Chastellier and Thilo, 1999; Thilo and de Chastellier, 2004).

The maturation block forms the central topic

A pre-requisite for phagosome-lysosome fusion is that the phagosome must mature (de Chastellier et al., 1995; de Chastellier and Thilo, 1997). Phagosomes containing pathogenic mycobacteria do not mature, keep fusing with early En and retain early endosome markers (Clemens and Horwitz, 1995; de Chastellier et al., 1995; Via et al., 1997). Therefore, to study mycobacteria's intracellular survival, focus must be placed on their resistance to overcome the maturation process, also referred to as the maturation block. Several molecular mechanisms have been proposed for the maturation block.

Since phagosome maturation involves an exchange of constituents which involves fusion events, fusion steps may be affected. Certain integral membrane proteins called soluble *N*-ethylmaleimide-sensitive factor-attachment protein receptors (SNAREs), *N*-ethylmaleimide-

sensitive factor (NSF) and NSF-attachment proteins (SNAPs) are essential for fusion between different organelles and vesicles (Pfeffer, 1996; Vieira et al., 2002). SNAREs on vesicles will selectively recognize and interact with SNAREs on target membranes to form stable complexes, bringing interacting membranes closely together to promote fusion (Pfeffer, 2007). SNAREs are classified into glutamine containing (or Q- SNAREs, also named t-SNAREs and mostly found on target membranes) and arginine-containing (or R-SNAREs, also named v-SNAREs, located mostly on vesicles) (Vieira et al., 2002; Pfeffer, 2007). Experiments show that fusion between early En and Ph require cytosol, ATP and NSF, while *N*-ethylmaleimide and antibodies against NSF inhibit fusion between early En and Ph and also affects phagosome-lysosome fusion in macrophages (Vieira et al., 2002). SNAREs, NSF and SNAPs are also implicated in endosome and phagosome maturation (Vieira et al., 2002), but Rab GTPases which recruit tethering molecules to membranes they are located on, act upstream to SNAREs in membrane fusion (Pfeffer, 2007).

Deretic and colleagues, from a viewpoint that the maturation block for mycobacterium-containing Ph occurs between the stages of Rab5 loss and Rab7 acquisition (Via et al., 1997), have focussed on Rab5-effectors and found that the membrane tethering molecule early endosome autoantigen 1 (EEA1) is the only Rab5-effector absent from M.tb-containing Ph as compared to bead-containing Ph (Fratti et al., 2001). EEA1 is a protein that has been localised to early En, has a cystein-rich domain named the FYVE finger and an IQ domain that binds calmodulin (Mu et al., 1995; Stenmark et al., 1996; Mills et al., 2001). EEA1 can bind Rab5 (Callaghan et al., 1999) at its two distantly separated Rab5 binding sites (Simonsen et al., 1998) and bind phosphatidylinositol 3-phosphate (PI3P) at EEA1's C-terminal located FYVE domain (Lawe et al., 2000). PI3P kinase, hVPS34, generates PI3P on early endosome membranes (Gillooly et al., 2001; Deretic et al., 2004). Studies suggest that EEA1 functions

in the fusion between early endocytic (Rab5 positive) vesicles by tethering the vesicular membranes (Vergne et al., 2004a; Lindmo and Stenmark, 2006).

PI3P-dependent processes are impacted on by M.tb's LAM and SapM (Vergne et al., 2004a; Deretic et al., 2006). Both molecules are secreted by M.tb (Strohmeier and Fenton, 1999; Saleh and Belisle, 2000). ManLAM inhibits the recruitment of EEA1 to mycobacteria-containing Ph (Fratti et al., 2001) by preventing the generation of PI3P on Ph through inhibition of the Ca^{2+} rise (Vergne et al., 2003). Ca^{2+} stimulates calmodulin to activate calmodulin kinase, leading to the recruitment of hVPS34 to the phagosome membrane (Vergne et al., 2003). Preventing the Ca^{2+} rise disables the calmodulin pathway that leads to PI3P production on Ph (Vergne et al., 2003). Previously, Kusner and colleagues have demonstrated that the cytosolic Ca^{2+} rise activates calmodulin which in turn activates calmodulin kinase and linked these Ca^{2+} -related activities to phagosome-lysosome fusion (Malik et al., 2000; Malik et al., 2001). Ph containing dead M.tb acquire calmodulin kinase and fuse with Ly, whereas Ph containing live M.tb display lowered levels of calmodulin and activated calmodulin kinase and do not fuse with Ly (Malik et al., 2001). The non-mannose capped form of LAM, AraLAM, does not inhibit the Ca^{2+} rise (Chua et al., 2004). The production of PI3P at the membrane is an upstream event to the recruitment of EEA1 to the membrane (Christoforidis et al., 1999). Specifically, M.tb inhibits the Ca^{2+} rise by acting on sphingosine kinase which produces sphingosine-1-phosphate (S1P), the second messenger that stimulates Ca^{2+} release from the endoplasmic reticulum (ER) (Malik et al., 2003; Kusner, 2005). The addition of S1P to mycobacteria-infected macrophages removes the block in phagosome-lysosome fusion and lowers mycobacterial viability (Garg et al., 2004).

EEA1 exclusion from mycobacteria-containing Ph is aided by ManLAM-stimulated activation of p38 mitogen-activated protein kinase (MAPK) which may lead to the activation

of GDI (GDP Dissociation Inhibitor) (Fratti et al., 2003a). GDI inhibits Rab5 and / or removes it from membranes (Chua et al., 2004). Because Rab5 binds EEA1 (Callaghan et al., 1999), its inactivation leads to a lowered recruitment of EEA1 to membranes (Fratti et al., 2003a). Therefore, the p38 MAPK activation of GDI, together with the inactivation of the Ca^{2+}, calmodulin and calmodulin kinase route of EEA1 exclusion from membranes, correlates with a block in phagosome maturation (Vergne et al., 2004a).

The other M.tb product influencing the PI3P levels on Ph is SapM, a PI3P phosphatase that eliminates any PI3P that might have bypassed the block by LAM (Vergne et al., 2005). Only live, but not heat-killed M.tb, can keep Ph liberated from PI3P, while blocking SapM leads to Ph containing live M.tb to acquire PI3P and subsequently mature (Vergne et al., 2005). The exclusion of PI3P from mycobacteria-containing Ph can be expected to influence the fusogenicity of these Ph toward early En, therefore possibly influencing mycobacteria's access to nutrients (Vergne et al., 2004b). Mycobacteria overcome this obstacle through yet another of its secreted molecules, namely phosphatidylinositol mannoside (PIM), which stimulates homotypic fusion between early En as well as fusion between early En and Ph (Vergne et al., 2004b) by mimicking the chemical structure of mammalian phosphatidylinositols (Chua et al., 2004). The action of PIM is not antagonistic to that of LAM, but is synergistic in the goal of intracellular survival for M.tb (Vergne et al., 2004b).

TACO (tryptophane aspartate-containing coat protein) has been implicated in the survival of intracellular mycobacteria (Ferrari et al., 1999). Usually, TACO is transiently present on Ph, but M.tb Ph remain TACO positive, resulting in these Ph not fusing with lysosomes and happens for live mycobacteria only (Ferrari et al., 1999). Several independent studies have questioned and refuted the reported role that TACO plays in the maturation block (Russell et al., 2002; Vergne et al., 2004a).

A characteristic difference between the various endocytic organelles is their luminal pH, which is important for normal endocytic processes. Typically, eEn have a pH of about 6.0, late En a pH of 5.5 and Ly a pH range of 4 to 5 (Huynh and Grinstein, 2007). Ph containing non-pathogenic bacteria become acidified to the same extent as Ly as they mature (Kuehnel et al., 2001), while the pH of Ph containing pathogenic mycobacteria is about 6.3 – 6.5 (Sturgill-Koszycki et al., 1994; de Chastellier et al., 1995) and has even been seen to increase to pH 6.6 – 6.7 during multiplication (de Chastellier et al., 1995). Non-acidification of Ph has been reported for live but not dead mycobacteria (Oh and Straubinger, 1996; Kuehnel et al., 2001). Avoiding a strongly hydrolytic environment is advantageous for mycobacteria's intracellular survival, but it is debatable whether non-acidification is a result or cause of the maturation block (Huynh and Grinstein, 2007). Acidification can mainly be ascribed to the proton-pumping action of the vacuolar (V)-ATPase (Lukacs et al., 1990) which is a multisubunit complex (Huynh and Grinstein, 2007). V-ATPases were earlier reported as excluded from mycobacterium-containing Ph (Sturgill-Koszycki et al., 1994), but might be present at low concentrations in these Ph (Schaible et al., 1998). Deretic and colleagues see a role for mycobacteria's ManLAM in preventing phagosome acidification (Fratti et al., 2003b). Syntaxin 6, a SNARE, which associates with EEA1 to deliver lysosomal constituents, including a V-ATPase subunit, from the Golgi network to endocytic organelles, is excluded from mycobacterium-containing Ph (Fratti et al., 2003b; Simonsen et al., 1999). As mentioned above, mycobacterium-containing Ph are EEA1 free through a block in PI3P generation and activation of p38 MAPK (Vergne et al., 2004a). Ph containing latex beads acquire syntaxin 6 gradually over time, whereas Ph containing ManLAM-coated beads display less syntaxin 6 as compared to Ph containing non-coated beads (Fratti et al., 2003b).

Microtubules and actin filaments form part of the cytoskeleton and are involved in the movement of and interactions between endocytic organelles (Mellman, 1996; Vieira et al.,

2002). It has been proposed that small phagosomes, containing 0.9μm polystyrene beads, move along microtubules whereas large phagosomes, containing 3.0μm beads, are propelled by actin filaments inside macrophages (Toyohara and Inaba, 1989). Several studies support microtubule-based movement as being important for phagosomal maturation (Vieira et al., 2002). The transfer of membrane proteins and fluid-phase marker to phagosomes containing latex beads is inhibited through depolymerising the microtubules (Desjardins et al., 1994b; Blocker et al., 1996). Phagosomes, although capable of bidirectional movement along microtubules, predominantly move centripetally towards the cell centre (Blocker et al., 1997) where late En and Ly aggregate (Matteoni and Kreis, 1987). A variety of molecular motors, most notably of the dynein and kinesin families responsible for centripetal and centrifugal motion respectively, are involved in organelle translocation (Vieira et al., 2002). Actin filaments and (actin binding proteins) have been localised to phagosomes (Defacque et al., 2000; Guerin and de Chastellier, 2000a). During infection, various pathogens rearrange the actin cytoskeleton for their own benefit (Dramsi and Cossart, 1998). M.av disrupts the actin filament network compared to cells infected with non-pathogenic bacteria (Mycobacterium smegmatis and Bacillus subtilis) or latex beads with a hydrophobic surface (Guerin and de Chastellier, 2000a). This disruption causes M.av-containing Ph to acquire endocytic contents marker atypically, i.e., instead of immediately, a lag of 10 to 20 minutes is observed (Guerin and de Chastellier, 2000b). Interestingly, M.av-Ph acquire membrane marker from the cell surface normally when the actin filament network is disrupted (Guerin and de Chastellier, 2000b). It is proposed that by disrupting the actin filament network, M.av influences the way in which Ph interact with En (Guerin and de Chastellier, 2000b; Thilo and de Chastellier, 2004). The mechanism whereby M.av disrupts the actin filaments is not known (Thilo and de Chastellier, 2004), but might form part of how mycobacteria control fusion events with endocytic organelles and therefore, indirectly, phagosome maturation. Various molecules have been implicated in actin-based propulsion. One study implicated the involvement of

protein kinase C, N-WASP (neural Wiskott-Aldrich syndrome protein) and Cdc42 in actin comet-tail formation for the propulsion of En and Ly (Taunton et al., 2000) while other studies indicate associated motor proteins of actin, namely myosins, in endocytic traffic (DePina and Langford, 1999; Raposo et al., 1999). In the elimination of apoptotic cells, ezrin-radixin-moesin (ERM) proteins and upstream-acting Rho kinases are involved in phagosome maturation (Erwig et al., 2006). ERM proteins link the actin cytoskeleton to the plasma membrane proteins (Ivetic and Ridley, 2004). The Arp2/3 (actin-related proteins 2 and 3) complex, an initiator of actin polymerization (Mullins et al., 1998) has a central role in regulating the actin cytoskeleton and is in turn regulated by various activators such as WASP proteins and myosins (May, 2001).

From the definition of organellar maturation (Gruenberg and Maxfield, 1995), two main aspects can be identified: recycling of membrane back to the cell surface and the exchange of constituents through fusion events. Other aspects of organelle maturation include acidification and the involvement of the cytoskeleton. Mycobacteria seem to influence processes of all these maturational aspects, most of which are discussed above. The recycling of membrane is addressed below.

One approach to discover underlying mechanisms of the maturation block is to study the morphological character of mycobacterium-containing Ph. Morphological observations, through electron microscopy (EM), support one aspect of the maturation process, namely recycling from early En and early Ph. Internalised receptors recycle back to the cell surface from tubular extensions of early En (Hopkins et al., 1994; Gruenberg and Maxfield, 1995). Such tubular extensions have been observed for the membrane of early En and also early Ph that undergo maturation (de Chastellier et al., 1995; de Chastellier and Thilo, 1997; Woodman

and Futter, 2008). It is suggested that tubule formation is a requirement for molecules to recycle back to the cell surface (de Figueiredo et al., 2001).

The phagosomal membrane surrounding pathogenic mycobacteria or beads with a hydrophobic surface, however, do not display tubular extensions, but is instead all-around closely apposed to the mycobacterial or bead surface (de Chastellier et al., 1995; de Chastellier and Thilo, 1997; Moreira et al., 1997; Mwandumba et al., 2004). In contrast, Ph containing degradable bacteria or beads with a hydrophilic surface have a loose fitting phagosomal membrane around the phagocytic particle (de Chastellier and Thilo, 1997). These observations have lead the authors to formulate a hypothesis for the basis of the maturation block by pathogenic mycobacteria: phagosome-lysosome fusion is prevented because the pre-requisite phagosome maturation is hampered by impaired recycling, where impaired recycling is a result of the close apposition between phagosomal membrane and mycobacterial surface (de Chastellier and Thilo, 1997). Impaired recycling from mycobacterium-containing Ph is evident from MHC I molecules having a delayed clearance from M.tb-containing Ph and a percentage of these Ph staining positive for transferrin receptor (TfR) which usually recycles within minutes, as tested at 3 hours and 1 day post-infection time points (Clemens and Horwitz, 1995). In cases where the close apposition is not maintained in an all-around manner, like for Ph containing two or more hydrophobic beads or *M. avium*, such Ph mature normally, as was evident by the presence of lysosomal marker (de Chastellier and Thilo, 1997). Phagosome maturation is possible because recycling can take place from the phagosome membrane areas between adjacent phagocytic particles where a close apposition was not possible (de Chastellier and Thilo, 1997). If an all-around close apposition is so important in preventing maturation of the phagosome, it must be present from the moment when a pathogenic mycobacterium enters its phagosome, i.e. at phagocytosis or mycobacterial replication (Thilo and de Chastellier, 2004). Indeed, for dividing *M. avium* the same authors

have observed an all-around close apposition right into the site of septum formation (de Chastellier and Thilo, 1997). The observation that Ph which contain opsonised pathogenic mycobacteria mature and fuse with Ly (Armstrong and Hart, 1975), implies that direct contact between the mycobacterial surface and phagosomal membrane is required for an all-around close apposition to block phagosome maturation (de Chastellier and Thilo, 1997). Recently, the requirement for an all-around close apposition has been tested by infecting bone marrow derived macrophages with *M. avium* to which latex beads have been coupled for the disruption of the close apposition (de Chastellier et al., 2009). The resulting Ph acquire lysosomal marker whereas Ph containing *M. avium* only, do not. Furthermore, after the release of beads from the mycobacteria inside phagolysosomes, the phagosome membrane became closely apposed to the bacterial surface, resulting in Ph with an immature character and without lysosomal marker (de Chastellier et al., 2009). These results clearly proof the importance of the close apposition to be maintained in an all-around manner to prevent phagosome maturation (de Chastellier et al., 2009). Cholesterol has been shown to be important in the maintenance of a close apposition between phagosome membrane and mycobacterial surface (de Chastellier and Thilo, 2006). Depleting cholesterol from bone-marrow derived macrophages infected with *M. avium* cause the M.av-containing Ph to mature and fuse with Ly (de Chastellier and Thilo, 2006). Although in this case the phagolysosomes containing the mycobacteria undergo autophagy that results in numerous mycobacteria contained in the same phagolysosome, when cholesterol is replenished, mycobacteria rescue themselves from the phagolysosomes to once again reside individually in Ph with a closely apposing phagosome membrane and which do not fuse with Ly (de Chastellier and Thilo, 2006). It is possible that sufficient cholesterol is needed to keep cholesterol-rich membrane portions (like lipid rafts) and their associated molecules as part of the phagosome membrane, because although lipid rafts have been implicated as necessary for phagosome maturation,

mycobacteria might establish the maturation block by manipulating lipid raft molecules (de Chastellier and Thilo, 2006).

Although immature Ph containing beads with a hydrophobic surface also display a close apposition between phagocytic particle and phagosome membrane, these Ph remain immature for at least 3 hours (de Chastellier and Thilo, 1997), but fuse with Ly by 24 hours (Desjardins et al., 1994a). In contrast, Ph containing live pathogenic mycobacteria can stay immature indefinitely (de Chastellier and Thilo, 1999). Although dead M.av initially have a close apposition with the phagosomal membrane, they do not remain in immature Ph (Thilo and de Chastellier, 2004). The maintenance of a close apposition is therefore linked to mycobacteria's viability, meaning that mycobacteria must do something actively to maintain the close apposition with the phagosome membrane (Thilo and de Chastellier, 2004).

Surface characteristics of pathogenic mycobacteria

Pathogenic mycobacteria's thick cell wall is their most striking feature. As described by Brennan (2003), the total cell wall consists of two segments, viewed as upper and lower. Adjacent to mycobacteria's plasma membrane is the mycolyl arabinogalactan-peptidoglycan complex, referred to as the cell wall core and comprising the lower segment. The upper segment contains free lipids with varying lengths of fatty acid chains. Cell wall proteins, phosphatidylinositol mannosides (PIMs), lipomannan (LM), lipoaribinomannan (LAM) and phthiocerol-containing lipids are interspersed between the fatty acid chains. PIMs have a phosphatidylinositol (PI) base and LM and LAM are extensions of PIM (Brennan, 2003). LAM is very significant in mycobacteria's pathogenesis (Strohmeier and Fenton, 1999). LAM can insert itself in cell membranes of cells infected with mycobacteria, spread through the cell and to neighbouring cells (Strohmeier and Fenton, 1999; Beatty et al., 2000) and is the predominant antigen in tuberculosis patients (Julian et al., 1997). LAM molecules can be

mannose-capped, termed ManLAM, or uncapped (arabinofuranosyl-terminated) and termed AraLAM (Chatterjee et al., 1992). ManLAM is believed to play a central role in the intracellular survival of pathogenic mycobacteria (Vergne et al., 2004a). Various mycobacterial surface molecules can bind to macrophage surface molecules, for example ManLAM binding to mannose receptors (in the phagocytosis of mycobacteria) (Schlesinger et al., 1994) or LM, M.tb's 19-kDa lipoprotein and other surface molecules binding to Toll-like receptors (stimulating macrophage immune responses) (reviewed in Jo et al., 2007). Obviously, among the mycobacterial surface molecules are those which form close interactions with the phagosome membrane molecules.

Composition of the phagosomal membrane

Due to mycobacterium-containing phagosomes' unusual fusion and membrane marker characteristics, it has become a longstanding goal to elucidate the phagosome membrane composition of these Ph in order to discover the underlying mechanisms behind mycobacterium-containing phagosomes' behaviour (Sturgill-Koszycki et al., 1997; Deretic and Fratti, 1999). In the light of the close apposition, the above goal can be refined to finding the molecules that are involved in mediating a close interaction between phagosome membrane and mycobacterial surface. These molecules may provide or be important clues to mechanisms underlying mycobacteria's intracellular survival. One study compares the phagosomal membrane between mycobacterium-containing phagosomes and latex bead-containing phagosomes through two-dimensional electrophoresis, but find only minor differences (Sturgill-Koszycki et al., 1997). In this regard, other researchers demonstrate that *M. avium*-containing Ph become gradually depleted about 3- to 4-fold of surface-derived glycoconjugates as compared to early En, although these Ph continuously fuse and exchange membrane components with early En (de Chastellier et al., 1995; de Chastellier and Thilo, 2002). Because the 3- to 4-fold level of depletion is applicable at 15 days post-infection, the authors propose that this action by mycobacteria is too late to help prevent phagosome

maturation at very early time points, but could play a role in maintaining the immature state of mycobacterium-containing Ph (de Chastellier and Thilo, 2002). Interestingly, the phagosome membrane of Ph containing hydrophobic beads, existing temporarily as immature Ph (de Chastellier and Thilo, 1997), do not undergo depletion of surface-derived glycoconjugates (de Chastellier et al., 1995). Whatever the membrane composition of the phagosome membrane surrounding pathogenic mycobacteria might be, it is expected to be different to Ph that do mature or can only temporarily remain immature.

Study Question

To identify any molecular mechanism of the maturation block, one must identify the molecules of the phagosomal membrane as well as select which molecules are of interest for further study. The observation that surface-derived glycoconjugates are depleted for M.av-containing Ph as compared to early En, but does not occur for Ph containing hydrophobic beads (de Chastellier et al., 1995; de Chastellier and Thilo, 2002), suggests that this depletion is an active process and therefore possibly form part of mycobacteria's manipulation of the phagosome, like excluding EEA1 and syntaxin 6. In a follow-up study by the above authors, it is demonstrated that the depletion of surface-derived glycoconjugates is also applicable to M.tb-containing Ph relative to early En, as shown by the graph (Pietersen et al., 2004) below.

"Relative grain density" represents surface-derived glycoconjugates and is derived from counting the grains that result from isotope-label (^{3}H-galactose) decay. The level of depletion and its time course is the same for both *M. avium* and *M. tuberculosis* (H37Rv) (Pietersen et al., 2004). Considering that the depletion of surface-derived glycoconjugates might be important to mycobacteria intracellularly, puts the focus on a select type of molecule to study, i.e., molecules that are cell-surface derived and glycosylated. Narrowing molecules down to a select type to study, gives an advantage over studies where all the phagosome membrane

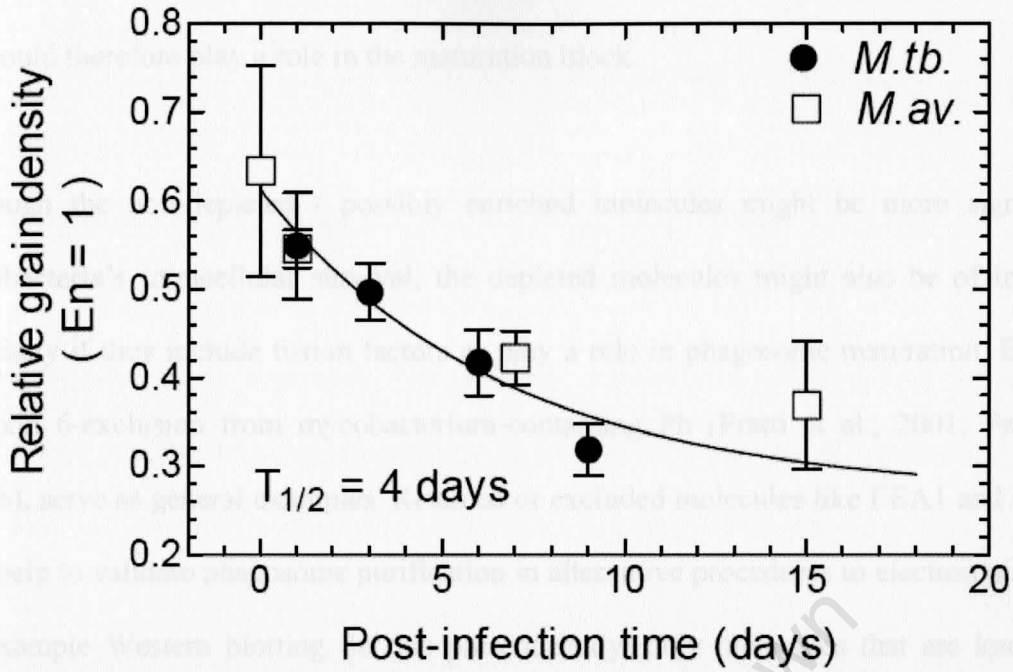

Fig.3. Change of phagosome membrane composition relative to early endosomes. To compare the membrane composition of phagosomes with that of early endosomes, the respective grain-density of phagosomes was divided by that of early endosomes. The data indicated a relative depletion of label on the phagosome membrane, the time course of which could be described by first-order kinetics with a half-life of about 4 days. Error bars indicate the standard error from 3 independently processed samples of fixed cells. Results for *M.avium* (open symbols) are as reported previously (de Chastellier and Thilo, 2002).
From Pietersen et al, 2004 in Eur. J. Cell Biol. 83 (2004); 153 - 158

molecules are considered as possibly significant for mycobacteria's intracellular survival. The question, therefore, in this regard is: what are the identities of the molecules involved in the observed depletion of surface-derived glycoconjugates.

Two possible scenarios might exist regarding the depletion of surface-derived glycoconjugates. Firstly, the depletion might be general for all the surface-derived glycoconjugates, i.e. all the concerned molecules are depleted to the same extent. This would require a general explanation. The second possibility is that some of the surface-derived glycoconjugates are depleted selectively while the relative abundance of others remains unchanged or may even be increased. This means, that in spite of an overall depletion, some surface-derived glycoconjugates might be enriched. Some of these molecules might mediate

the observed close interaction between the mycobacterial surface and phagosome membrane and could therefore play a role in the maturation block.

Although the non-depleted / possibly enriched molecules might be more significant in mycobacteria's intracellular survival, the depleted molecules might also be of importance, especially if they include fusion factors or play a role in phagosome maturation. EEA1- and syntaxin 6-exclusion from mycobacterium-containing Ph (Fratti et al., 2001; Fratti et al., 2003b), serve as general examples. Retained or excluded molecules like EEA1 and syntaxin 6 may help to validate phagosome purification in alternative procedures to electron microscopy, for example Western blotting. In this present study, only molecules that are known to be surface-derived and glycosylated will be considered for possible significance in the maturation block.

Chapter 1

Phagosome Purification

In order to characterise surface-derived glycoproteins in the membrane of *M. avium*-containing phagosomes, the phagosomes had to be isolated and purified. Ideally, the phagosomes had to be separated from all other cellular material. The first objective (after phagosome purification) was to perform quantitative comparisons against other cellular vesicles. For a later stage, qualitative assessments like protein identification were envisaged.

In general, the purification of phagosomes (Ph) is based on their density. Ph usually have a unique density which allows them to separate from all other organelles and vesicles on a density gradient. Various substances have been employed for the separation and isolation of vesicles and organelles according to their density. Among these are sucrose, Percoll and Ficoll (Pertoft, 2000). In the literature, the purification of mycobacteria-containing Ph is often described through the use of sucrose density-gradients (Fratti et al., 2001) and was therefore chosen as a first approach to purify mycobacteria-containing Ph.

The final phagosome purification method would include phagosome isolation from radioactive galactose-labelled primary bone marrow-derived macrophages that would be pre-infected with virulent transparent (Tr) *M. avium*. In initial experiments for phagosome purification, however, a simplified procedure, which included the use of a readily available mouse macrophage cell line, $P388D_1$, and the avirulent opaque (Op) strain of *M. avium*, was used. Also, the *M. avium* (Op), instead of the cells, were radioactively labelled in order to follow their position inside Ph on the gradient.

Because Ph were to be analysed for their cell surface-derived glycoconjugates, it was also important to know the position on the gradient of other vesicles that contained these markers. For this reason, a mixture of plasma membrane (PM) and endosomes (En) was prepared and tested alongside the Ph for its position on the sucrose gradient.

Endocytic organelles obtained label by labelling the cell-surface glycoconjugates with either ^{3}H- or ^{14}C-galactose and subsequently internalising the labelled molecules by incubation at 37°C to reach the organelles. Limiting the time of label internalisation controlled which organelles received label. To prepare labelled En, cell-surface label was internalised for 5 minutes followed by the removal of uninternalised label. About 90% of the cell-surface label could be removed enzymatically, while the remaining 10% became part of a mixed pool of PM and En, because they could not be separated. This resulted in a mixture of PM and En in terms of labelled glycoconjugates.

The use of sucrose gradients, as applied in this study, did not give the desired result. The important results obtained from the sucrose gradients are that En/PM and lysosomes (Ly) occurred in the same position on the gradient as the Ph (Figures A1.1 and A1.2 in the Appendix, p108). The main criterion for phagosome purification was the complete separation between Ph and En/PM because the Ph needed to be compared to the En/PM. Changing the sucrose concentrations resulted only in a partial improvement. It was concluded that a sucrose gradient was not the best option to use.

Thus far, the sucrose gradients were unsuccessful. Two options presented themselves, namely to continue pursuing a sucrose gradient method, or to consider a gradient that does not use sucrose as a separation medium. In Figure A1.2, denser Ly occupied closely the same position as the Ph, meaning these two types of vesicles have closely the same density. In work done by

Haylett and Thilo (1986) to analyse dense (secondary) Ly, a 27 % Percoll column was used to successfully separate secondary Ly from En/PM. From these observations it was predicted that the Ph would have a similar separation from the En/PM in a 27 % Percoll gradient. In other words, a complete separation between Ph and En/PM was expected on a 27 % Percoll gradient. This was strong motivation to first test the 27 % Percoll gradient before reconsidering a sucrose gradient.

Percoll, consisting of silica particles that are coated with polyvinylpyrrolidone (PVP), is a well-known medium to separate cells and cellular constituents because it is non-toxic to cells and does not change the viability or morphological character of samples (Blitzer and Donovan, 1984; Pertoft, 2000; Schaub et al., 2005). Percoll, which is a self-forming gradient under centrifugation, was prepared as a mixture with buffer. The same experimental approach that was used for the sucrose gradients was used to evaluate the suitability of the 27% Percoll column for the purification of M.av-Ph.

Figure 1.1 summarises the results obtained for centrifuging different samples on 27 % Percoll. Comparing graph A of Figure 1.1 (En/PM from non-infected cells) with graph B (labelled mycobacteria representing Ph from a separate gradient), it can be seen that En/PM were close to the top of the 27 % Percoll gradient and the Ph close to the bottom. Graphs A and B of Figure 1.1 are reproduced in Figure A2 in the Appendix. These results represented good separation between Ph and En/PM. These two radioactivity peaks coincided with the two visible, opaque bands that could be observed in the centrifuge tube. There was usually an upper band towards the top of the tube (at the position of the En/PM) and a lower band close to the bottom of the tube where the Ph occurred. The fraction numbers confirmed that the visible bands exactly matched the radioactivity peaks. Only the clear Percoll-coloured background was visible between the upper and lower bands in the centrifuge tube.

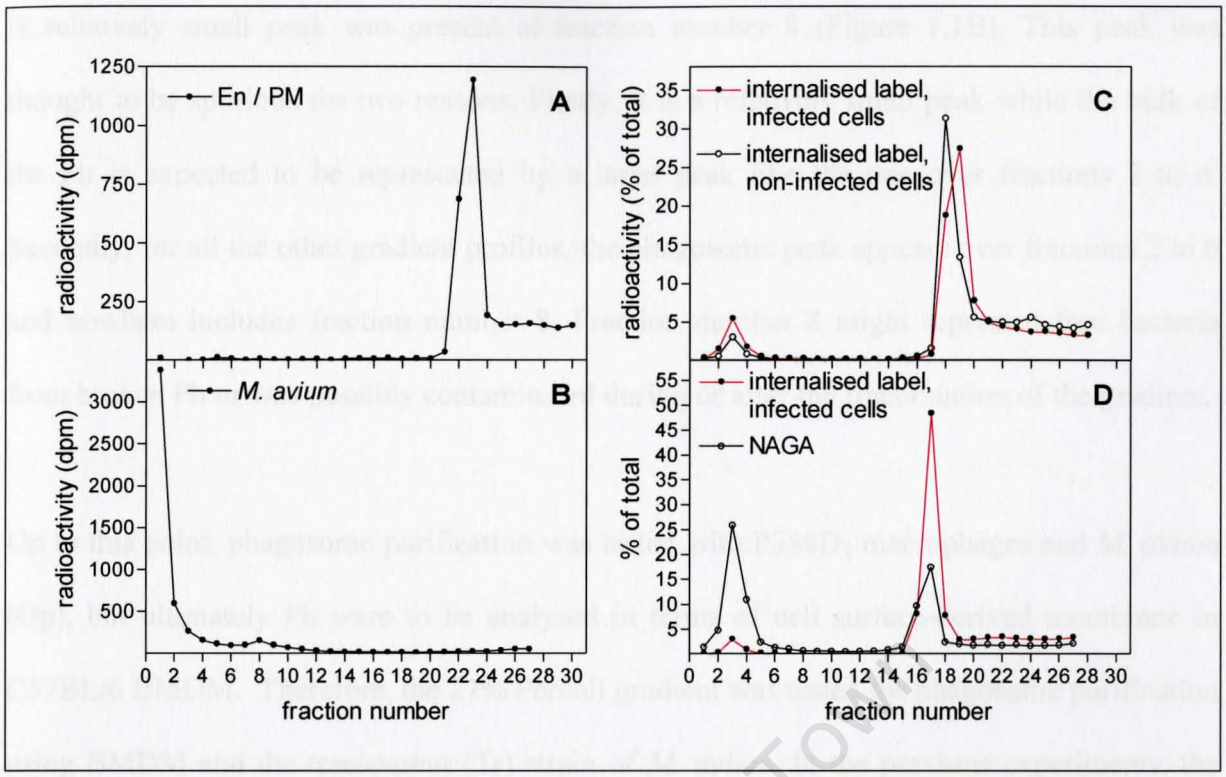

Figure 1.1: Sedimentation on 27% Percoll for the isolation and purification of M.av-Ph
A: Non-infected P388D$_1$ cells were labelled with ^{3}H-galactose, followed by internalisation of label for 5 minutes and the enzymatic removal of uninternalised label. PNS was loaded on top of a 27% Percoll column and centrifuged (as described in Methods). The gradient was fractionated from the bottom and aliquots counted for radioactivity. **B:** P388D$_1$ cells were infected with ^{3}H-galactose labelled *M. avium* (Op) for 60 minutes and chased for 30 minutes. PNS was loaded on top of a 27% Percoll column and centrifuged as in A. **C:** Bone marrow-derived macrophages (BMDM) were divided into two groups. One group was infected with *M. avium* (Tr) while the other remained non-infected. At 7 days post-infection (p.i.), the cells were labelled with ^{3}H-galactose, the label was internalised for 2h and surface label enzymatically removed (as described in Methods). A PNS was prepared for each group of cells and loaded on separate 27% Percoll columns and centrifuged as in A. **D:** To compare how the position of Ly coincide with that of internalised label, a new BMDM culture was infected with *M. avium* (Tr). At 7 days post-infection, the cells were treated as in C. Aliquots from the gradient were counted for radioactivity and also analysed for NAGA content. A comparison between A and B indicates that Ph could be completely separated from the En/PM. The level of cell surface-derived label in the Ly (which are collected with the Ph) was originally thought to be negligible because it was found that only 2% of the cell-surface label goes to dense Ly for P388D$_1$ cells (Haylett and Thilo, 1986). Here, however, dense Ly accounted for 6% (and Ph 11%) of the total label recovered from the gradients. Two published methods for Ph purification did not manage to remove the dense Ly from the Ph. At that stage the 27% Percoll gradient offered the best purification method for M.av-Ph.

A relatively small peak was present at fraction number 8 (Figure 1.1B). This peak was thought to be spurious for two reasons. Firstly, it is a relatively small peak while the bulk of the Ph is expected to be represented by a large peak like the one over fractions 2 to 6. Secondly, for all the other gradient profiles, the phagosome peak appears over fractions 2 to 6 and nowhere includes fraction number 8. Fraction number 8 might represent free bacteria from broken Ph or was possibly contaminated during or after the fractionation of the gradient.

Up to this point, phagosome purification was tested with P388D_1 macrophages and *M. avium* (Op), but ultimately Ph were to be analysed in terms of cell surface-derived membrane in C57BL/6 BMDM. Therefore, the 27% Percoll gradient was tested for phagosome purification using BMDM and the transparent (Tr) strain of *M. avium*. In the previous experiments, the mycobacteria were labelled, but now the phagosome membrane had to carry label. As described in the Introduction, Ph receive cell-surface label when they exchange labelled glycoconjugates with early En (which receive their label from the labelled PM) during incubation at 37° C (de Chastellier et al., 1995). Thus, after the cell surface (PM) of infected cells was labelled, the cells were incubated for 2 hr to allow for the intracellular distribution of label, during which a steady-state distribution of the internalised label was reached. This internally distributed label was compared between infected and non-infected cells as shown by Figure 1.1C.

Following from the position of the labelled bacteria – which were inside Ph – in Figure 1.1B, the radioactivity peak (●) over fractions 1 – 5 in Figure 1.1C was concluded to be the Ph. For both the infected and non-infected cells, the upper peaks (over fractions 15 to 19) of Figure 1.1C represent the En/PM, similarly to Figure 1.1A. Although the cell type used for Figure 1.1C differed to that for Figures 1.1A and B, the overall result of high and low density peaks occurring over closely the same fractions in these figures, suggests that cell type might only

have had a very small influence on the position of the vesicles. For instance, for the P388D_1 cells (Figure 1.1B), the Ph peaked in fraction number 1 while for BMDM (Figure 1.1C) the Ph peaked in fraction number 3. The position of the En/PM peak is also influenced by the size (or volume) of the Percoll gradient. In the non-infected cells, the lower peak (over fractions 1 to 6) represents the Ly. Ly obtain surface-derived label by fusion with matured En, i.e. not before 5 minutes from the start of incubation at 37°C. The absence of a peak for the high density fractions in Figure 1.1A is in line with published results for P388D_1 cells regarding the time-dependent appearance of surface-derived glycoconjugates in Ly (Haylett and Thilo, 1986). Seeing that the Ly and Ph occurred over the exact same fraction numbers in the gradient, the radioactivity, as represented by the lower peak for the infected cells, includes that of both the Ly and the Ph. The larger area under the curve (AUC) for the Ph peak (which is 10) as compared to the Ly (5.4), shows that the more abundant radioactivity is associated with the Ph.

The experiment to Figure 1.1C was reproduced in Figure A3 (Appendix). The good, clear separation between Ph and En/PM (as seen for Figures 1.1A and 1.1B from separate gradients) is confirmed by Figures 1.1C and A3, where both labelled En/PM and Ph were present on the same gradient.

From Figure 1.1C it can be seen that Ly and Ph occurred over the same gradient fractions. To confirm if these two vesicle types do occupy the same position on the gradient, the experiment of internalising the label into infected cells was repeated and the distribution of Ly in the gradient was determined by measuring the lysosomal enzyme NAGA (as was done for the sucrose gradients) using aliquots from the same fractions for which radioactivity was determined as shown in Figure 1.1D.

It is clear that the Ly share the positions of the Ph as well as the En/PM in a 27% Percoll gradient, thus corresponding to the two visible bands in the centrifuge tube. As was described by Haylett and Thilo (1986) regarding the position of Ly in the 27% Percoll gradient, the Ly coinciding with the Ph are the dense part of the continuous density spectrum of Ly, while the complementary fraction of lower density banded with En/PM.

The amount of cell surface-derived label in the Ly was expected to be negligible, as mentioned in Figure 1.1, but was seen to be about half of the total amount in the Ph. The same amounts were calculated for Figure A3. Although the amount of cell surface-derived label in the Ly was calculated for non-infected cells, it is probably the same for infected cells, because no reason is known to suggest otherwise. Two published methods for Ph purification did not manage to remove the Ly from the Ph (Desjardins et al., 1994; Alvarez-Dominguez et al., 1996). From the above results it is clear that the densities from M.av-Ph and dense Ly are either exactly the same or extremely close. There was no reason to expect that a sucrose gradient might separate dense Ly from M.av-Ph. The 27% Percoll gradient, therefore offered the best purification for M.av-Ph. The lysosomal contamination had to be considered when analysing results.

It was asked if label could be dragged down to the high density fractions by vesicles or organelles that do reach the position of the Ph. To answer this, a radioactive PNS preparation, where only the En/PM carried label, from non-infected cells was mixed with non-radioactive PNS containing M.av-Ph and centrifuged on 27% Percoll to see if radioactivity could be found at the bottom of the gradient. The result appears in Figure 1.2. A bottom band was visible for both gradients, but no radioactivity was detectable at the position where the Ph was expected to be. This meant that no label from the low-density Percoll fraction was dragged down to the dense Percoll fraction.

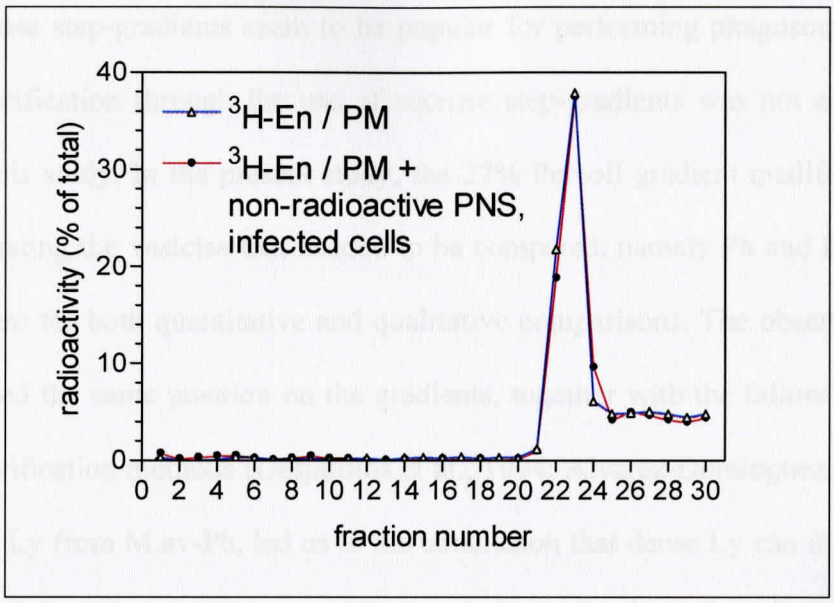

Figure 1.2: Sedimentation on 27% Percoll to test if label is dragged down in the gradient
Two PNS preparations were made. The first PNS was from non-infected P388D$_1$ cells that were labelled with ^{3}H-galactose, followed by internalisation of label for 5 minutes and the enzymatic removal of uninternalised label. The second PNS was from P388D$_1$ cells that remained unlabelled, but were infected with *M. avium* (Op) for 1 h and chased for 30 minutes. Half of the ^{3}H-PNS was mixed with the non-radioactive PNS (●) and the other half adjusted to the same volume with buffer (△). These two final preparations were loaded on separate 27% Percoll columns and centrifuged. The gradients were fractionated and aliquots counted for radioactivity. The presence of Ph in the PNS did not cause the label on En/PM to sediment to the high-density fractions.

Although sucrose step-gradients seem to be popular for performing phagosome purification, phagosome purification through the use of sucrose step-gradients was not as successful as attempted in this study. In the present study, the 27% Percoll gradient qualified in the main aspect of separating the vesicles that needed to be compared, namely Ph and En/PM. The Ly posed a problem for both quantitative and qualitative comparisons. The observations that Ph and Ly occupied the same position on the gradients, together with the failure of a few other phagosome purification methods (Desjardins et al., 1994; Alvarez-Dominguez et al., 1996) to separate dense Ly from M.av-Ph, led us to the conclusion that dense Ly can in general not be separated from M.av-Ph by density centrifugation. The 27% Percoll gradient was therefore chosen as an acceptable method for phagosome purification at the time.

Chapter 2

Radioactivity profiles of cell surface-derived glycoproteins

After having established a method for phagosome purification, the next objective was to analyse the Ph in terms of surface-derived glycoconjugates. The proposal for this study came from the observation that surface-derived glycoconjugates were found to be depleted about 3- to 4-fold in M.av-Ph as compared to early endosomes, even though these vesicles exchange contents and intermingle membrane components continuously (de Chastellier et al., 1995; de Chastellier and Thilo, 2002). The goal, here, was to determine the identity of the glycoproteins involved in the quantitative differences.

Experimental approach

Surface-derived glycoconjugates needed to be compared between early En and M.av-Ph through an approach that would allow their quantification and identification. Polyacrylamide gel electrophoresis (PAGE) was the technique of choice to satisfy both requirements of the approach. To be able to analyse the surface-derived glycoproteins, they were either labelled enzymatically with ^{3}H- or ^{14}C-galactose as originally described (Thilo, 1983). Early En acquire label when endocytosis takes place during incubation of surface-labelled cells at 37°C, while Ph acquire label, i.e. labelled molecules, when eEn fuse with Ph.

The use of different isotopes, i.e. tritium and carbon-14 (both in the same chemical form, i.e. galactose), offers the advantage of combining different isotope-labelled molecules in the same lane on the PAGE for both a direct and detailed comparison. The two isotopes can be separated by oxidation to $^{3}H_2O$ and $^{14}CO_2$ in a Sample Oxidizer prior to detection by scintillation counting. The labelled surface-derived glycoproteins could therefore be effectively compared between two different cell compartments.

For this study, BMDM were infected with the virulent Tr strain of *M. avium* for 4 hours at a multiplicity of infection (MOI) of 20 and chased after washing for seven days. The depletion of the surface-derived glycoconjugates from the phagosomal membrane was a gradual process which was followed up to 15 days after infection, but a steady state level is reached from seven days onwards (de Chastellier and Thilo, 2002). Seeing that the level of labelled glycoprotein-depletion at day 7 closely resembled that at day 15 (de Chastellier and Thilo, 2002), the p.i. time of day 7 was chosen as the testing point in the current study for the remodelling of the phagosome membrane by *M. avium* in terms of surface-derived glycoconjugates.

EM analysis

Electron microscopy (EM) was performed for morphological assessment of the Ph. BMDM were infected with *M. avium* and 7 days after infection were fixed and processed for EM. Figure 2.1A shows a general view of a BMDM with seven day old M.av-Ph. The majority of the mycobacteria were in Ph that were free of lysosomal material and had a closely apposed phagosome membrane surrounding the bacteria. In the bottom right corner there are two dividing *M. avium* bacilli with an all-around closely apposing phagosome membrane, even into the site of septum formation. The same observation was reported by de Chastellier and Thilo (1997) as support for the viewpoint that pathogenic mycobacteria need to maintain an all-around closely apposing phagosome membrane in order to remain as immature Ph. The above observations indicate that the macrophages were properly infected with virulent and dividing bacteria.

An enlarged picture of a phagosome is shown by Figure 2.1B. The phagosome membrane, indicated by thin arrows, is all-around closely apposed to the bacterial surface. Ly did not fuse with this phagosome, which supports that it is an immature phagosome. Normally, Ph take 5

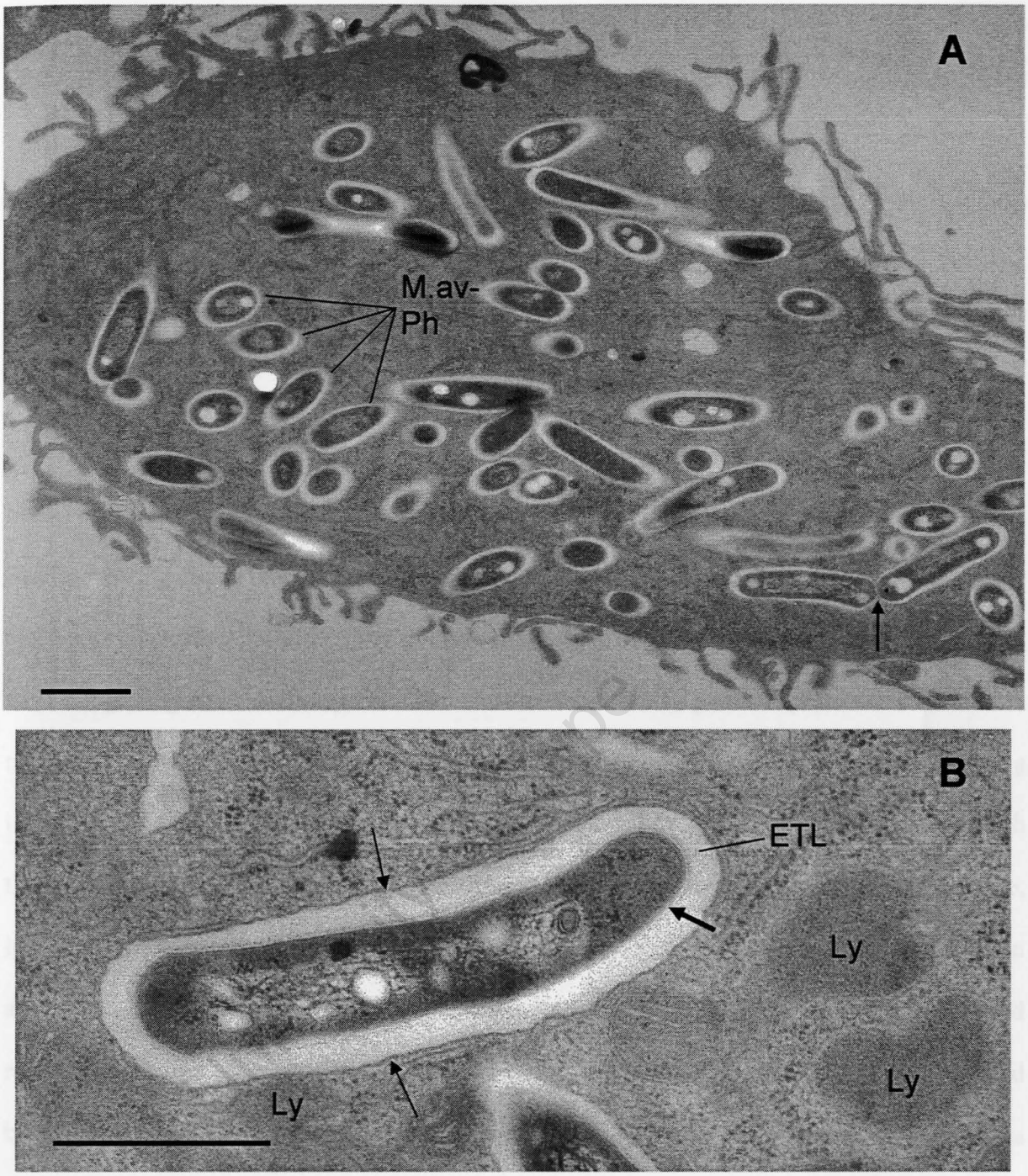

Figure 2.1: Evaluation of proper infection and immature status of M.av-Ph by EM
BMDM were infected with *M. avium*. At 7 days p.i., the cells were fixed and processed for EM (as described in Methods). **A**: General view of a macrophage with immature M.av-Ph. Each Ph generally contained a single bacterium. Immature M.av-Ph were characterised by an all-around close apposition of the phagosome membrane to the mycobacterial surface. The close apposition was maintained at the site of septum formation (arrow) for dividing mycobacteria. **B**: Enlarged view of a M.av-Ph. The thin arrows indicate the phagosome membrane. The electron translucent layer (ETL), situated between the phagosome membrane and the mycobacterial PM (thick arrow), corresponds to the lipid-rich cell wall of mycobacteria. Ly are situated close to the phagosome without fusing with them. Bar = 1 μm in **A** and 0.5 μm in **B**. The macrophages were properly infected and the majority of the Ph remained immature. (All EM was kindly performed by Dr C de Chastellier, Marseille.)

to 15 minutes to mature before they fuse with Ly (Pitt et al., 1992; de Chastellier et al., 1995; Oh and Swanson, 1996). These observations are therefore in line with the character of immature Ph.

2.1 PM and infection

The quantitative difference for surface-derived glycoconjugates between Ph and eEn was observed through the techniques of autoradiography and EM (de Chastellier et al., 1995). Radioactive decay of the isotope (radioactive galactose) was assessed at the level of the electron microscope because EM can distinguish between the various endocytic organelles with a high degree of accuracy. The aim of this study was to perform protein identification, meaning the technique of EM needed to be substituted for PAGE analysis by comparing isolated Ph and eEn. Unfortunately, obtaining pure eEn is not possible. Within the approach that was to be followed, labelled eEn could be prepared by labelling the cell-surface, internalising the label for not more than 5 minutes (to prevent the label from reaching late En and Ly) and then remove up to 90% of uninternalised label from the surface. This would result in a mixture of labelled En and the remaining 10% of label on the PM. It was decided better to compare Ph to PM to avoid a mixed sample. A few experiments were done with a mixture of labelled PM and En for comparison.

In the experimental approach, a BMDM culture was divided into two groups, each group for a specific treatment (e.g. infected and non-infected), followed by labelling of cell-surface glycoconjugates with either ^{3}H- or ^{14}C-galactose. Re-incubating the cells at 37°C allowed for internalisation of the labelled molecules to steady-state distribution. Different organelles were isolated and the labelled glycoproteins compared via PAGE analysis. One-dimensional (1-D)

PAGE was employed first to obtain overall results which also served as a guide for subsequent two-dimensional (2-D) PAGE analysis.

Figure 2.2 shows a Coomassie-stained sodium dodecyl sulphate (SDS)-PAGE as an example of one of the first experiments comparing M.av-Ph from infected cells against PM from non-infected cells. For this PAGE, BMDM were divided into two groups and only one group was infected with *M. avium.* Seven days after infection, the infected and non-infected cells were labelled with ^{3}H-galactose. Only the label of the infected cells was internalised for 2 h and uninternalised label removed. The M.av-Ph were isolated from 27% Percoll. For the ^{3}H-PM sample total PNS was used. Extensive sample preparation for the PM was not necessary because only the radioactivity was followed. All the electrophoresis work was done under denaturing conditions.

Coomassie-stained protein bands can be seen for the Ph sample, but seem to be totally absent for the PM sample in Figure 2.2. The most likely reason for this is that the phagosome sample contained more protein due to the presence of the mycobacteria (from the phagosomes). Because standardisation of the PAGE samples was based on radioactivity, the non-radioactive bacteria increased the total protein but not the radioactivity in the phagosome sample. The bulk of the radioactivity, even at steady-state distribution, is associate with the PM and endosomes (Figure 1.1, Chapter 1; Haylett and Thilo, 1986). However, enough radioactivity was present on the PM lane to construct a profile which appears in Figure 2.3B (which is discussed below).

To obtain a profile of the radioactive glycoproteins (glycolipids were expected to electrophorese off the PAGE due to their size) on the PAGE, the following steps were taken. After electrophoresis and having dried the SDS-PAGE, the lanes with the Ph and PM samples

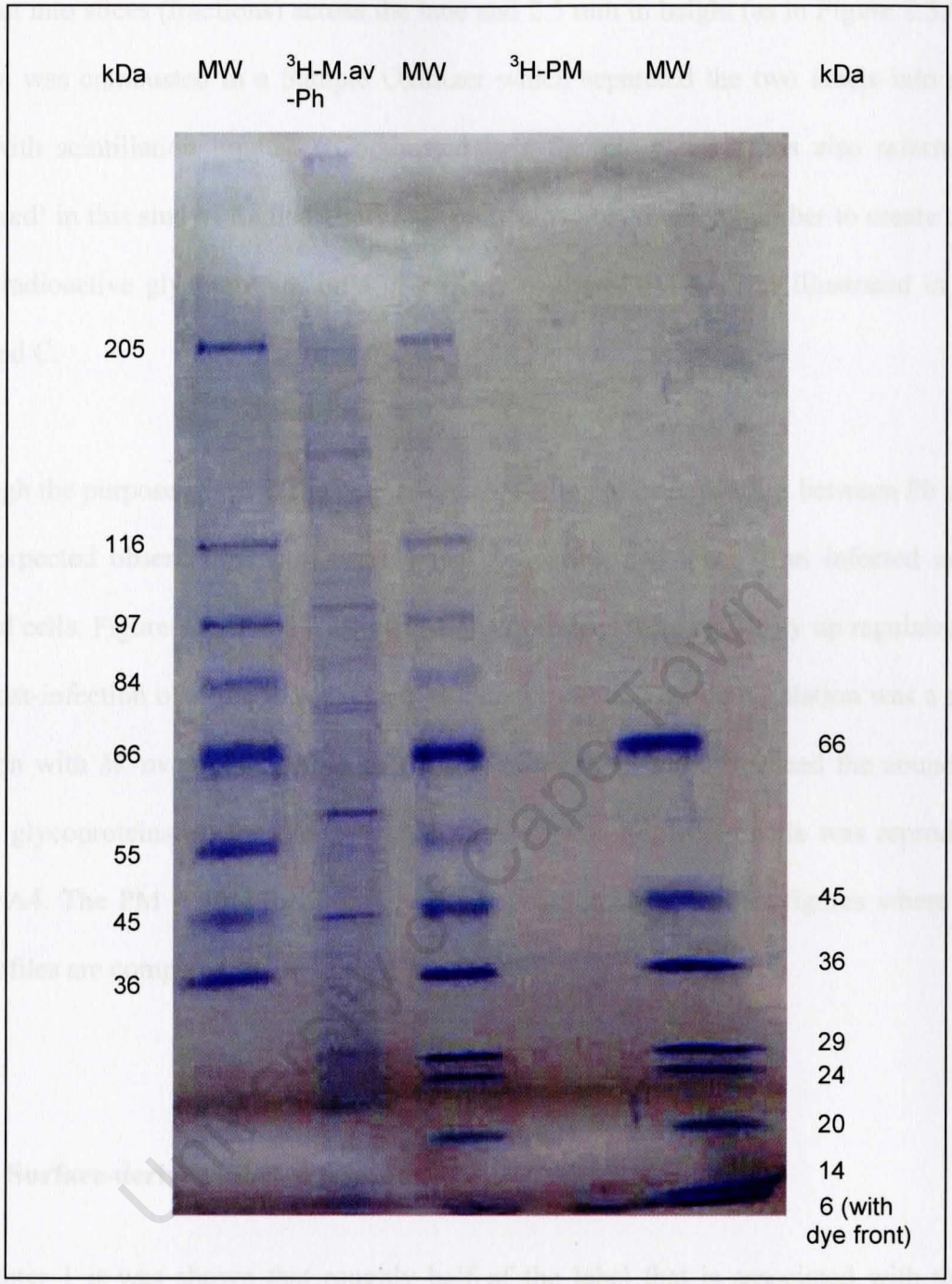

Figure 2.2: Coomassie-stained 1-D SDS-PAGE showing bands for Ph and PM samples as an example of the gel electrophoresis experiments BMDM were divided into two groups. One group was infected with *M. avium* while the other remained non-infected. At 7 days p.i., the infected and non-infected cells were labelled with ^{3}H-galactose. Only the label of the infected cells was internalised for 2 h and uninternalised label removed (as described). Separate PNS preparations were made for the two groups of cells and only the PNS from the infected cells was centrifuged on a 27% Percoll column. The M.av-Ph were isolated as the high-density fraction (bottom band in the centrifuge tube) from the Percoll gradient. Total PNS was used as the ^{3}H-PM sample. The radioactivity of the ^{3}H-Ph and ^{3}H-PM samples were measured and equal radioactivity amounts subjected to 1-D SDS-PAGE, using a gradient gel of 8 to 15% acrylamide. No bands were visible for the PM sample. Because gel loading was based on radioactivity and not protein amount, the Ph sample, which included the bacteria, obviously had enough total protein for visualisation through Coomassie staining, but not the PM sample for which the total protein amount must have been below the detection limit of the stain.

were cut into slices (fractions) across the lane and 2.5 mm in height (as in Figure 2.3A). Each fraction was combusted in a Sample Oxidizer which separated the two labels into separate vials with scintillation liquids. ('Combusted in a Sample Oxidizer' is also referred to as 'Oxidized' in this study.) Radioactivity was plotted against fraction number to create a profile of the radioactive glycoproteins on a given lane of the SDS-PAGE as illustrated in Figures 2.3B and C.

Although the purpose of the 1-D electrophoresis was to compare profiles between Ph and PM, an unexpected observation was made when comparing PM label from infected and non-infected cells. Figures 2.3B and C show PM glycoproteins were markedly up regulated after 7 days post-infection over the MW range of 205 to 116 kDa. This up regulation was a result of infection with *M. avium* and serves as evidence that *M. avium* influenced the abundance of certain glycoproteins on the PM. The PM profile for non-infected cells was reproduced in Figure A4. The PM profile for infected cells appears in several other figures where Ph and PM profiles are compared (e.g. Figure 2.7).

2.2 Surface-derived label in lysosomes

In Chapter 1 it was shown that roughly half of the label that is associated with the high-density fraction (bottom band) on a 27% Percoll gradient is part of dense Ly. Seeing that dense Ly could not be separated from M.av-Ph, an attempt was made to correct for the label in the Ly through PAGE analysis. The aim was to incorporate this correction into the comparison of labelled glycoproteins between Ph and the PM. Therefore, a BMDM culture was divided into three groups and from two of the groups of cells ^{14}C-PM and ^{3}H-labelled M.av-Ph were prepared as described and detailed under Figure 2.4A. The third group of cells was not infected and labelled with ^{3}H-galactose followed by internalisation of the label for

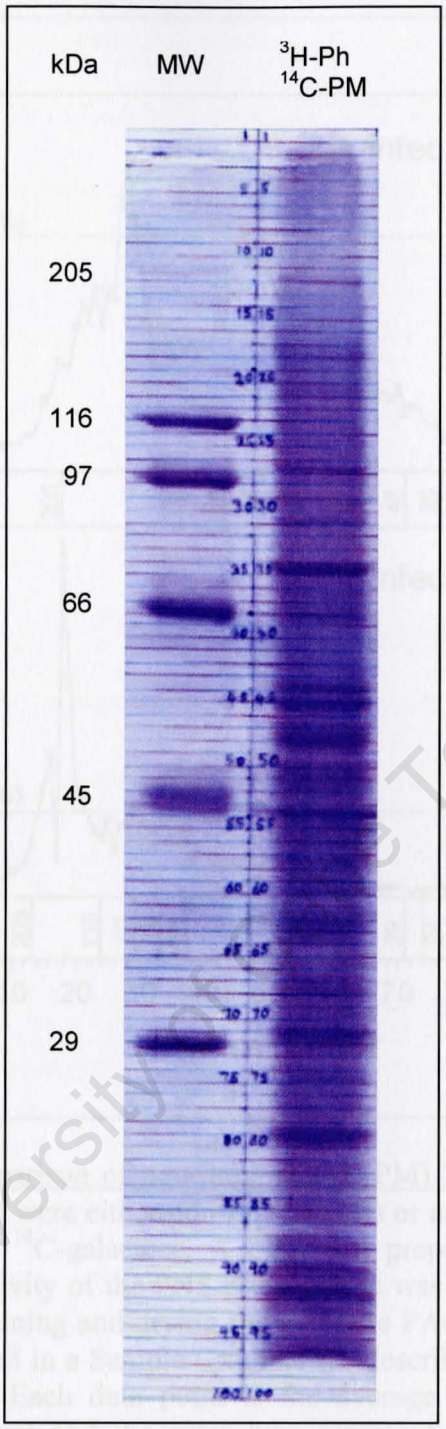

Figure 2.3A: Coomassie-stained SDS-PAGE showing how lanes were divided into fractions
BMDM were divided into two groups. One group was infected with *M. avium* while the other remained non-infected. At 7 days post-infection, the infected cells were labelled with ^{3}H-galactose, the label was internalised for 2 h and uninternalised label removed. The non-infected cells were labelled with ^{14}C-galactose. ^{3}H-Ph and ^{14}C-PM were isolated by cell fractionation and density gradient centrifugation (as described). The radioactivity of the two samples was determined and equal radioactivity portions from the respective samples were mixed and subjected to 1-D SDS-PAGE. Lanes were divided into fractions of 2.5 mm height as indicated by the horizontal lines. The blue numbers indicate fraction numbers. The fractions were subsequently Oxidized.

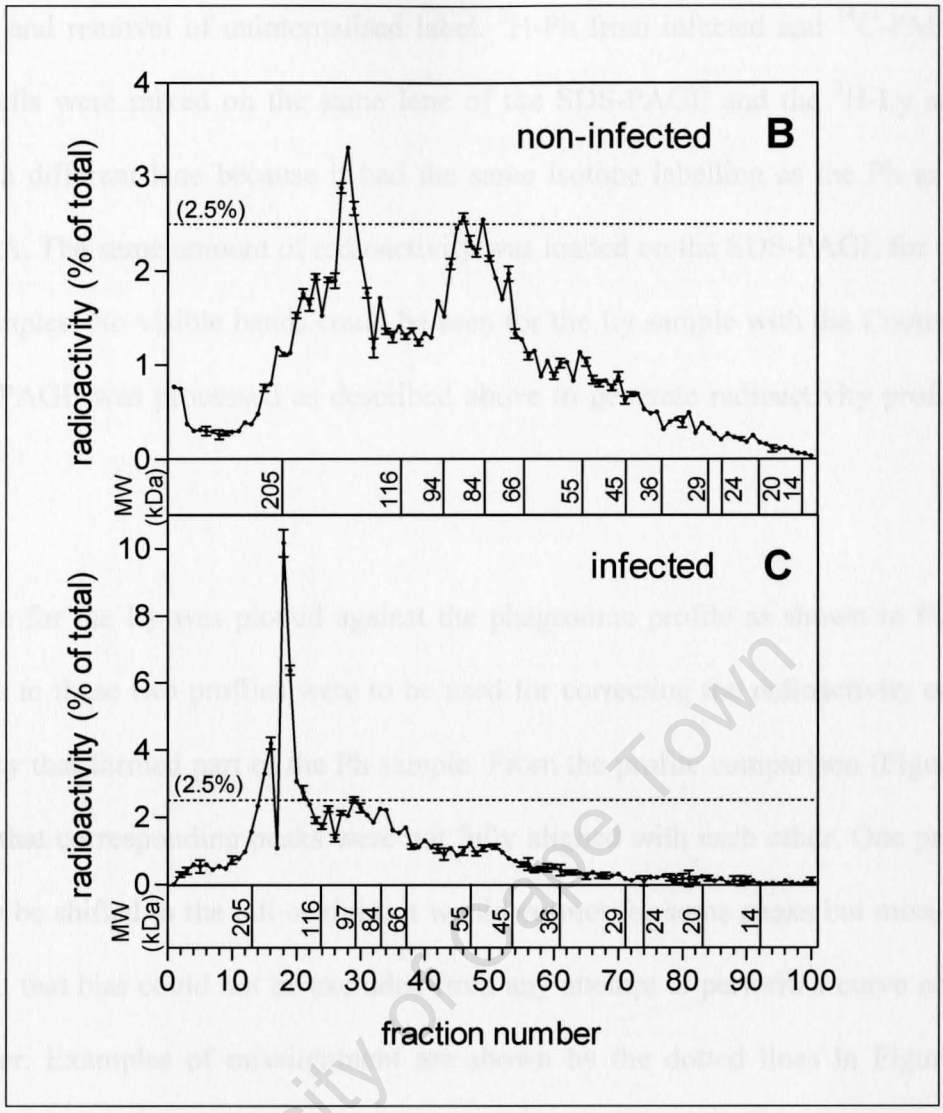

Figure 2.3B and C: Comparison of non-internalised (PM) label between non-infected and infected cells BMDM that were either non-infected (**B**) or at 7 days p.i. with *M. avium* (**C**), were labelled with ^{3}H- or ^{14}C-galactose. A PNS was prepared for the infected and non-infected cells. The radioactivity of the PNS preparations was measured and analysed on 8 to 15% SDS-PAGE. After staining and drying the gels, the PAGE lanes were fractionated and each fraction was combusted in a Sample Oxidizer (as described). Radioactive content of the fractions was determined. Each data point is the average of 2 or 3 scintillation counts (radioactivity determinations) and the error bars represent standard deviation. A definite change in glycoprotein abundance occurred at the PM as a result of the 7 day infection with *M. avium*. Specifically, over the MW range of 205 to 116 kDa there was a general increase (up regulation) of surface glycoproteins. The dotted line in both graphs is at the 2.5% interval and means that the surface glycoproteins over 94 to 66 kDa (as the other significant rise in the profile in B) did not change in abundance.

two hours and removal of uninternalised label. ^{3}H-Ph from infected and ^{14}C-PM from non-infected cells were mixed on the same lane of the SDS-PAGE and the ^{3}H-Ly sample was loaded in a different lane because it had the same isotope labelling as the Ph as shown by Figure 2.4A. The same amount of radioactivity was loaded on the SDS-PAGE for the Ph, PM and Ly samples. No visible bands could be seen for the Ly sample with the Coomassie stain. The SDS-PAGE was processed as described above to generate radioactivity profiles for the samples.

The profile for the Ly was plotted against the phagosome profile as shown in Figure 2.4B. The values to these two profiles were to be used for correcting the radioactivity contribution from the Ly that formed part of the Ph sample. From the profile comparison (Figure 2.4B), it was clear that corresponding peaks were not fully aligned with each other. One profile could not simply be shifted to the left or right; it would correct for some peaks but misalign others. This meant that bias could not be excluded from any attempt to perform a curve correction in this manner. Examples of misalignment are shown by the dotted lines in Figure 2.4B. In conclusion it was inaccurate to compare profiles from samples that were electrophoresed on different lanes of a SDS-PAGE. General or overall comparisons were possible, but not detailed ones.

The shape of the phagosome profile, as depicted in Figure 2.4B, turned out not to be the standard profile shape for the labelled glycoproteins in the phagosome membrane (which is discussed later). The experiment to this phagosome profile was one of the first for PAGE analysis. This profile shape was however not seen again and was therefore considered not to be the standard profile shape as concluded from duplicate experiments. Irrespective of the profile shape, it was accepted that a curve correction between samples from different lanes was not possible in general.

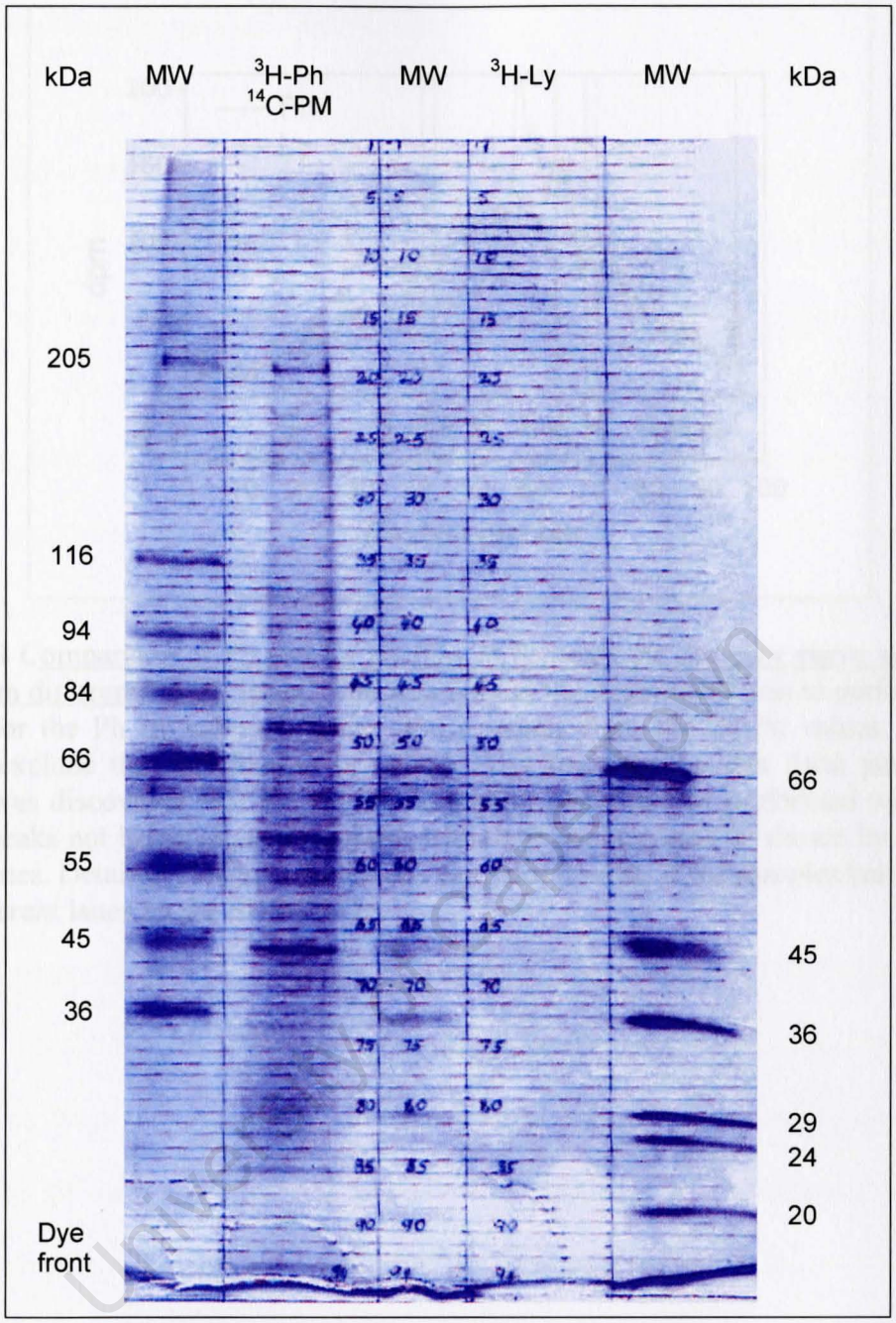

Figure 2.4A: Coomassie-stained 1-D SDS-PAGE to address the issue of combining samples in the same lane BMDM were divided into three groups. One group was infected with *M. avium* while the other two remained non-infected. At 7 days p.i., the infected cells and one non-infected group were labelled with ^{3}H-galactose, the label was internalised for 2 h and uninternalised label removed. The other non-infected cells were labelled with ^{14}C-galactose. ^{3}H-Ph (from the infected cells) and ^{3}H-Ly (from non-infected cells) were separately isolated by cell fractionation and density gradient centrifugation. Cells with the ^{14}C-PM (uninternalised label) were homogenised and a PNS prepared. Total PNS was used as the ^{14}C-PM sample. The radioactivity for the three samples was measured, equal radioactivity amounts of ^{3}H-Ph and ^{14}C-PM were mixed while the ^{3}H-Ly sample was prepared separately and at the same radioactivity amount. The samples were subjected to 1-D SDS-PAGE. Lanes on the dried PAGE were cut into strips (as indicated by the horizontal lines) and combusted in a Sample Oxidizer followed by scintillation counting. The blue numbering indicates the fraction numbers. The results are shown in Figure 2.4B.

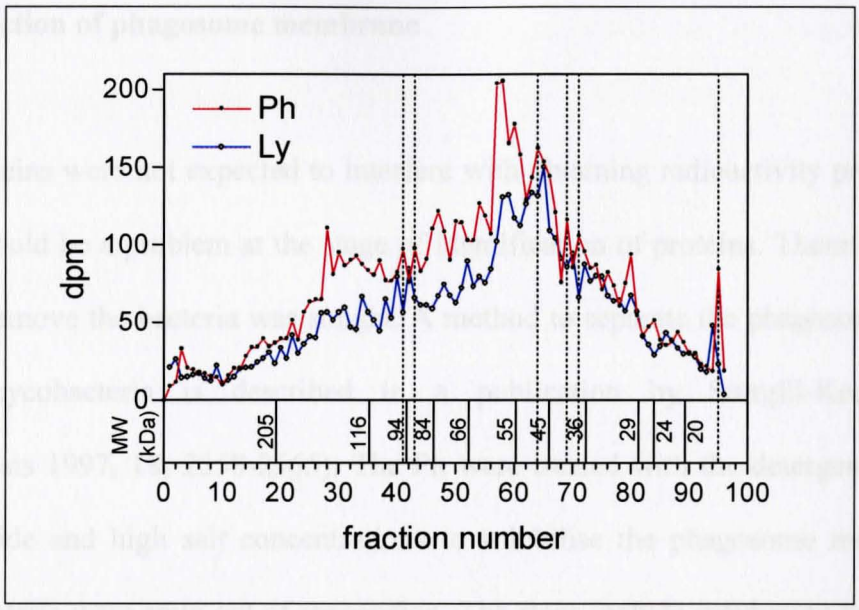

Figure 2.4B Comparison of Ph and Ly profiles to demonstrate the poor curve alignment for samples from different PAGE lanes The idea behind the experiment was to perform a profile correction for the Ph by subtracting the ^{3}H-Ly values from the ^{3}H-Ph values. This would effectively exclude the contribution in radioactivity from the Ly that form part of the Ph sample. It was discovered that the profile correction could not be performed without errors due to the peaks not being aligned properly with their counterparts, as shown by examples at the dotted lines. Detailed profile comparisons were not feasible if the samples being compared were in different lanes on the SDS-PAGE.

2.3 Extraction of phagosome membrane

Bacterial proteins were not expected to interfere with obtaining radioactivity profiles from 1-D gels, but could be a problem at the stage of identification of proteins. Therefore, a method to lessen or remove the bacteria was sought. A method to separate the phagosome membrane from the mycobacteria is described in a publication by Sturgill-Koszycki et al (Electrophoresis 1997, 18, 2558-2565). The Ph were treated with the detergent n-octyl β-$_D$-glucopyranoside and high salt concentrations to solubilise the phagosome membrane after which the bacteria were spun out of suspension. The steps include incubating the Ph with the detergent at 0.5 times the critical micellar concentration (CMC) in buffer for 5 minutes on ice followed by two washes with 0.6 M KCl containing 0.45 times the CMC of n-octyl β-$_D$-glucopyranoside (Sturgill-Koszycki et al., 1997). The supernatants were collected and pooled. Sonication was added to the described method to aid the solubilisation of the membrane (and was used at a later stage to remove luminal proteins to (especially) lessen the Ly proteins in the sample). Also, 0.5 times CMC was used throughout and not 0.45 times the CMC for the washing steps. High salt concentrations are incompatible with isoelectric focussing (which forms part of the next analysis step, namely 2-D electrophoresis), therefore, the salt was decreased to less than 50 mM by washing in the membrane extraction buffer (excluding salt) and centrifuging through a 10 kDa MW cut off membrane which also concentrated the sample to a small volume. The above procedure is referred to as membrane extraction in this study.

It was important that the membrane extraction was effective. The effectiveness of the membrane extraction procedure was ascertained by scintillation counting of small aliquots of the extracted membrane and comparing it to the amount at the beginning, before membrane extraction. Ideally, a 100% yield for the extracted radioactive membrane was sought. The

reported method reports that all the macrophage proteins can be removed from the mycobacteria (Sturgill-Koszycki et al., 1997).

It was found that the membrane extraction, as described above, left some (up to 30%) radioactive membrane on the bacterial pellet. To obtain the remaining radioactive membrane from the pellet, the membrane extraction procedure was performed for a second time. It was found that a second extraction removed all or nearly all the radioactivity as demonstrated by Figure 2.5.

Figure 2.5 shows how much radioactive membrane remained on the pellets after each membrane extraction. The amounts of radioactive membrane were established by linear analysis from the aliquots of extracted membrane. Basically, aliquots were counted before and after membrane extraction. On average, the first round of extraction yielded 70% of the total radioactivity while all or nearly all of the remainder was extracted with the second extraction.

2.4 Comparison of Ph to PM

It was shown above that infection with *M. avium* caused a change in the abundance of glycoproteins at the cell surface. Now, comparisons between Ph and PM samples were made to find out if glycoprotein abundance was different in the Ph as compared to the cell surface of infected cells.

The approach to the gel electrophoresis experiments was modified to accommodate the subsequent 2-D analysis. 1-D separation served as a guide to ultimately isolate individual proteins from 2-D separations for identification. To have a better comparison between 1-D

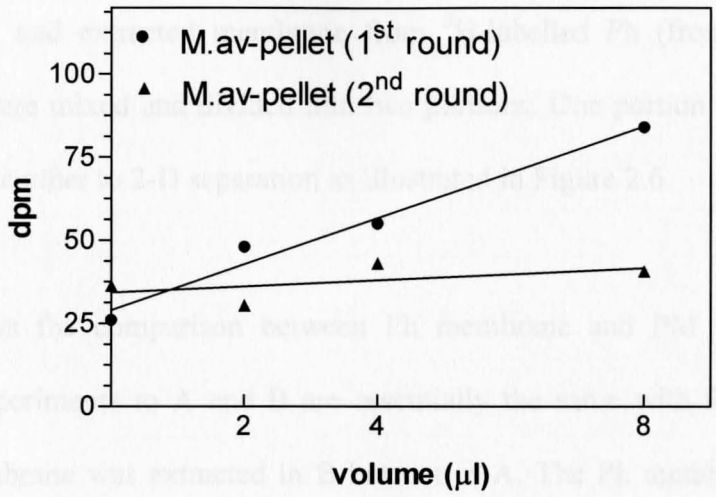

	post 1st round extraction (dpm/µl)	post 2nd round extraction (dpm/µl)
Slope	6.9 ± 0.74	0.91 ± 0.95
Y-intercept	29 ± 3.4	34 ± 4.4
P value	0.0113	0.4385
Deviation from zero	Significant	Not Significant

Figure 2.5: Remaining radioactive membrane on the M.av-pellets after membrane extraction
BMDM were infected with *M. avium* and at 7 days p.i. were labelled with ^{3}H-galactose. The label was internalised for 1 h and uninternalised label removed. A PNS was prepared and the M.av-Ph isolated by cell fractionation and density gradient centrifugation. The Ph were treated with detergent and high salt to solubilise the radioactive phagosome membrane (as described). Aliquots of the extracted membrane and pellets were counted for radioactivity. The linear analysis (inserted table) shows the slope (slope ± standard deviation) in dpm/µl. The slopes, together with the volumes of extracted membrane, were used to calculate the portions of membrane that was extracted. The amount of extracted membrane for the 1st and 2nd round was 70% and 33% respectively. In general, extractions beyond this point only returned background values. According to Sturgill-Koscycki et al (Electrophoresis 1997, 18, 2558-2565), their method removed all host-derived proteins from the bacteria. The membrane extraction method worked well enough to be reliable.

and 2-D separations, both 1-D and 2-D separations were performed on the same SDS-PAGE. ^{14}C-labelled PM and extracted membrane from ^{3}H-labelled Ph (from the same batch of infected cells) were mixed and divided into two portions. One portion was subjected to 1-D separation and the other to 2-D separation as illustrated in Figure 2.6.

Figure 2.7 shows the comparison between Ph membrane and PM (from infected cells) profiles. The experiments to A and B are essentially the same with the exception that the phagosome membrane was extracted in B but not in A. The Ph membrane profile shows a depletion of glycoproteins over the MW range of about 210 – 150 kDa and an enrichment over the range of about 66 – 40 kDa as compared to the PM for both A and B. The same overall result was thus obtained for A and B, irrespective of membrane extraction. The consistency of the results can be seen in the duplicated experiments in Figure A5. The profiles show that the section between the enriched and depleted ranges (about 116 to 66 kDa) display minor differences between the Ph membrane and PM. Although there were small differences between duplicate experiments, the overall shape remained the same and the result of enrichment and depletion consistent.

2.5 Comparison of M.av-Ph to mLB-Ph

So far, comparisons were between Ph membrane and PM, as a next step, the PM was now substituted for a more relevant alternative, namely Ph containing latex beads with a hydrophobic character. The idea for the use of beads comes from earlier observations (de Chastellier and Thilo, 1997) where the intracellular fate of hydrophobic latex beads (LB) was compared to that of *M. avium*. It was observed that hydrophobic latex bead Ph (LB-Ph) behaved like eEn by not fusing with Ly because they were immature Ph. However, LB-Ph

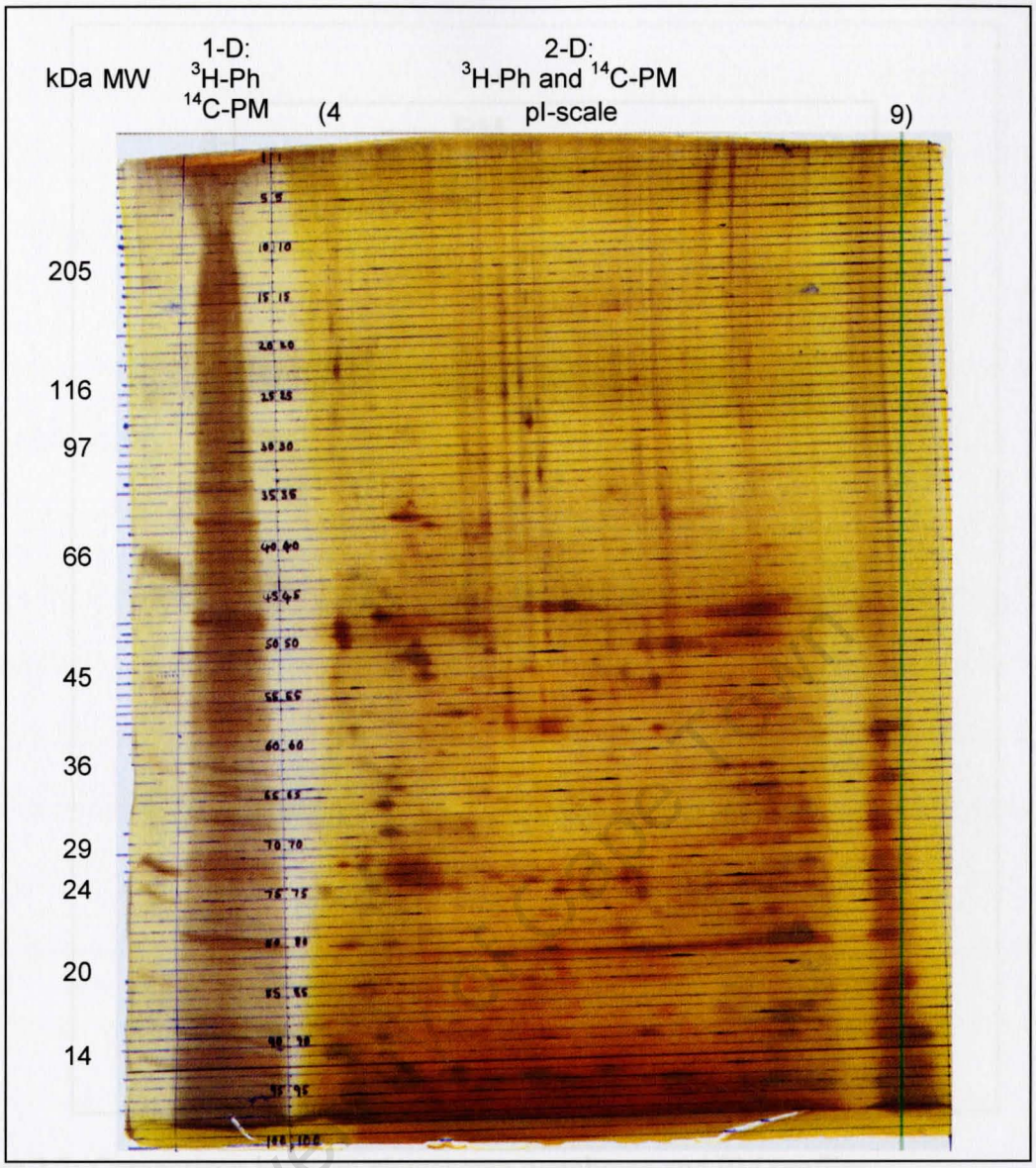

Figure 2.6: Silver-stained 2-D SDS-PAGE (comparing Ph membrane and PM) of which the 1-D lane was Oxidized BMDM that were infected with *M. avium* were divided into two groups. At 7 days p.i., one group of cells was labelled with ^{3}H-galactose and the label internalised for 2 h to label the Ph. The surface label was enzymatically removed. A PNS preparation was centrifuged on a 27% Percoll column and the Ph isolated as described. The phagosome membrane was separated from the mycobacteria according to a modified procedure from Sturgill-Koszycki et al (1997). Essentially, the Ph were treated with the membrane-specific detergent n-octyl β-$_{D}$-glucopyranoside and high salt concentrations to solubilise the phagosome membrane (as described in Methods). For PM, the other group of cells was labelled with ^{14}C-galactose and a PNS was prepared without further treatment. Both the phagosome and PM preparations were measured for radioactivity and mixed in equal radioactivity amounts. One part of the mixture was used for 2-D gel electrophoresis and another part of the mixture (for 1-D separation) was applied to the same polyacrylamide gel that was used for the second dimension electrophoresis. After staining and drying the SDS-PAGE, the 1-D lane was fractionated and each fraction was combusted in a Sample Oxidizer. Radioactive content of the fractions was determined. The results appear in Figure 2.7B.

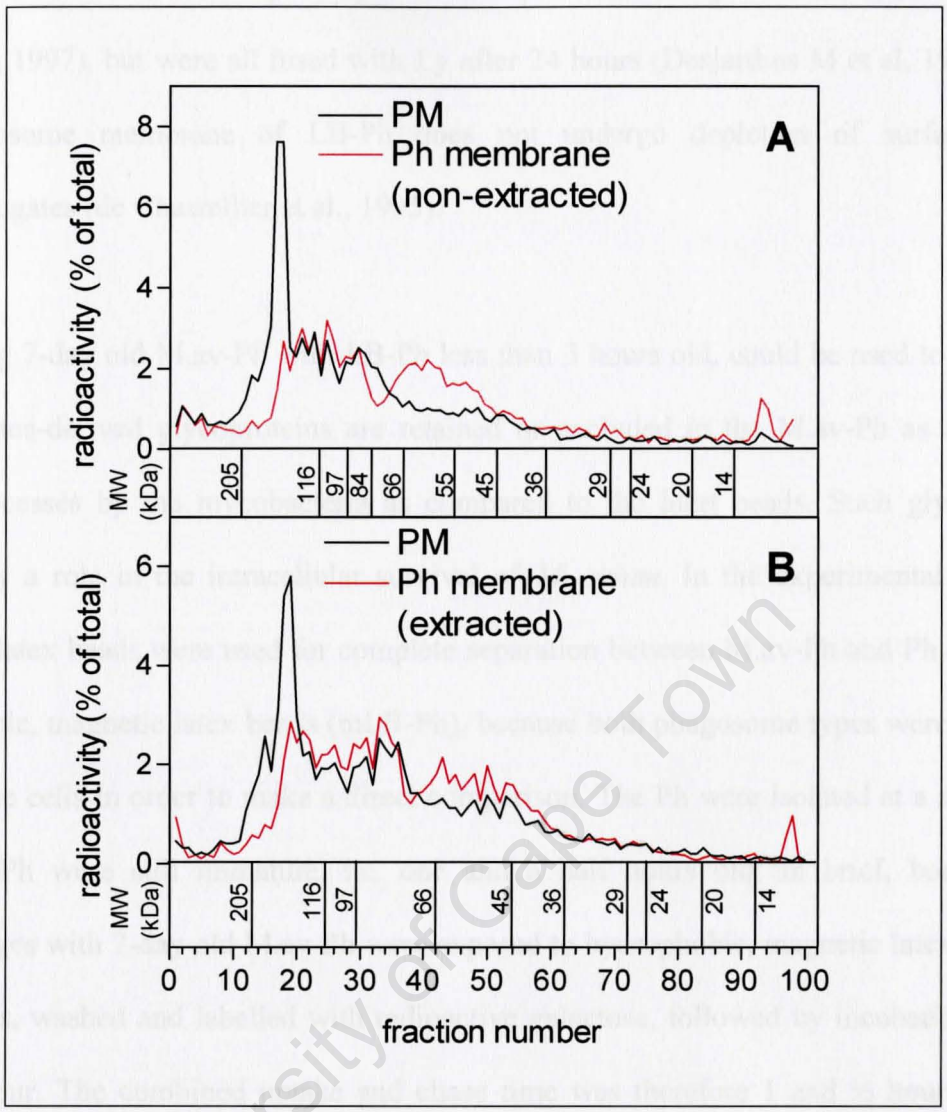

Figure 2.7: Comparison between phagosome membrane and PM profiles
A: BMDM were divided into two groups. One group was infected with *M. avium* and at 7 days p.i., the cells were labelled with ^{3}H-galactose and the label was internalised for 2 h. The surface-label was enzymatically removed. Ph were separated on a 27% Percoll gradient. For PM, infected cells were labelled with ^{14}C-galactose and a PNS was prepared without further treatment. Both the phagosome and PM preparations were measured for radioactivity, mixed in equal radioactivity amounts and subjected to an 8 to 15% SDS-PAGE. The SDS-PAGE was processed as before to determine the radioactive content of the lane fractions. **B:** The experiment was performed as described in Figure 2.6. For both A and B, the phagosome membrane profiles displayed enrichment in the 66 to 45 kDa range and depletion around the 205 kDa area as compared to the PM. There was good similarity between the profiles for extracted and non-extracted phagosome membrane (which supported the reliability of the membrane extraction).

could only avoid fusion with Ly for up to 3 hours (from the time points tested) (de Chastellier and Thilo, 1997), but were all fused with Ly after 24 hours (Desjardins M et al, 1994). Also, the phagosome membrane of LB-Ph does not undergo depletion of surface-derived glycoconjugates (de Chastellier et al., 1995).

Comparing 7-day old M.av-Ph with LB-Ph less than 3 hours old, could be used to determine what surface-derived glycoproteins are retained or excluded in the M.av-Ph as a result of active processes by the mycobacteria as compared to the inert beads. Such glycoproteins might play a role in the intracellular survival of *M. avium*. In the experimental approach, magnetic latex beads were used for complete separation between M.av-Ph and Ph containing hydrophobic, magnetic latex beads (mLB-Ph), because both phagosome types were generated in the same cells in order to make a direct comparison. The Ph were isolated at a stage when the mLB-Ph were still immature, i.e. one and a half hours old. In brief, bone-marrow macrophages with 7-day old M.av-Ph were exposed to hydrophobic, magnetic latex beads for 30 minutes, washed and labelled with radioactive galactose, followed by incubation at 37°C for one hour. The combined uptake and chase time was therefore 1 and ½ hours. At later stages (beyond 3 hours) the mLB-Ph would become matured and the advantage of the comparison lost.

As with the M.av-Ph that were evaluated by EM to see if they were immature, the mLB-Ph were subjected to the same analysis as shown in Figure 2.8. A total incubation time of only 1 and ½ hours was chosen to ensure that the mLB-Ph would be immature while the M.av-Ph were seven days old. Panel A of Figure 2.8 shows a macrophage containing both M.av-Ph and mLB-Ph. Most Ph contained a single mLB or *M. avium* and no lysosomal material was present. The enlarged view of a mLB-Ph, Panel B, clearly shows an all-around closely

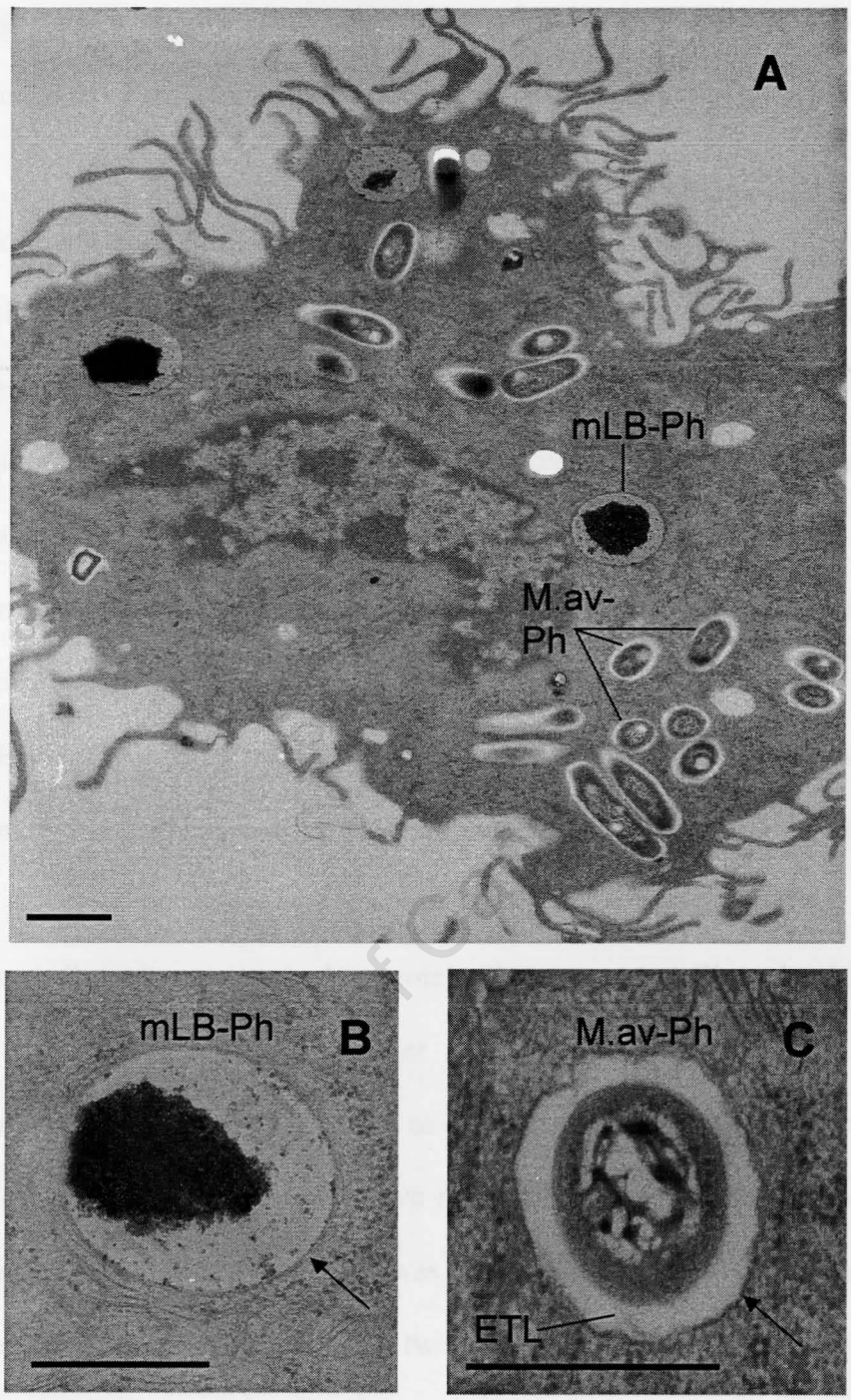

Figure 2.8: Electron micrographs showing infection with both hydrophobic mLB and *M. avium* BMDM were infected with *M. avium* and at 7 days p.i., the cells were exposed to mLB for 30 minutes and chased for one hour (as described in Methods). The cells were fixed and processed for EM (as described). **A**: General view of a macrophage with both mLB-Ph and M.av-Ph. **B**: An enlarged view of a mLB-Ph for which an all-around closely apposing phagosome membrane can be seen (arrow, also for C). **C:** An enlarged M.av-Ph. Mycobacteria's ETL (**C**) is a distinguishing characteristic between the two types of Ph. The bar is 1 μm in **A** and 0.5 μm in **B** and **C**. The hydrophobic mLB-Ph, like the M.av-Ph, were immature Ph.

apposing phagosome membrane, indicated by the arrow. These observations show that both M.av-Ph and mLB-Ph were immature Ph in the same cells.

Figure 2.9 shows enriched Ph as they were collected in the final step just before membrane extraction took place. This showed that intact Ph were isolated at the end of the phagosome purification procedure. Ly can be seen with the M.av-Ph in Figure 2.9A. To lessen the luminal lysosome proteins in the phagosome sample, the sample was sonicated after phagosome isolation but before membrane extraction. Sonication was not performed on earlier experiments that compared the phagosome membrane to PM because the presence of lysosomal proteins was not viewed as a potential problem for PAGE analysis at that time. Enriched mLB-Ph (Figure 2.9B) did not have the problem of lysosomal contamination. For both phagosome types the phagosome membrane can be seen for many of the Ph.

For comparing cell surface-derived glycoproteins between M.av-Ph and mLB-Ph, BMDM containing 7-day old M.av-Ph were further infected with mLB, followed by labelling, isolation of the Ph and membrane extraction as described. However, membrane extraction for mLB-Ph could not remove all the radioactive membrane from the mLB as shown in Figure A6. The remaining membrane on the mLB was removed by boiling the beads in SDS sample buffer. The reason for dividing the cells into two groups was to have both types of Ph labelled with either of the two isotopes (^{3}H and ^{14}C), making it possible to compare M.av-Ph directly with mLB-Ph by mixing and applying the extracted membrane with alternative label on the same PAGE lane (as was done for the comparison between PM and phagosome membrane).

The SDS-PAGE in Figure 2.10 was prepared as a 1-D only PAGE because 2-D PAGE analysis turned out to be problematic, as explained in the following section. Although several prominent bands are showing for the SDS-PAGE in Figure 2.10, they do not necessarily

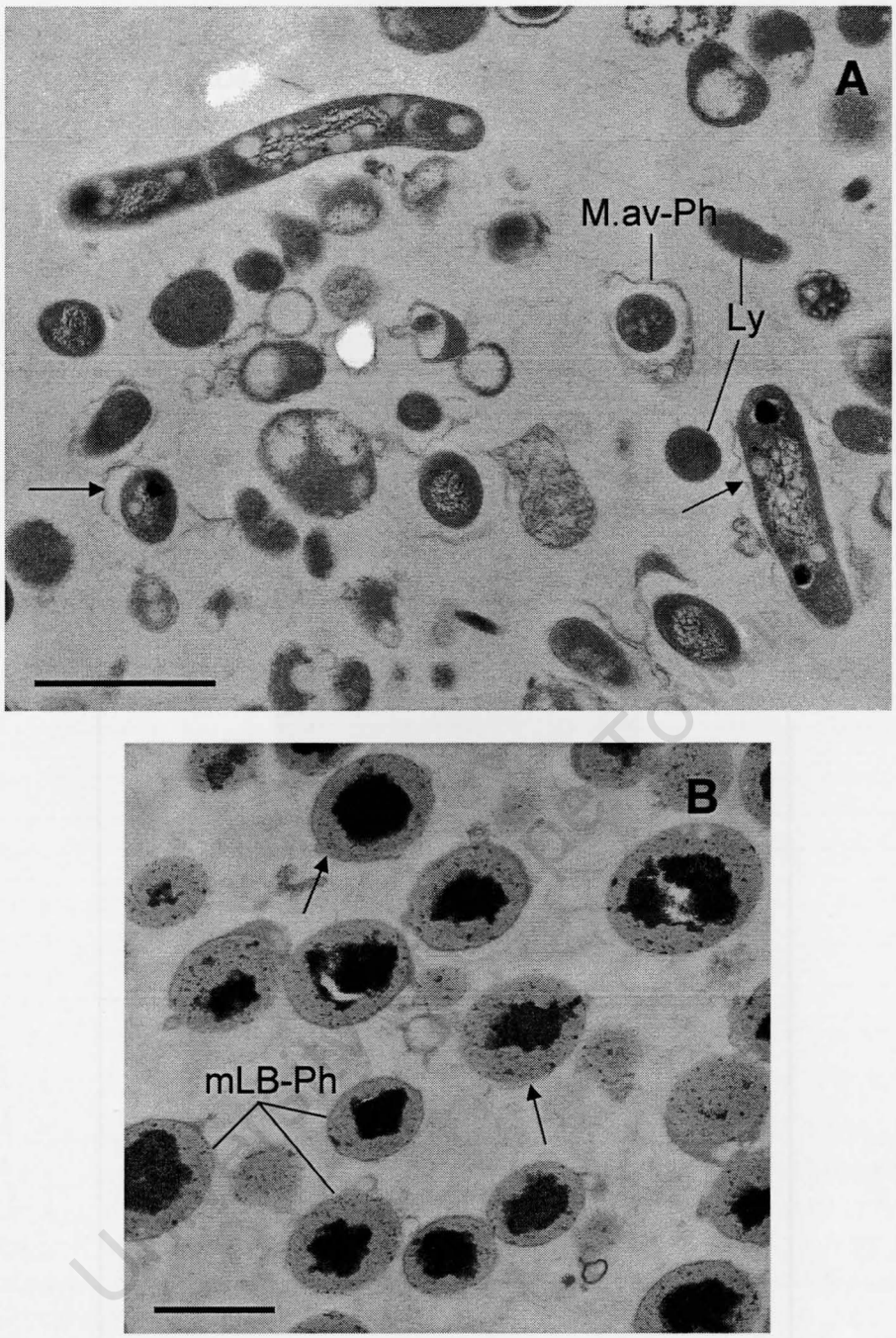

Figure 2.9: Electron micrographs showing isolated M.av-Ph and mLB-Ph
BMDM were infected with *M. avium*. At 7 days p.i., the cells were exposed to hydrophobic mLB for 30 minutes and chased for 1 h (as described). The cells were scraped and a homogenate was prepared. The mLB-Ph were first separated magnetically from the homogenate before a PNS was prepared and centrifuged on a 27% Percoll column. The M.av-Ph were isolated from the Percoll gradient. The mLB-Ph were washed three times with buffer. Both phagosome types were pelleted and the resultant pellets were fixed and processed for EM (as described). **A**: Enriched M.av-Ph with Ly present as a contaminant. **B**: Enriched mLB-Ph. The arrows indicate the phagosome membrane. Bars = 1 μm. After all the treatments that the Ph went through, most of them still had intact or discernable membrane before membrane extraction took place.

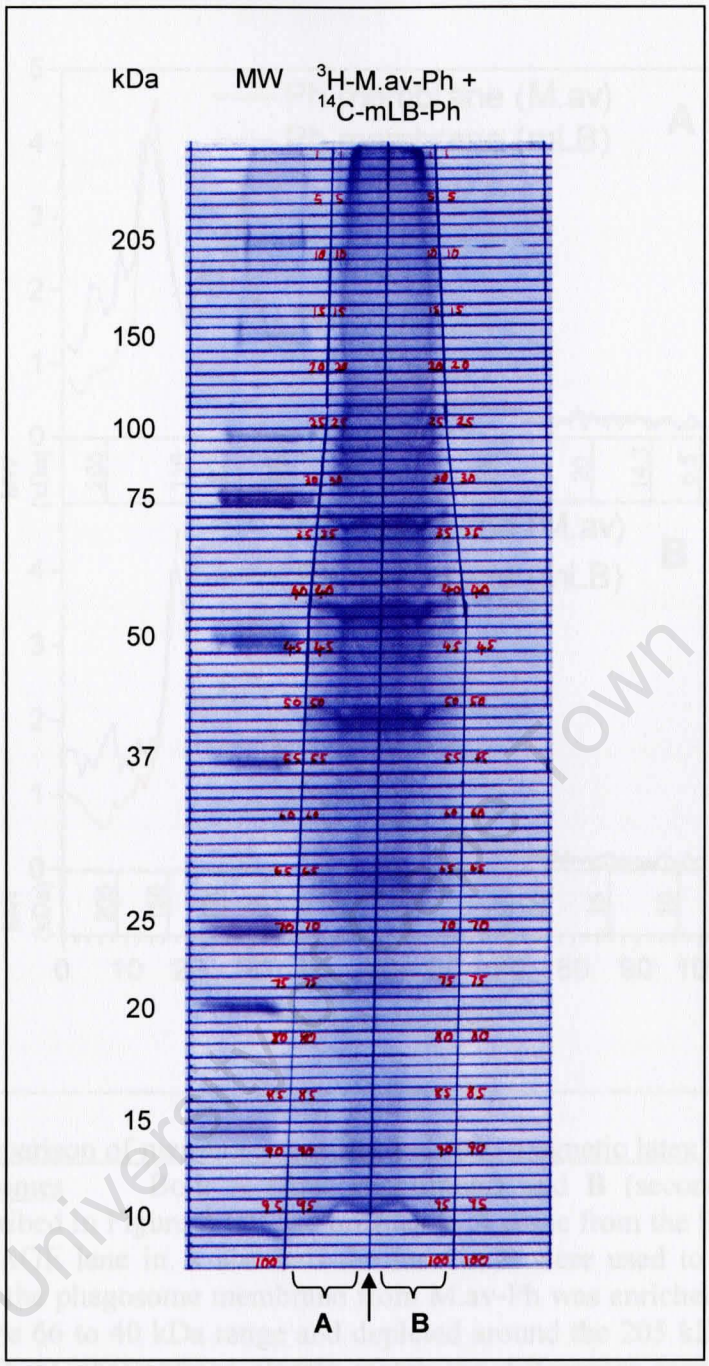

Figure 2.10: Coomassie-stained 1-D SDS-PAGE showing bands for Ph membrane from M.av-Ph and mLB-Ph BMDM were infected with *M. avium* and at 7 days p.i. were exposed for 30 minutes to hydrophobic mLB. Half the cells were labelled with ^{3}H-galactose and half with ^{14}C-galactose. The label was internalised for 1 h and uninternalised label removed. Separate homogenates were prepared from the two groups of cells and the mLB-Ph were first separated magnetically from the homogenates before PNS preparations were made (as described in Methods). The PNS preparations were centrifuged on 27% Percoll columns and the M.av-Ph isolated. Membrane extraction was performed on the mLB-Ph and M.av-Ph. The radioactivity of the phagosome membranes was determined. For this PAGE ^{14}C-phagosome membrane from mLB-Ph was mixed with ^{3}H-phagosome membrane from M.av-Ph in a ratio of 3 to 1 (^{3}H to ^{14}C, as explained in the text) and subjected to 1-D SDS-PAGE, using a gradient gel of 8 to 15% acrylamide (as described in Methods). The total lane was divided into two halves, A and B, as indicated by the line (arrow). One half was used to produce the labelling profiles (appearing in Figure 2.11B) and the other half kept for protein identification. The fraction numbers are indicated in red and represent 2.5 mm sections down the lane.

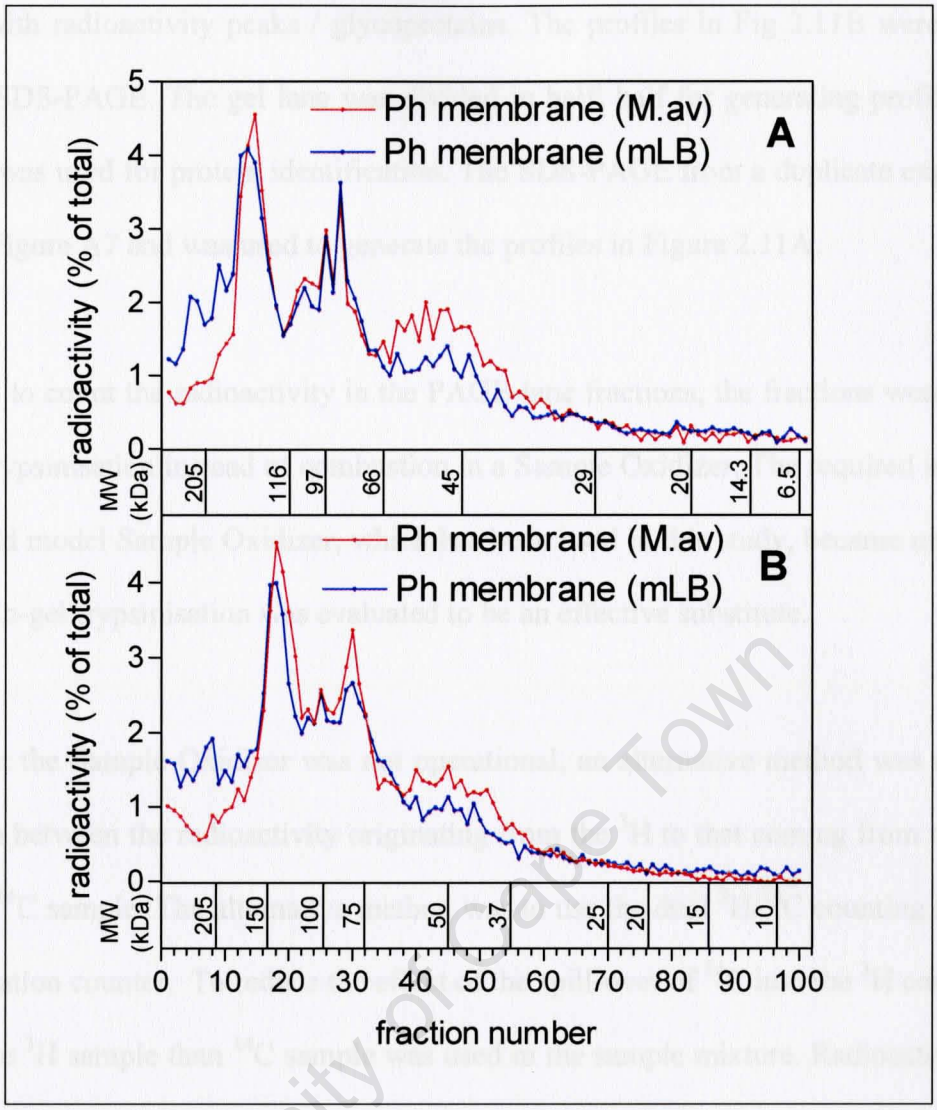

Figure 2.11: Comparison of membrane profiles between magnetic latex bead- and *M. avium*-containing phagosomes Both **A** (first experiment) and **B** (second experiment) were performed as described in Figure 2.10. The profiles in **A** come from the SDS-PAGE in Figure A7. The whole PAGE lane in **A** and half the lane in **B** were used to create profiles. The profiles show that the phagosome membrane from M.av-Ph was enriched for surface-derived glycoproteins in the 66 to 40 kDa range and depleted around the 205 kDa area, as compared to the mLB-Ph. These observations closely match the differences seen for the comparison between M.av-Ph and PM.

coincide with radioactivity peaks / glycoproteins. The profiles in Fig 2.11B were generated from this SDS-PAGE. The gel lane was divided in half: half for generating profiles and the other half was used for protein identification. The SDS-PAGE from a duplicate experiment is shown in Figure A7 and was used to generate the profiles in Figure 2.11A.

To be able to count the radioactivity in the PAGE-lane fractions, the fractions were subjected to in-gel trypsinisation instead of combustion in a Sample Oxidizer. The required servicing of the very old model Sample Oxidizer, which has been used in this study, became unfeasible to maintain. In-gel trypsinisation was evaluated to be an effective substitute.

Seeing that the Sample Oxidizer was not operational, an alternative method was required to distinguish between the radioactivity originating from the ^{3}H to that coming from the ^{14}C in a mixed $^{3}H/^{14}C$ sample. The alternative method was to use the dual $^{3}H/^{14}C$ counting function of the scintillation counter. To reduce the effect of the spill-over of ^{14}C into the ^{3}H count, about 3 fold more ^{3}H sample than ^{14}C sample was used in the sample mixture. Radioactivity counts were normalised as shown.

Figure 2.11 compares the profiles for the membrane of M.av-Ph against that for mLB-Ph. The experiments to A (first experiment) and B (second experiment) were done in the same way with the exception that only half of the total PAGE lane was used in B to produce the profiles. Good reproducibility is seen between the two experiments A and B. The M.av-Ph membrane profile shows an enrichment over the MW range of about 66 – 40 kDa and a depletion over about 150 – 350 kDa (as estimated from a MW migration distance) as compared to the mLB-Ph membrane in both A and B. The section between the enriched and depleted ranges that stretches from 150 to 66 kDa matches very closely between the M.av-Ph and the mLB-Ph membrane profiles. Therefore, apart from the 'depleted range' that covers a larger range as

compared to the comparison between Ph and PM (Figure 2.7), the comparison between M.av-Ph and mLB-Ph membrane profiles gave the same overall result to the comparison between M.av-Ph and the PM. This makes the enriched and depleted proteins still the most interesting result and therefore the focus of attention. The results of the protein identification appear in Chapter 3.

2.6 Two-dimensional gel electrophoresis

The purpose of the 2-D electrophoresis was to link individual surface-derived glycoproteins in Mav-Ph to a condition of enrichment or depletion (as guided by the observations from the 1-D PAGE results) and hence identify those proteins.

Autoradiography was intended to confirm and indicate in which areas on the 2-D PAGE the surface-derived glycoproteins were located in order to select protein spots for identification. Autoradiography turned out to be less effective than using the Oxidizer and will therefore be referred to briefly.

In initial experiments, about 6 000 dpm of radioactive sample was used for 2-D SDS-PAGE. Figures A8.1 to A9.2 show the PAGEs and autoradiographs. No signal could be detected and the most likely reason was thought to be too little radioactivity on the PAGEs. Increases in the amount of radioactive membrane used for 2-D electrophoresis were tested, of which the maximum (50 000 dpm on an IPG strip and also on a 1-D lane) was prepared from P388D_1 macrophages. The PAGE and autoradiograph are shown in Figures A10.1 and A10.2. The observed improvement for what was considered the maximum obtainable yield of radioactive membrane for an experiment was too meagre for this approach to be feasible. This showed

that autoradiography with the Phosphor Imager was not the method to follow to analyse the 2-D PAGEs.

In a separate experiment, a 2-D PAGE, incorporating 1-D separation, was analysed through autoradioagraphy and by Oxidizing gel fractions. A total of 10 000 dpm was applied to the 1-D lane and 30 000 dpm to the IPG strip. The PAGE appears in Figure 2.12A and the autoradiograph in Figure 2.12B. The exposure time for autoradiography was for 7 days and apart from the MW markers and two bands between 205 and 116 kDa no other spots or bands could be seen. From previous profiles, the focus was placed on the enriched surface-derived glycoproteins in M.av-Ph, occurring in the MW region of about 66 to 40 kDa (Figure 2.7). Therefore, the 2-D region corresponding to this MW region (the selected 2-D area), shown in Figure 2.12C, was subsequently Oxidized. Due to the larger surface area of the selected 2-D section and because of cost implications (due to the special scintillation liquids used by the Sample Oxidizer) it was decided to use the combined height of two 1-D fractions, meaning a height of 5 mm and width of 1 cm as the size for the gel fractions as illustrated by the grid in Figure 2.12C. Any specific area of interest could always be fractionated more (cut into smaller pieces) for a subsequent PAGE. Another solution could also be to use IPG strips of a narrow pH range that separate the proteins in that range much further apart. The PAGE fractions were combusted in a Sample Oxidizer (which was still in use at the time) as before followed by scintillation counting. For the best view of the radioactivity peaks, the data was plotted as three-dimensional (3-D) views.

Figure 2.12D shows the 3-D view of the profiles for the Ph and PM. The data was plotted in dpm after the background was subtracted. This figure shows that the method of combusting the samples was much more sensitive and therefore better than using the Phosphor Imager. An important advantage was that the combustion method also worked for ^{3}H samples, which

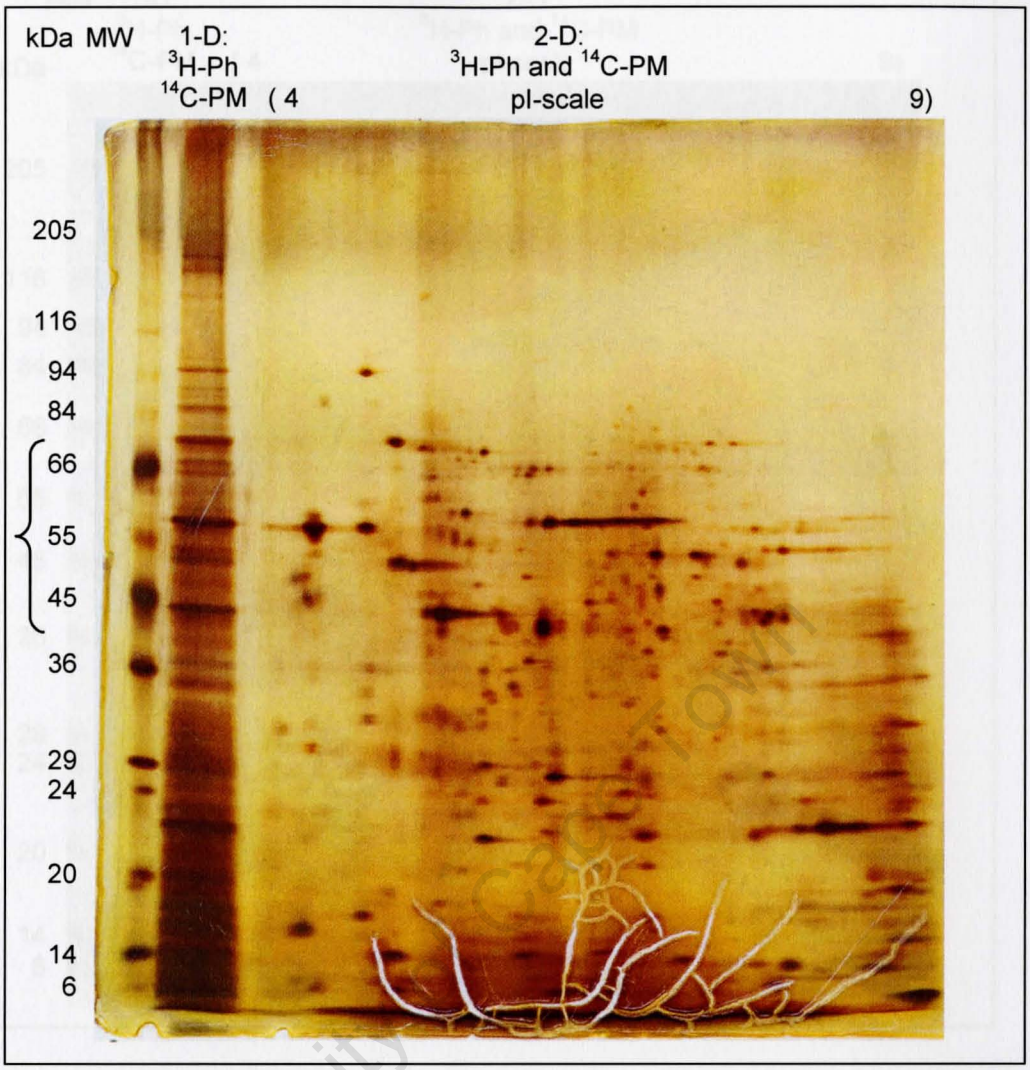

Figure 2.12A: Silver-stained 2-D SDS-PAGE with Ph membrane and PM
BMDM that were infected with *M. avium* were divided into two groups. At 7 days p.i., one group of cells was labelled with ^{3}H-galactose and the label internalised for 2 h. The surface label was enzymatically removed. A PNS preparation was centrifuged on a 27% Percoll column and the Ph isolated. For PM, the other group of cells was labelled with ^{14}C-galactose and a PNS was prepared. Both the phagosome and PM preparations were measured for radioactivity and mixed in equal radioactivity amounts. One part of the mixture was used for 2-D gel electrophoresis and the other part for 1-D separation, using the same SDS-PAGE (as described). A total amount of 30 000 dpm in radioactive membrane was applied to the IPG strip and 10 000dpm on the 1-D lane. The SDS-PAGE was stained, dried and developed on a Phosphor Imager (as described). The autoradiograph is shown in Figure 2.12B. Afterwards, a selected section of the 2-D area, indicated by the bracket and shown in Figure 2.12C, was fractionated and combusted in a Sample Oxidizer. Radioactive content of the fractions was determined. The resulting profiles appear in Figure 2.12D.

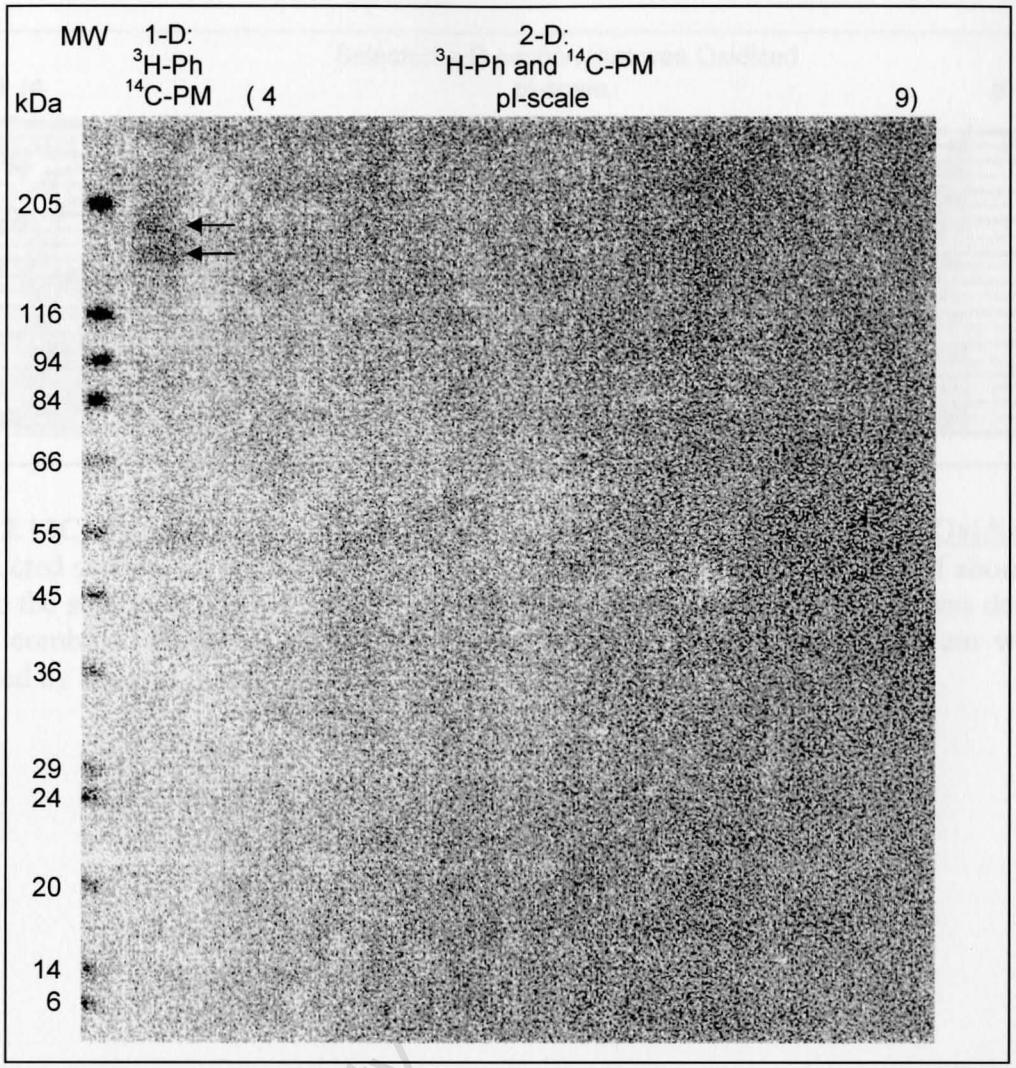

Figure 2.12B: Autoradiograph of the 2-D SDS-PAGE in Figure 2.12A
The PAGE was on the Phosphor Imager for a week. Other than the MW markers, two bands (arrows) developed from the 1-D lane. No bands developed from the 2-D area of the PAGE. In this case a higher concentration of radioactivity was used and therefore expected to show bands or spots in the 2-D area. The reason for not seeing bands could have been due to the amount of radioactivity being still too low for detection on the Phosphor Imager. (A section of this PAGE was measured using the Sample Oxidizer.)

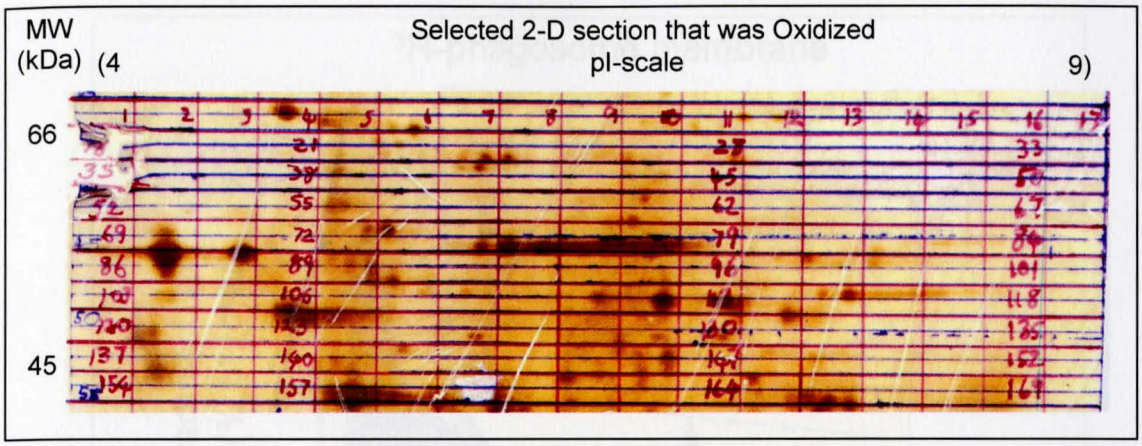

Figure 2.12C: Selected section of the 2-D PAGE (from Figure 2.12A) that was Oxidized
The selected section covers a MW range of about 66 to 40 kDa and a pI range of about 4 to 9. Because the selected 2-D area covered a larger surface area than a 1-D lane, it was decided to use the combined height of two 1-D fractions, meaning 5 mm height and 1 cm width (as illustrated by the grid in red). The red numbering indicates the fraction numbers.

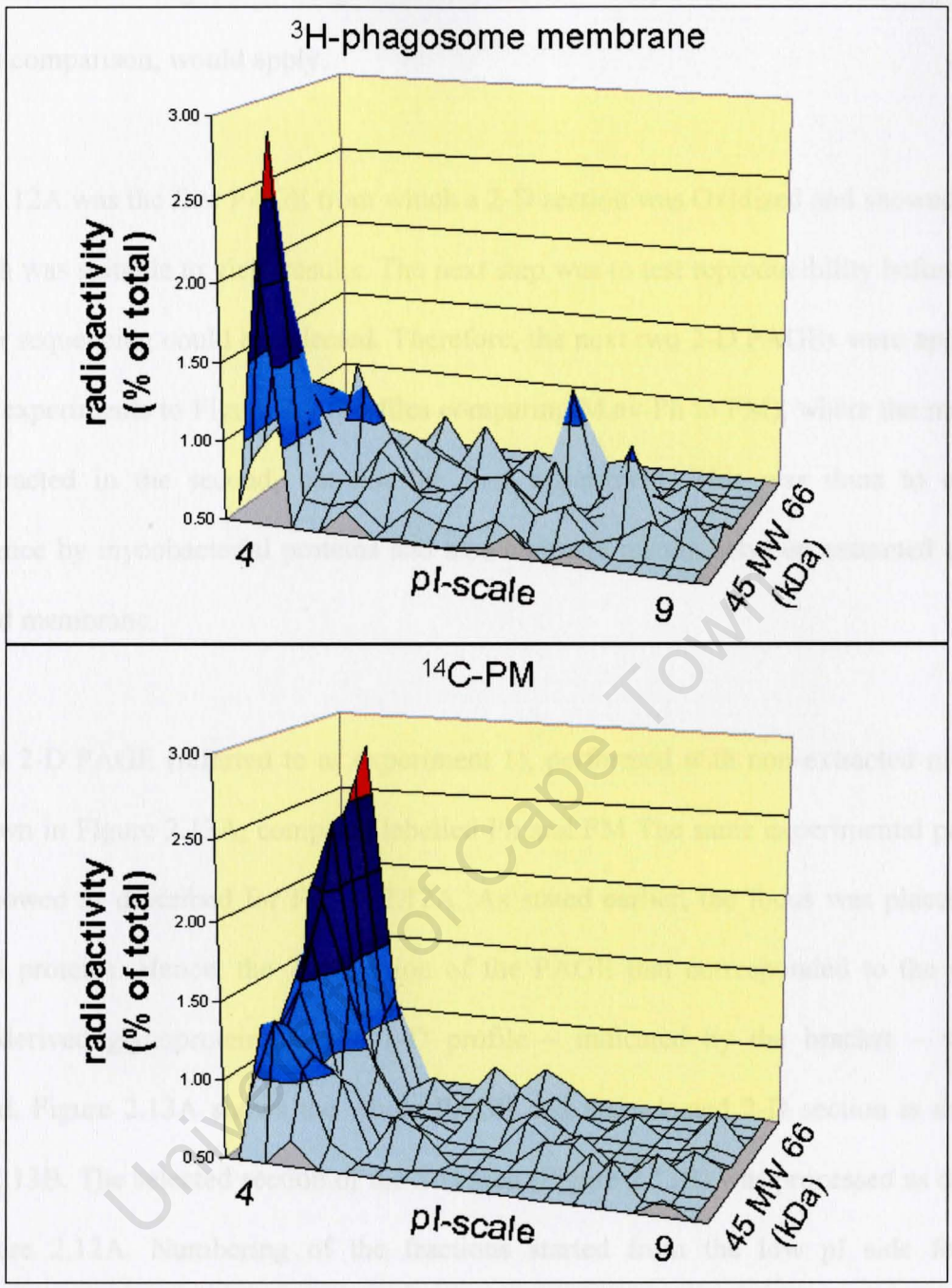

Figure 2.12D: 3-D view of the profiles for phagosome membrane and PM from Figure 2.12C Well-defined peaks were obtained from using the Sample Oxidizer method. All of the highest peaks and therefore the strongest labelled or most abundant radioactive glycoproteins in the selected region had a low pI value.

meant that the advantages of mixing differently labelled samples in order to have a direct and accurate comparison, would apply.

Figure 2.12A was the first PAGE from which a 2-D section was Oxidized and showed that the approach was suitable to yield results. The next step was to test reproducibility before protein spots for sequencing could be selected. Therefore, the next two 2-D PAGEs were approached like the experiments to Figure 2.7 (profiles comparing M.av-Ph to PM), where the membrane was extracted in the second, but not the first experiment. This was done to eliminate interference by mycobacterial proteins and also compare results between extracted and non-extracted membrane.

The first 2-D PAGE (referred to as experiment 1), performed with non-extracted membrane and shown in Figure 2.13A, compares labelled Ph and PM The same experimental procedure was followed as described for Figure 2.12A. As stated earlier, the focus was placed on the enriched proteins. Hence, the 2-D section of the PAGE that corresponded to the enriched surface-derived glycoproteins in the 1-D profile – indicated by the bracket – was also Oxidized. Figure 2.13A shows the whole PAGE and the selected 2-D section is shown by Figure 2.13B. The selected section of the 2-D area (Figure 2.13B) was processed as described for Figure 2.12A. Numbering of the fractions started from the low pI side for easier comparison to other 2-D PAGEs. Most of the visibly stained proteins were on the low pI side of the selected area.

For the second experiment the whole PAGE is shown in Figure 2.14A and its selected 2-D section in Figure 2.14B. In this case the phagosome membrane was extracted. Fewer proteins can be observed on the gel as compared to Figure 2.13A. This was to be expected in view of the exclusion of the mycobacterial proteins. The staining resulted in an unusually dark

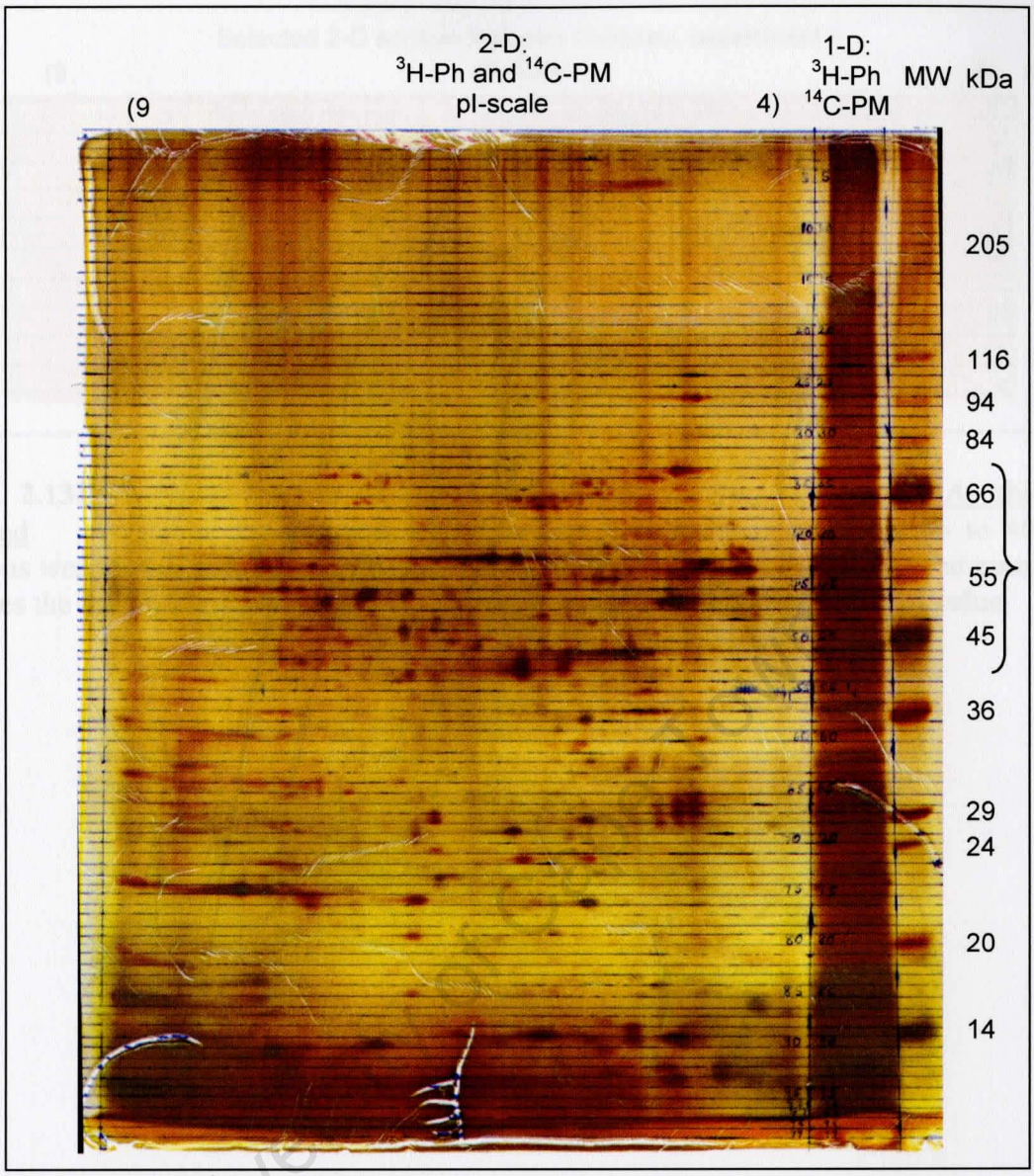

Figure 2.13A: Whole silver-stained 2-D SDS-PAGE of which a section of the 2-D area was Oxidized BMDM that were infected with *M. avium* were divided into two groups. At 7 days p.i., one group of cells was labelled with ^{3}H-galactose and the label internalised for 2 h. Remaining surface label was enzymatically removed. A PNS was prepared and the Ph isolated from a 27% Percoll gradient. For PM, the other group of cells was labelled with ^{14}C-galactose and a PNS was prepared. Both the phagosome and PM preparations were measured for radioactivity and mixed in equal radioactivity amounts. One part of the mixture was used for 2-D gel electrophoresis and the other part for 1-D separation, using the same SDS-PAGE. The SDS-PAGE was stained and dried. A selected section of the 2-D area (shown in Figure 2.13B), based on the 1-D profile (Figure 2.7A) and indicated by the bracket, was fractionated and fractions were combusted in a Sample Oxidizer. Radioactive content of the fractions was determined.

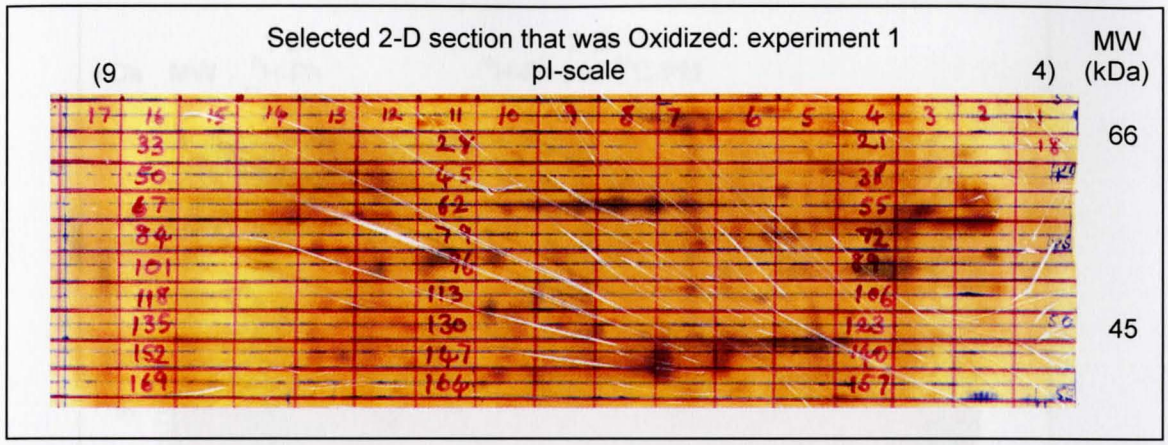

Figure 2.13B: Selected section of the 2-D SDS-PAGE (from Figure 2.13A) that was Oxidized As stated, the selected section covers a MW range of about 66 to 40 kDa. Fractions were 5 mm in height and 1 cm wide as shown by the grid in red. The red numbering indicates the fraction numbers. Most of the visibly stained proteins had a low pI value.

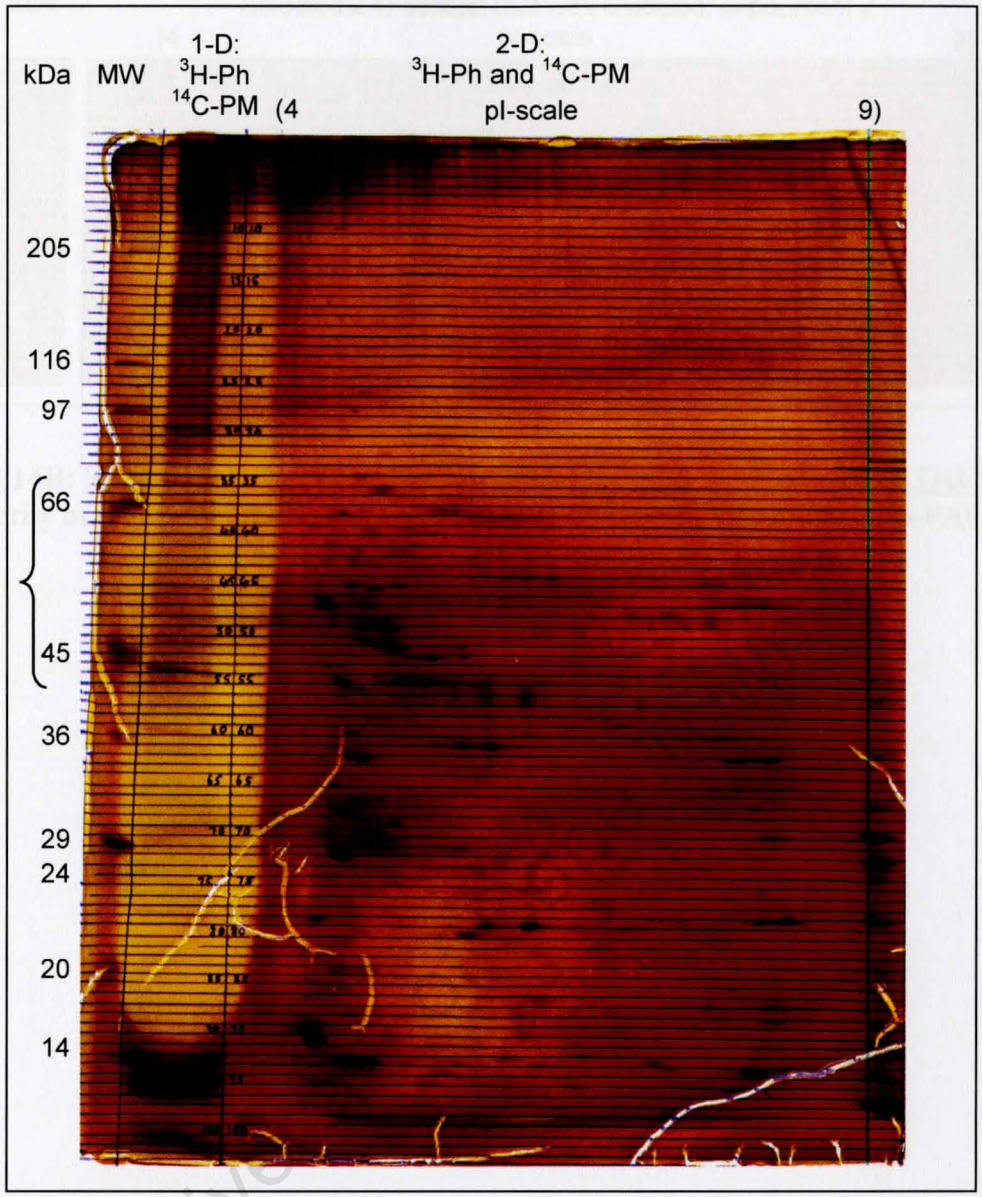

Figure 2.14A: Whole silver-stained 2-D SDS-PAGE of which a section of the 2-D area was Oxidized: reproduced experiment to Figure 2.13A In this case the phagosome membrane was extracted (separated from the mycobacteria, as described). The selected section that was combusted in a Sample Oxidizer is indicated by the bracket and shown in Figure 2.14B. The 1-D profiles appear in Figure A5B. There are less visible proteins on this PAGE. The staining resulted in an uneven and dark background which possibly obscured some proteins from being visualised.

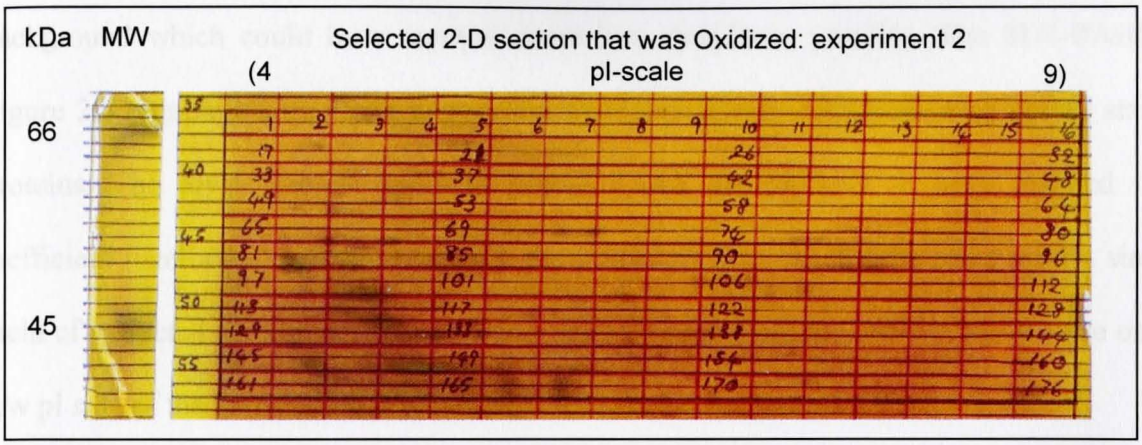

Figure 2.14B: Selected section of the 2-D PAGE (from Figure 2.14A) that was Oxidized
The majority of the visibly stained proteins were on the low pH side of the SDS-PAGE.

background which could have masked some low abundance proteins. The SDS-PAGE in Figure 2.6 (which is a duplicate experiment to Figure 2.14A) displayed more visibly stained proteins. The fewer protein spots in Figure 2.14A are unlikely to have resulted from inefficient membrane extraction because the procedure was exactly the same with a similar yield of extracted membrane. Again, as in Figure 2.6, more of the visible proteins were on the low pI side of the PAGE.

Radioactivity profiles for the selected 2-D sections were constructed as described and presented as 3-D views in Figures 2.15A and 2.15B. For comparison, profiles for the Ph membrane from Figures 2.13B (first experiment) and 2.14B (second experiment) have been grouped. The same was done for the PM profiles. The highest peaks (indicating either more abundant or more highly glycosylated glycoproteins) were from proteins on the low pI side of the PAGE. Both for the phagosome membrane and for the PM the two profiles were different. This showed that the reproducibility was poor. Although the similarities for the PM profiles were better than for the Ph membrane profiles, the results were not convincing with respect to reproducibility. A different view of the radioactivity peaks to better illustrate the differences and similarities between the profiles for the selected 2-D section is shown in Figure A11. These views clearly show the reproducibility problem that was encountered.

Because the 2-D electrophoresis approach was very important, the possible cause for the poor reproducibility was investigated. From the literature it seems that poor solubility of the proteins and their transfer from the first to the second dimension are the most frequently encountered problems that relate to poor reproducibility (Molloy, 2000). One sign of poor solubility would have been precipitation of the samples, but this was not observed. It was therefore decided to find out how well protein was transferred from the first to the second dimension.

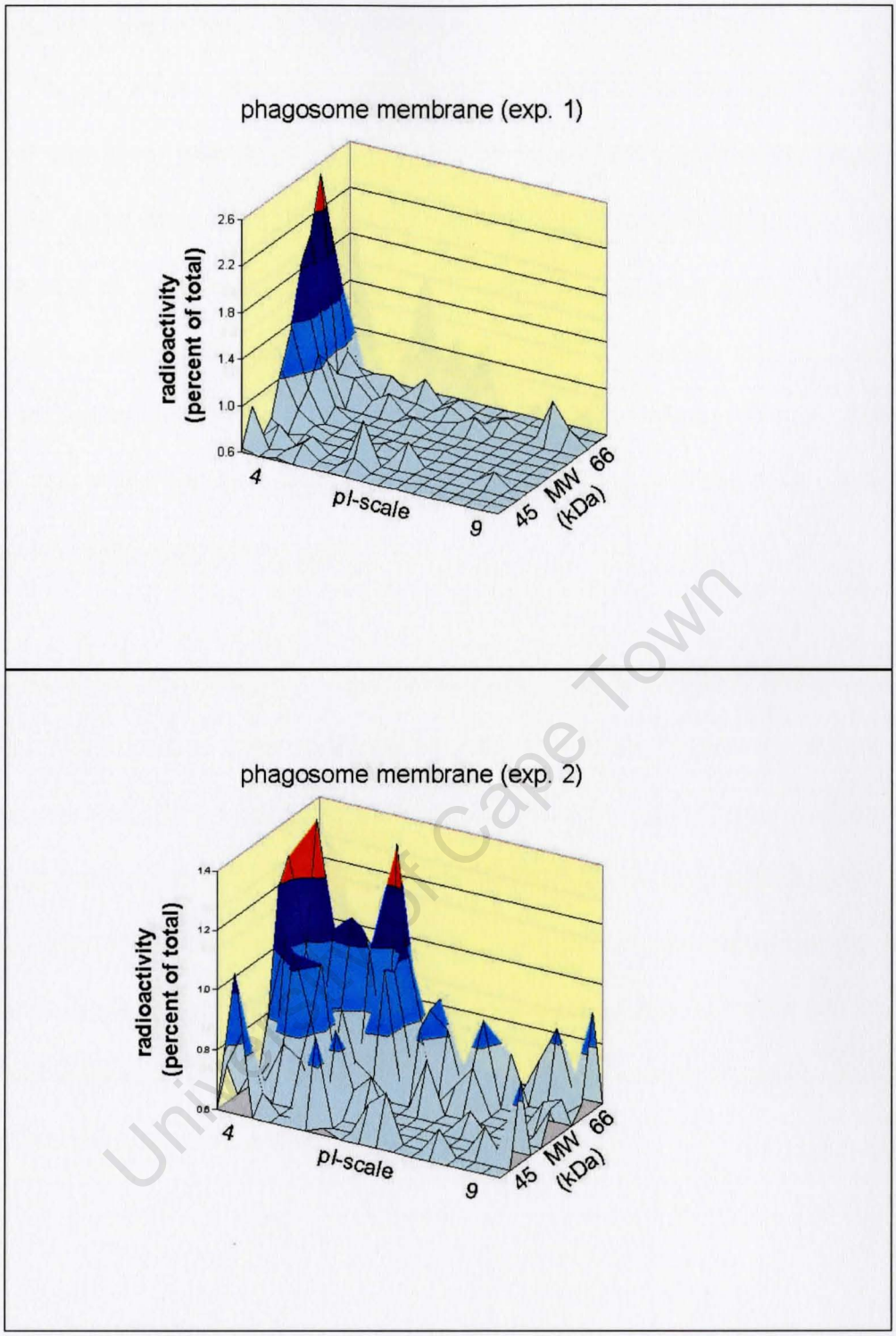

Figure 2.15A: Comparison between the profiles of phagosome membrane from the selected 2-D sections in Figures 2.13B and 2.14B (Only in experiment 2 the phagosome membrane was extracted.) Most of the strongly labelled radioactive proteins had a low pI value. More differences than similarities were observed between the two experiments.

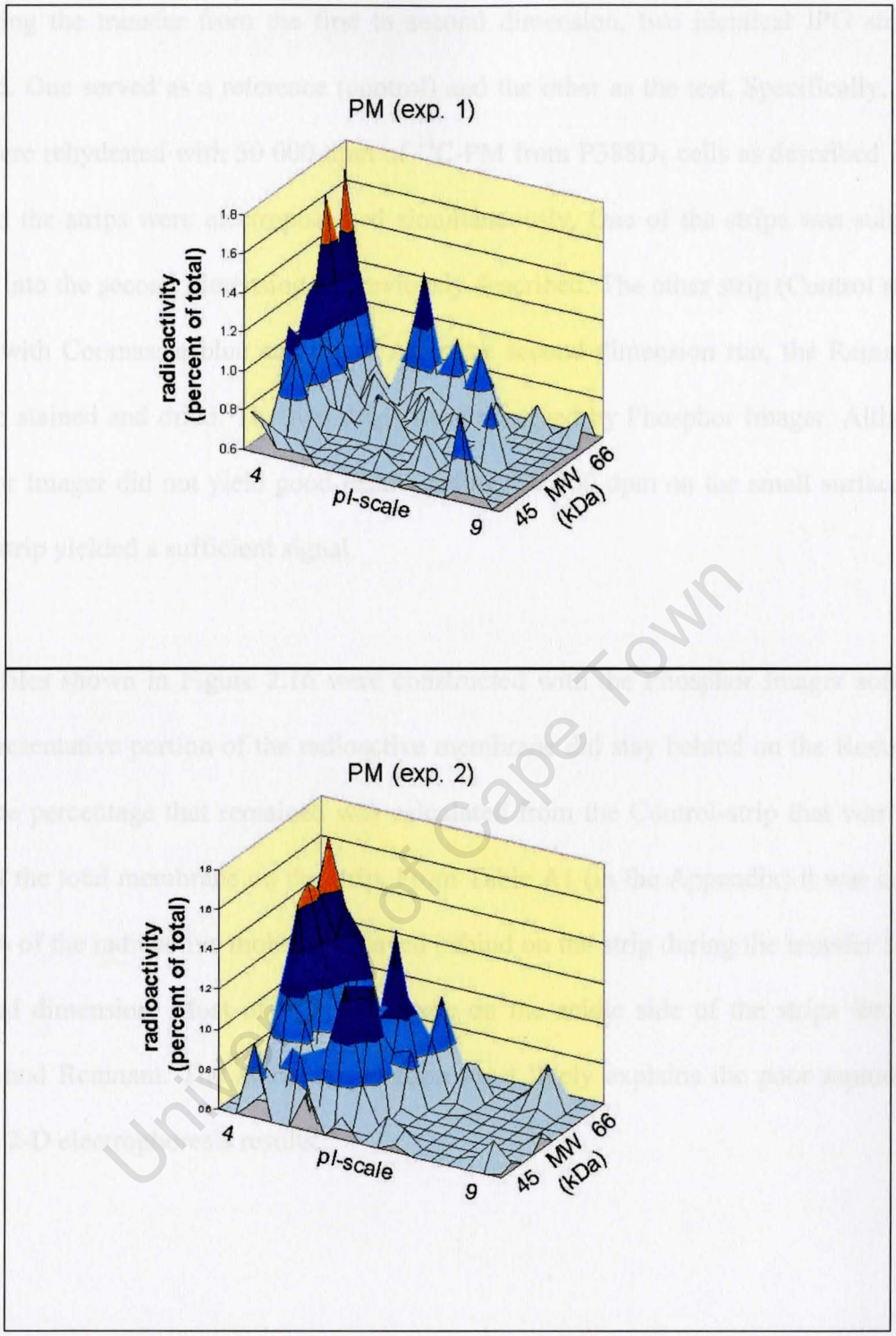

Figure 2.15B: Comparison between the profiles of PM from the selected 2-D sections in Figures 2.13B and 2.14B Also here, the strongly labelled proteins had a low pI value. Overall, the reproducibility was too poor for the 2-D SDS-PAGEs to be used successfully.

For testing the transfer from the first to second dimension, two identical IPG strips were prepared. One served as a reference (control) and the other as the test. Specifically, two IPG strips were rehydrated with 50 000 dpm of ^{14}C-PM from P388D$_1$ cells as described in Figure 2.16 and the strips were electrophoresed simultaneously. One of the strips was subjected to transfer into the second dimension as previously described. The other strip (Control strip) was stained with Coomassie blue and dried. After the second dimension run, the Remnant strip was also stained and dried. The two strips were observed by Phosphor Imager. Although the Phosphor Imager did not yield good results before, 50 000 dpm on the small surface area of an IPG strip yielded a sufficient signal.

The profiles shown in Figure 2.16 were constructed with the Phosphor Imager software. A non-representative portion of the radioactive membrane did stay behind on the Remnant IPG strip. The percentage that remained was calculated from the Control-strip that was taken as 100% of the total membrane on the strip. From Table A1 (in the Appendix) it was calculated that 35% of the radioactive molecules stayed behind on the strip during the transfer from first to second dimension. Most of the peaks were on the acidic side of the strips for both the Control and Remnant. The above observation most likely explains the poor reproducibility with the 2-D electrophoresis results.

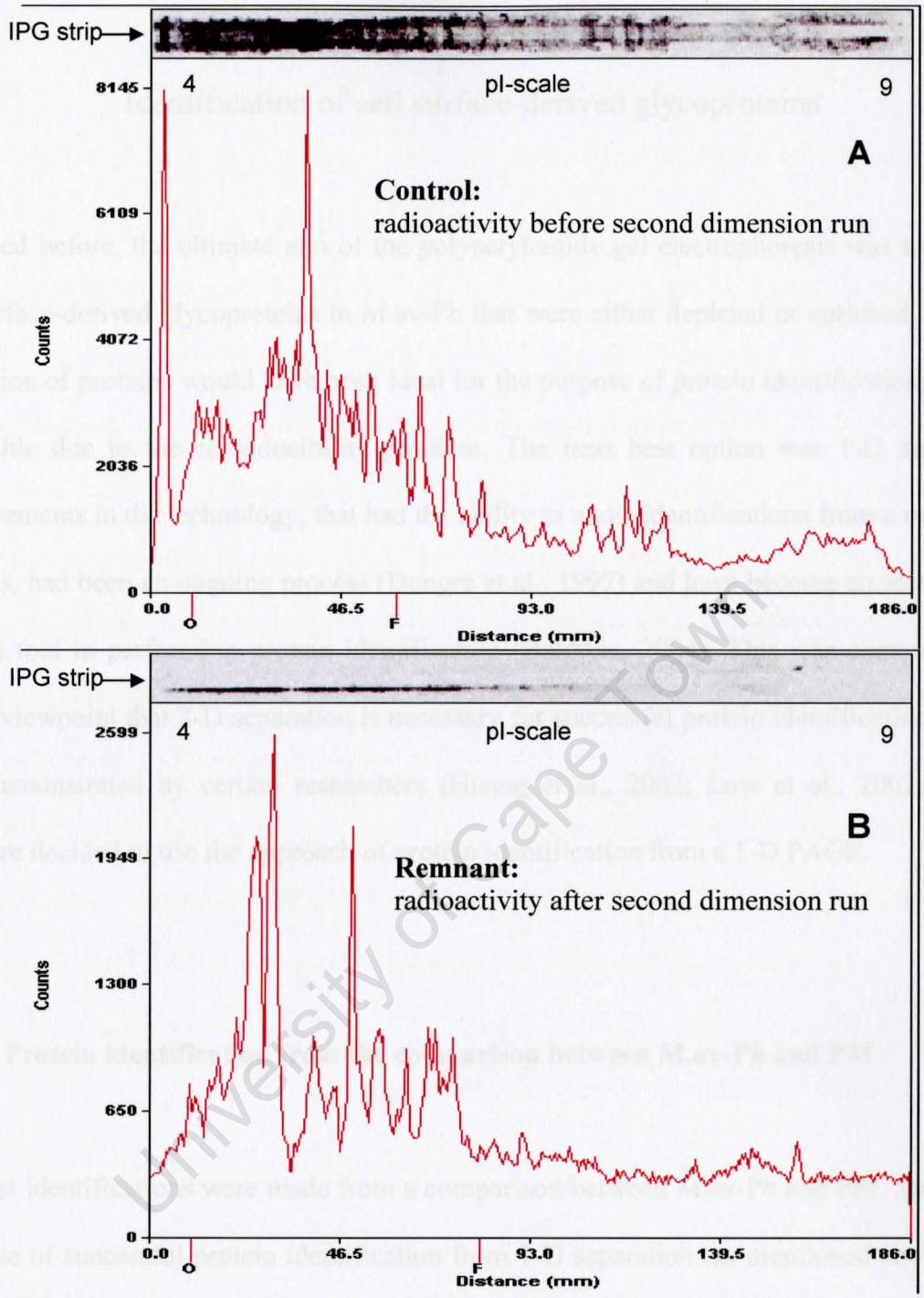

Figure 2.16: Phosphor Imager profiles of IPG strips comparing the amount of radioactivity before and after second dimension electrophoresis Two IPG strips were hydrated with the same amount (in radioactivity) of ^{14}C-PM from P388D$_1$ macrophages. After isoelectric focusing was performed, the ends were trimmed off (as described in Methods) and the one strip, **A** (serving as the control: the amount of radioactive protein present before the second dimension run), was immediately treated with protein fixing solution while the other strip, **B** (serving as the remnant: the amount of radioactive protein left after the second dimension run), was applied to a SDS-PAGE for the second dimension run before it too was treated with protein fixing solution. The IPG strips were stained, dried and exposed on a Phosphor Imager. (Note: the true length of the strip (x-axis) was 150 mm and not as indicated by the Phosphor Imager programme, which also automatically sets the y-axis scale.) A substantial portion of the radioactive proteins was not transferred to the second dimension PAGE, which might explain the problem with the reproducibility of the 2-D results.

Chapter 3

Identification of cell surface-derived glycoproteins

As stated before, the ultimate aim of the polyacrylamide gel electrophoresis was to identify cell surface-derived glycoproteins in M.av-Ph that were either depleted or enriched. The 2-D separation of proteins would have been ideal for the purpose of protein identification, but was unfeasible due to the reproducibility problem. The next best option was 1-D separation. Improvements in the technology, that had the ability to make identifications from a mixture of proteins, had been an ongoing process (Dongre et al., 1997) and have become an increasingly reliable tool in performing protein identification (Baldwin, 2004). This was contrary to the earlier viewpoint that 2-D separation is necessary for successful protein identification as have been demonstrated by certain researchers (Huang et al., 2002; Low et al., 2002). It was therefore decided to use the approach of protein identification from a 1-D PAGE.

3.1 Protein identification from the comparison between M.av-Ph and PM

The first identifications were made from a comparison between M.av-Ph and PM. Supporting evidence of successful protein identification from 1-D separation (as mentioned above) gave enough confidence to expect the approach to work for a mixture of membrane proteins. It was decided to select a small number of fractions and to concentrate on the MW range that was seen to contain enriched surface-derived glycoproteins in M.av-Ph, meaning 66 to 40 kDa. A secondary purpose to the experiment was to ascertain the reliability of making identifications from a 1-D separation.

Figure 3.1 shows the SDS-PAGE comparing PM and extracted Ph membrane from M.av-Ph that was prepared for the purpose of protein identification. Although it was earlier observed that comparing profiles from different lanes was less accurate, it was deemed necessary to know to which sample a certain identification belongs. To minimize the inaccuracy of comparing samples from different lanes, the samples were applied adjacent to each other on the PAGE. The SDS-PAGE was stained with Coomassie blue but was not dried. Silver staining (in general), which modifies certain proteins (Gharahdaghi et al., 1999), was avoided. As described earlier, it was necessary to have a radioactivity profile for each SDS-PAGE to know in which fractions the enriched and depleted surface-derived glycoproteins were located. To satisfy both requirements of having radioactivity profiles and doing protein sequencing, only half of the lanes were combusted in the Sample Oxidizer while the other halves were reserved for sequencing. For accurate cutting of the wet gel, 5 mm high fractions, which were double the height for fractions from a dried PAGE, were cut. Fractions were first cut across the total width of the two lanes, before further cutting into half fractions. Fraction halves from the Ph and PM samples having the same fraction number were combusted together in the Sample Oxidizer.

For Figure 3.1, the profiles were constructed directly from radioactivity values, meaning without normalisation, because only a selected portion (MW of about 66 to 36 kDa) of the PAGE lane was Oxidized. Values from blank samples were subtracted as background. The profile shapes compare well to earlier results in regard to the enrichment of surface-derived glycoproteins for M.av-Ph over the MW range of 66 to 36 kDa as shown in Figure 2.7. Selections for protein identification were made on the basis of the profiles showing enrichment in the Ph membrane. Fractions number 1, 3, 4, 5, 6 and 8 were selected for Ph membrane and 3, 4, 5, 6 and 8 for the PM. These fractions were subjected to protein sequencing.

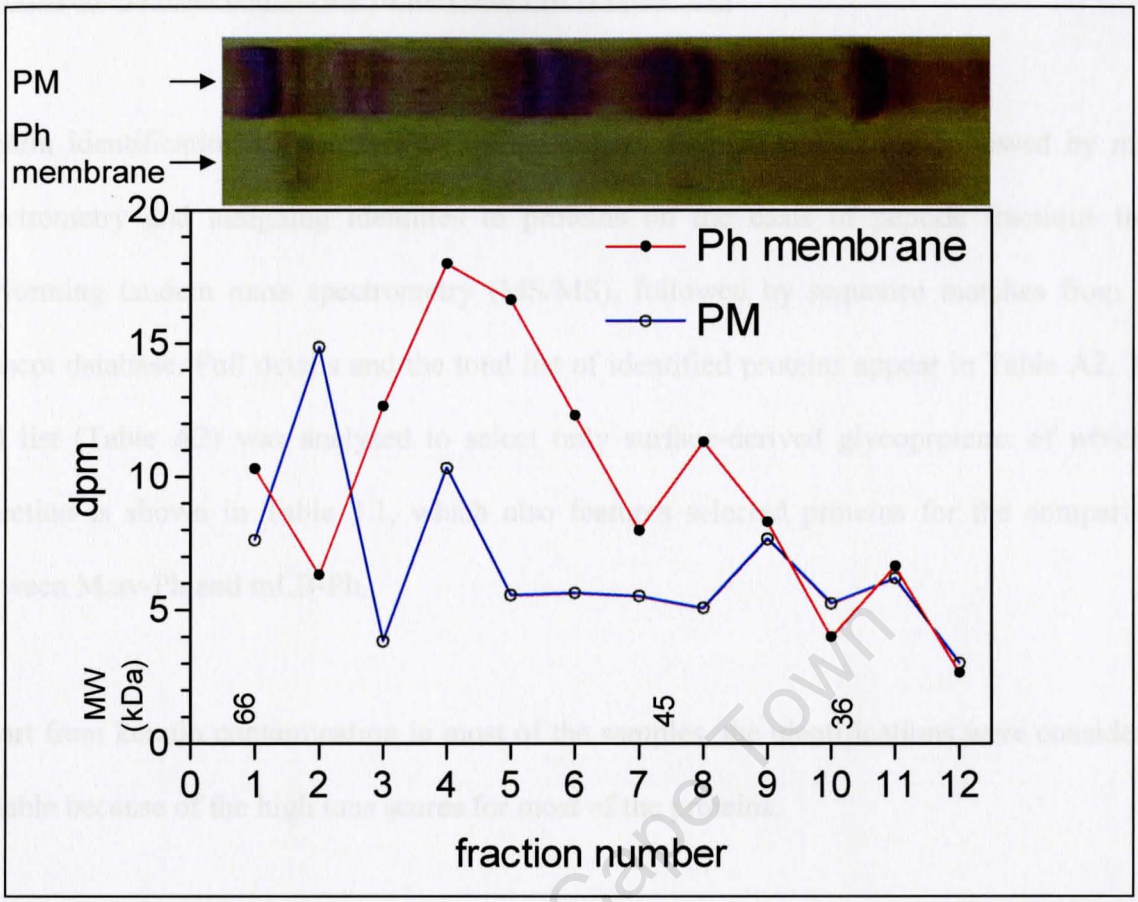

Figure 3.1: Comparison between Ph membrane and PM profiles for the purpose of protein identification BMDM were infected with *M. avium* and at 7 days p.i. were divided into two groups. For Ph, the cells were labelled with ^{3}H-galactose and the label was internalised for 2 h and surface label enzymatically removed. PNS was centrifuged on 27% Percoll and the Ph isolated from the gradient. The phagosome membrane was extracted. For PM, cells were labelled with ^{14}C-galactose and a PNS prepared. Both the Ph membrane and PM preparations were measured for radioactivity and equal radioactivity amounts subjected to SDS-PAGE using separate lanes. Relatively low radioactivity amounts (about 3000 dpm) were loaded. After staining with Coomassie blue, half of the PAGE lanes were fractionated (over the indicated MW range) and Oxidized. Radioactive content of the fractions was determined and based on the profiles, certain fractions from the remaining half-lanes were subjected to protein sequencing. The profiles compared well with previous results which showed enrichment over the MW range of 66 to 36 kDa for surface-derived glycoproteins in M.av-Ph as shown in Figure 2.7.

Identifications from comparing M.av-Ph to PM (Figure 3.1)

Protein identification was performed by starting at in-gel trypsinisation followed by mass spectrometry and assigning identities to proteins on the basis of peptide fractions from performing tandem mass spectrometry (MS/MS), followed by sequence matches from the Mascot database. Full details and the total list of identified proteins appear in Table A2. The full list (Table A2) was analysed to select only surface-derived glycoproteins of which a selection is shown in Table 3.1, which also features selected proteins for the comparison between M.av-Ph and mLB-Ph.

Apart from keratin contamination in most of the samples, the identifications were considered reliable because of the high ions scores for most of the proteins.

In comparing the identified proteins between phagosome membrane and PM, the ideal finding would have been for the same surface-glycoprotein to be present in corresponding phagosome membrane and PM gel fractions. Furthermore, the radioactivity profiles for such gel fractions must indicate that the surface-glycoproteins in the Ph are enriched as compared to the PM. A surface-glycoprotein fitting the above description can with certainty be referred to as surface-derived and enriched in M.av-Ph. No such protein was identified from the comparison in Figure 3.1. The next best situation was to search for known surface-located glycoproteins in the list of identified proteins for the phagosome membrane. One phagosome membrane protein in Table 3.1, namely the dendritic cell-associated transmembrane protein precursor, fits this description. The corresponding gel fraction, PM8, did not contain this protein, but does not automatically mean that it was absent from the PM8 gel fraction or not part of the PM sample, according important considerations as laid out by Baldwin (2004). The underlying reason is that in any given sample that is subjected to protein sequencing, it is

Table 3.1: Selected surface-derived glycoproteins of interest from the comparison between M.av-Ph and PM (Figure 3.1) as well as M.av-Ph and mLB-Ph (Figure 3.2) From the list of identified proteins in Tables A2 and A3, a selection of the surface-derived glycoproteins, thought to be of particular interest, was made.

Protein name	Gel fraction	Mass * (Da)	Peptides	Total score	Up / Down regulated in context of M.av-Ph	Subcellular localisation	Function
A: comparison between M.av-Ph and PM (Figure 3.1)							
dendritic cell-associated transmembrane protein precursor (known as DC-HIL) [a]	Ph8	63 634	4	85	Up	On cell-surface and in cytoplasm [1]; endosome-like compartment [2]	Cell adhesion [1]; possibly involved in DC migration [1]; negatively regulates T lymphocyte activation [3]
MHC class I histocompatibility antigen H-2D(b) alpha chain [b]	PM8	38 378	4	192	- [c]	On cell surface [4]	Antigen presentation [5]
H-2 class I histocompatibility antigen, D-D alpha chain precursor (H-2D(D)) [b]	PM8	41 084	4	163	-	On cell surface [4]	Antigen presentation [5]
Tapasin [b]	PM8	49 725	4	160	-	Endoplasmic reticulum [6]	Assembly of MHC class I molecules, stabilise the peptide loading complex [6, 7]
B: comparison between M.av-Ph and mLB-Ph (Figure 3.2)							
Niemann Pick type C1	8, 10	145 475	12	318	Down	Late En and Ly, have been found on PM [8]	Transport lipids including cholesterol from En and Ly, but precise function unknown [8]
Macrosialin (CD68)	8, 10	35 322 [d]	2	94	Down	Predominantly late En, up to 15% on cell surface [9]; also on early En and Ph [10]	Bind oxLDL (including cholesterol) at the cell surface, but exact function is unknown [11]

Continued …

Protein name	Gel strip	Mass (Da)	Pep-tides	Total score	Up / Down regulated In context of M.av-Ph	Subcellular localisation	Function
Sialoadhesin	10, 11	185 331	19	648	Down	On cell surface [12]	Suggested to play a regulatory role in the innate immune system, mediate interactions between cells [13]
H-2D cell surface glycoprotein	49	38 606	9	261	Up	On cell surface [4]	Antigen presentation [5]
Tapasin	49	50 010	2	87	Up	As above	As above
Nogo-B	51	38 543	5	167	Up	In ER predominantly [14], on cell surface [15]	Possibly forms channels at the cell surface or in the ER [15]
putative transmembrane glycoprotein (known as DC-HIL)	55	64 439	4	115	Up	As above	As above
CD45/ leukocyte common antigen (L-CA)/ T200	12, 13	142 716	4	117	Down	On cell surface [16], (Can be in lipid rafts [17])	Linked to regulation and / or immune responses [17]
Protein tyrosine phosphatase	10	146 224	2	70	Down	Cell surface, cytoplasm, nucleus [18]	Signaling, immune responses [18]
Tumor rejection antigen, gp96	8	237 934	2	69	Down	ER and SR (sarcoplasmic reticulum) lumen; cell surface under stress conditions [19]	Plays a role in innate and acquired immunity [20]; Functions as a molecular chaperone [19]
Sphingosine-1-phosphate lyase	44	64 293	2	71	Up	"Membrane bound", primarily in ER, might be in other organelles [21]	Catalyze the breakdown of sphingosine-1-phosphate [22]

Continued …

Protein name	Gel strip	Mass (Da)	Pep-tides	Total score	Up / Down regulated In context of M.av-Ph	Subcellular localisation	Function
Integrin alpha M	14, 15, 18	128 541	10	237	Down	On cell surface [23]	Signal transduction for adhesion and cell migration [23]
Alanyl (membrane) aminopeptidase (CD13)	18	110 038	16	501	Same	Plasma Membrane [24]	Cholesterol absorption, endocytosis, signal transduction, antigen presentation and phagocytosis [24, 25]

*: Molecular weight as given by Mascot database.

a: DC-HIL: "dendritic cell-associated heparin sulfate proteoglycan-dependent integrin ligand" [1]; Other notes appear in the text.

b: These proteins from PM8-fraction are included because a closely related MHC I molecule appears in strip 49 from the comparison between M.av-Ph and mLB-Ph, as discussed in the text. (This shows that these molecules are present on the PM.)

c: Up or down regulation is only proposed in terms of M.av-Ph.

d: Non-glycosylated. Macrosialin is heavily glycosylated, ranging from 87 to 115kDa (Holness et al., 1993).

References: **1**: Shikano et al., 2001; **2**: Bachner et al., 2002; **3**: Chung et al., 2007; **4**: Maloy et al., 1981; **5**: Sawicki et al., 2001; **6**: Momburg and Tan, 2002; **7**: Raghavan et al., 2008; **8**: Karten et al., 2009, **9**: Holness et al., 1993; **10**: Silva and Gordon, 1999; **11**: Ng et al., 2009; **12**: Ducreux et al., 2009; **13**: Crocker and Varki, 2001; **14**: Fontoura and Steinman, 2006; **15**: Dodd et al., 2005; **16**: Thomas et al., 1985; **17**: Saunders and Johnson, 2010; **18**: Mustelin et al., 2005; **19**: Cho et al., 2004; **20**: Doody et al., 2004; **21**: Bandhuvula and Saba, 2007; **22**: Zhou and Saba, 1998; **23**: Harris et al., 2000; **24**: Mina-Osorio, 2008; **25**: Kramer et al., 2005.

never that all the peptides of a single protein or every peptide from a mixture of proteins get registered by the protein sequencing instrument and protein in low concentrations in the sample can be particularly affected (Baldwin, 2004). Highly glycosylated proteins which label relatively intensely, but is present in low abundance in the sample, might therefore not be well represented among the identified proteins. Therefore, glycoproteins in the phagosome membrane fractions that are known to be surface-located and appearing in 'enriched' fractions, were accepted as surface-derived glycoproteins that are enriched in the M.av-Ph.

For the same argument that a surface-located glycoprotein which is identified only in a phagosome membrane fraction and might be present in the corresponding PM fraction, but is not detected due to a low concentration, it can also be asked if a surface-glycoprotein that is only identified in a PM fraction and not the corresponding phagosome membrane fraction, could be present in the corresponding phagosome membrane fraction. More importance was placed on the actual detection of a surface-located glycoprotein in the phagosome membrane fractions, while reasonable argument for the possible presence of a glycoprotein in mycobacteria-containing phagosomes will depend on reported findings for the glycoprotein in question.

From comparisons between PM and phagosome membrane (Figures 2.7 and 3.1) it was concluded that glycoproteins over the MW of about 66 to 36 kDa are enriched in M.av-Ph, but can it also be said that the PM glycoproteins might be down regulated over the same MW region? Down regulation in a general sense might not be applicable, but does not rule out the possibility of down regulation in specific fractions. In Figure 2.3B and C it was shown that mycobacteria up regulate certain glycoproteins on the PM, whereas down regulation, including for the 66 to 36 kDa region, was not obviously evident. The PM profile comparison in Figure 2.3 is for samples from different lanes (on different PAGEs) and such a situation has

its limits of comparison as discussed for Figure 2.4. An example of possible down regulation in Figure 3.1 can be made for the fraction PM3, which is on the downward trend of the profile, as compared to the corresponding fraction Ph3, which shows an upward trend. Therefore, although the PM glycoproteins over the MW region of 66 to 36 kDa (Figure 3.1) might not be down regulated in general, specific ones might be. The PM glycoproteins in Table 3.1 have been included because most function in the immune system and it is well documented that pathogenic mycobacteria influence immune functions for their intracellular survival (reviewed in Jozefowski et al., 2008). The proteins in Table 3.1 are further explored in the Discussion.

3.2 Protein identification from the comparison between M.av-Ph and mLB-Ph

The more interesting protein identification was for the comparison between Mav-Ph and mLB-Ph. The specific experiment that served this purpose has already been described in Figures 2.10 (SDS-PAGE) and 2.11 (radioactivity profiles) and is represented in Figure 3.2, but with a different normalisation. As mentioned in the text in Chapter 2, the highest peaks (appearing between the MW ranges of about 150 to 66 kDa) of the comparative profiles were closely matched in height. In general, the profiles from duplicate experiments displayed a deviation to one another. For these reasons, it is argued that these closely matching peaks might match exactly in height if more repetitions of the same experiment were made. Therefore, normalisation matching the profiles at the highest peaks was performed. This did not change the overall results.

For protein identification, the following fractions from the half lane (Figure 3.2) were selected: fractions number 3 to 15 were chosen because these include (in general) the depleted

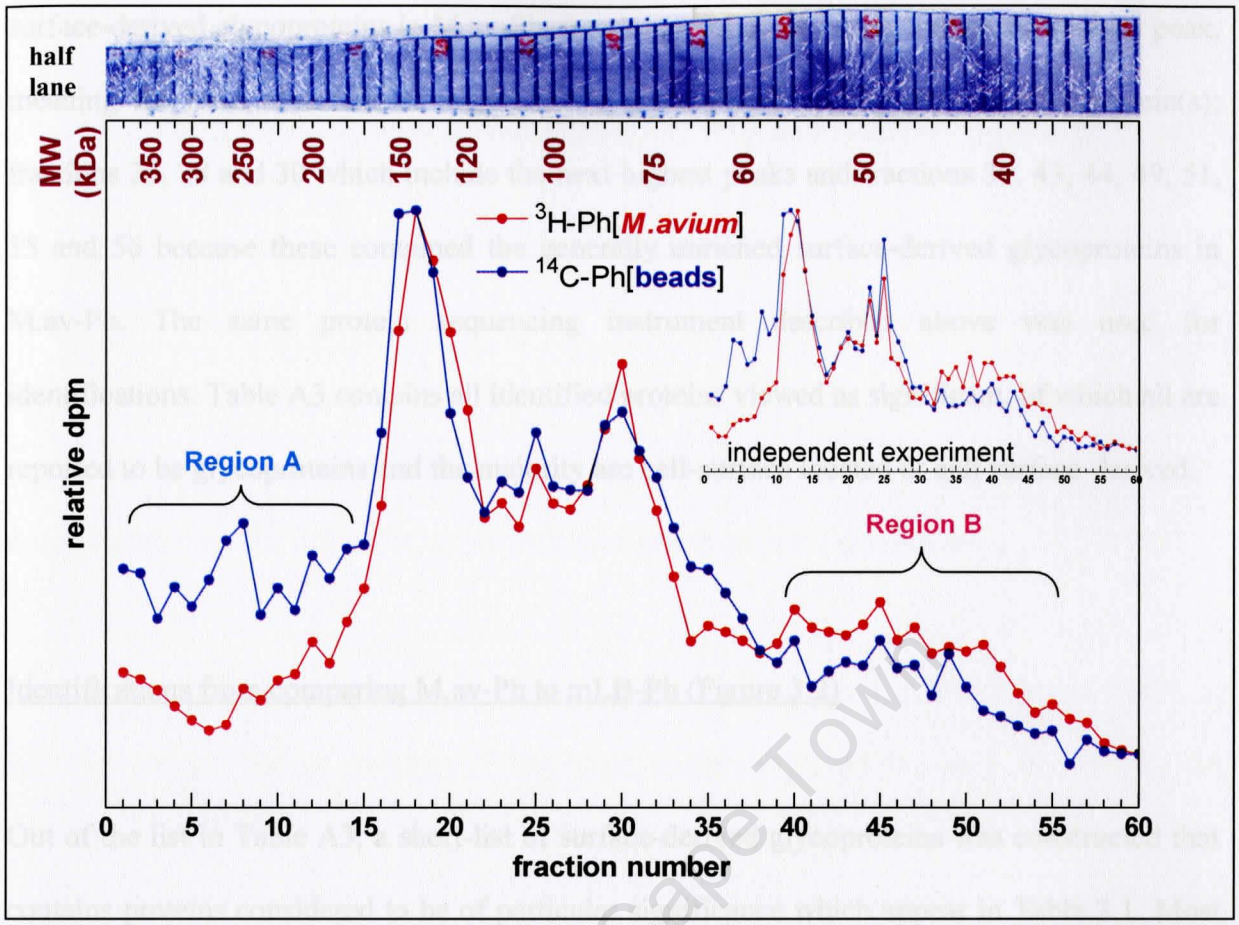

Figure 3.2: Comparison between phagosome membrane profiles from M.av-Ph and mLB-Ph for the purpose of protein identification These are the same profiles that appear in Figure 2.11, but a different normalisation has been applied as discussed in the text. The main profiles are related to Figure 2.11B and the inserted (independent experiment) profiles to Figure 2.11A. The half lane that was used for protein identification appears above the profiles. Region A (bracket on the left) refers to the generally depleted surface-derived glycoproteins and Region B to the generally enriched surface-derived glycoproteins in the phagosome membrane of M.av-Ph as compared to mLB-Ph. In this study, particular emphasis has been placed on enriched molecules because of the viewpoint that enrichment might be the result of specific action by mycobacteria to retain molecules on the phagosome membrane that are important in mycobacterium's intracellular survival. Depletion, on the other hand, might largely be non-specific, although not less important. (This figure has been modified from notes by L. Thilo.)

surface-derived glycoproteins in M.av-Ph; fraction number 18 which contain the highest peak, meaning the most abundant or most heavily glycosylated surface-derived glycoprotein(s); fractions 25, 28 and 30 which include the next highest peaks and fractions 39, 43, 44, 49, 51, 55 and 56 because these contained the generally enriched surface-derived glycoproteins in M.av-Ph. The same protein sequencing instrument described above was used for identifications. Table A3 contains all identified proteins viewed as significant, of which all are reported to be glycoproteins and the majority are cell-surface located or cell surface-derived.

Identifications from comparing M.av-Ph to mLB-Ph (Figure 3.2)

Out of the list in Table A3, a short-list of surface-derived glycoproteins was constructed that contains proteins considered to be of particular significance which appear in Table 3.1. Most of the surface-derived glycoproteins for M.av-Ph in Region A (in Figure 3.2) can be considered depleted on the phagosome membrane and those in Region B enriched. Two issues need to be raised in this regard. Firstly, Ly are always isolated with M.av-Ph and have been shown to carry about 50% of the total radioactivity in the M.av-Ph sample as discussed in Chapter 1 and shown in Figure 1.1.

The radioactivity profile of surface-derived glycoproteins in dense Ly (Haylett and Thilo, 1986) indicate that the main region affected by lysosomal contribution is in the 66 to 116 kDa range for $P388D_1$ macrophages, which if applicable here also, only include and therefore influence fractions 20 to 35 in Figure 3.2. Here, species differences must be respected, but the idea of relating the possible influence of a radioactivity profile for Ly, highlights an important consideration. Correcting for the radioactivity in Ly from an actual representative profile will

enhance observations of enrichment and depletion, or alternatively decrease and / or nullify the differences associated with the observations.

The second issue has to do with the specific values of comparative peaks versus their up or downwards trend. For comparative peaks that show a relatively small difference, like fractions 40 and 45 (Region B), as well as having the same directional trend, might actually have an insignificant difference. Likewise, if the directional trend is in opposite directions for comparative samples, the quantitative difference might be more significant.

Among the roles that the proteins in Table 3.1 play, lipid homeostasis and immune functions in macrophages feature strongly. These proteins are explored in more detailed in the Discussion.

Chapter 4

Phagosome characterisation by Western blot analysis

Western Blot analysis was performed to confirm that Ph containing M.av or mLB were immature Ph by checking for markers normally associated with eEn, i.e. Rab5 and transferrin receptor (TfR) as well as the late endocytic markers Rab7 and LAMP1.

4.1 WB analysis of immature Ph

Samples of M.av-Ph and mLB-Ph were tested in a comparative manner. Because M.av gradually changes the composition of the phagosome membrane (de Chastellier et al., 1995; de Chastellier and Thilo, 2002), it was decided to test M.av-Ph at an early and later time point. This would show if markers were present on the M.av-Ph immediately or acquired later and if markers change in intensity if present from the start.

To prepare M.av-Ph and mLB-Ph for the purpose of Western blot analysis, the same procedure was followed as described in Chapter 2, but excluding the radioactive labelling, as described under Figure 4.1.1. On day 0, the cells were first infected with *M. avium*, washed and re-incubated for 2 hours before infecting with mLB. Figure 4.1.1 shows the Western blot (WB) results for Rab5 content in the phagosome membranes. The antibody (Ab) used against Rab5 specifically recognises the B isoform of Rab5. Day 0 (D0) and day 7 (D7) refer to the age of the M.av-Ph only. The mLB-Ph were always 1 and ½ hours old (to ensure they were immature), but were either isolated with D0 or D7 M.av-Ph and were therefore given the same annotation to distinguish between the two situations.

Figure 4.1.1 shows that both the M.av-Ph and mLB-Ph were positive for Rab5B (lanes 2, 3, 5 and 6). Comparing the M.av-Ph between D0 and D7, a clearly stronger signal can be seen for D7, meaning that the amount of Rab5B increased from D0 to D7. The possibility that Ly may occur in varying amounts from sample to sample, can not be ruled out.

Similar signal strengths were obtained for both mLB-Ph samples (which were the same age), meaning the amount of Rab5B was the same. As a control, Ly (dense fraction from a 27% Percoll gradient) from non-infected cells were analysed for Rab5B content. Ly were Rab5B positive. The same result was obtained for other Western blots from different preparations (for example Figure 4.4.1 which is discussed later). This was therefore a consistent observation. The strength of the signal in Ly is comparable to the signal for seven day old M.av-Ph. This implies that the Rab5B signal in the M.av-Ph sample partly came from the Ly or perhaps a contaminant containing Rab5B that is collected with the Ph / Ly from the 27% Percoll gradient. Rab5 has only been reported to localise to eEn and the PM (Wilson and Wilson, 1992) which were completely separated from the Ph. It is unclear why the Ly were Rab5B positive.

The PM sample (low density fraction on the 27% Percoll gradient from which the M.av-Ph were isolated), containing PM, En and light Ly was Rab5B positive as expected. The M.av and mLB pellets were also tested to see if any molecules remained. Both pellets were positive for Rab5B after membrane extraction. This implies that some Rab5B molecules remained on the mycobacteria and beads, but nonspecific Ab attachment could also be the reason.

The Rab5B had to have come from the macrophages, because free bacteria (lane 9) had no Rab5B. As mentioned in Chapter 2, more phagosome membrane usually remained on the mLB as compared to the M.av after membrane extraction. To remove the remaining

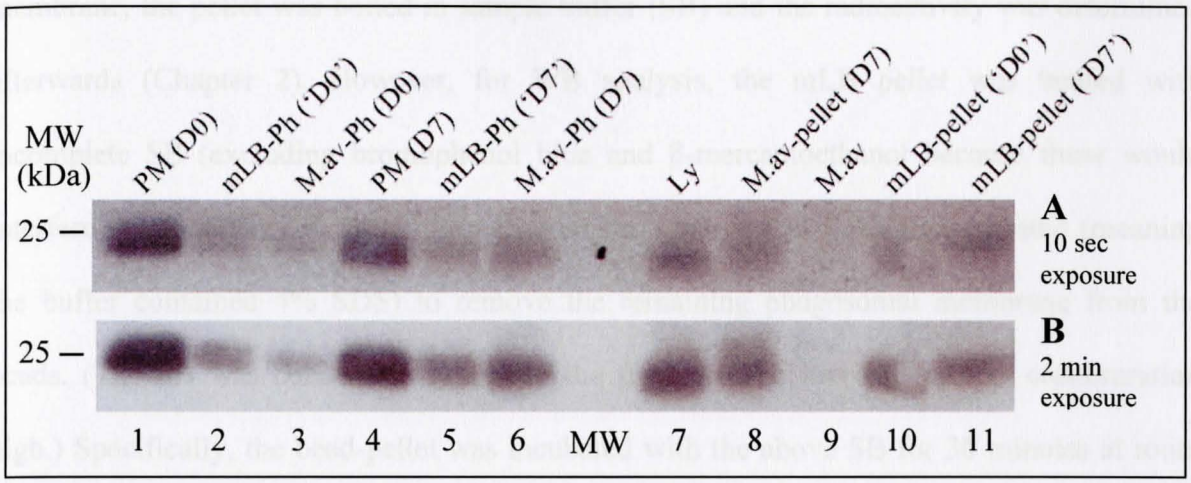

Figure 4.1.1: Presence of Rab5B in M.av-Ph and mLB-Ph

BMDM were infected with *M. avium* and divided into two batches. Two hours after having washed and re-incubated the cells (for day 0 samples), one batch of cells was exposed for 30 minutes to hydrophobic mLB and chased for 1 h. The other batch of cells, at 7 days p.i. with *M. avium* (for day 7 samples), was also exposed to hydrophobic mLB in the same way as the first batch. (Day 0 and 7 refer to the age of the M.av-Ph. For the mLB-Ph samples D0 and D7 are written between single quotation marks, i.e. 'D0' and 'D7', to indicate that they differ from these time points.) Immediately after the 1 h chase of the mLB, a homogenate was prepared, the mLB-Ph removed magnetically and a PNS prepared which was centrifuged on 27% Percoll followed by the isolation of the M.av-Ph. Membrane extraction was performed on the mLB-Ph and M.av-Ph. PM (top Percoll-gradient band which include En) in the gradients from which M.av-Ph were isolated, was also isolated to serve as a positive control. Lysosomes (bottom Percoll-gradient band) from non-infected cells were prepared as a negative control. Membrane extraction was performed on the PM and Ly samples. The protein concentration of the samples was determined and equal protein amounts subjected to 1-D SDS-PAGE followed by Western blotting (as described in Methods). The WB was probed with rabbit polyclonal anti-human Rab5B antibody followed by peroxidase labelled anti-rabbit antibody. The exposure time was 10 sec for **A** and 2 min for **B**. Lane **1:** PM, day 0 (D0); **2:** mLB-Ph, 'D0'; **3:** M.av-Ph, D0; **4:** PM, D7; **5:** mLB-Ph, 'D7'; **6:** M.av-Ph, D7; **7:** Lysosomes from uninfected cells; **8:** M.av-pellet (post extraction) to M.av-Ph, D7; **9:** M.av (mycobacteria directly from cold storage); **10:** bead-pellet to mLB-Ph, 'D0' and **11:** mLB-pellet to mLB-Ph, 'D7'. (The spot in the MW marker lane, **A**, shows the position of the 25 kDa marker.) All the phagosomes were positive for the early endocytic marker Rab5B, indicating their immature condition. Lysosomes, however, were also Rab5B positive, making the M.av-Ph result questionable. The mycobacteria and bead pellets were also positive, indicating that some Rab5B molecules remained tightly bound to the pellets or that non-specific binding took place.

membrane, the pellet was boiled in sample buffer (SB) and the radioactivity was determined afterwards (Chapter 2). However, for WB analysis, the mLB pellet was treated with incomplete SB (excluding bromophenol blue and β-mercaptoethanol because these would interfere with protein concentration measurements) that was 4 times concentrated (meaning the buffer contained 4% SDS) to remove the remaining phagosomal membrane from the beads. (The SB was concentrated to keep the final volume low and protein concentration high.) Specifically, the bead-pellet was incubated with the above SB for 30 minutes at room temperature followed by 30 minutes on ice. Lower temperatures were chosen to preserve the protein. The boiling of the sample was only done after all the membrane was thought to be removed. Without radioactivity as an indication that all the phagosomal membrane was removed, it could only be assumed that the extraction was successful. M.av-Ph and mLB-Ph were Rab5B positive, indicating the immature status of these Ph. However, the fact that Ly were also Rab5B positive makes the result questionable.

EM analysis showed that the above Ph did not contain lysosomal material and hence concluded to be immature. The lysosomal contamination made it difficult to conclusively confirm the immature character of these Ph through WB analysis.

The above WB (Figure 4.1.1) experiment was prepared in duplicate. The duplicate WB was analysed for LAMP1 content. The results are shown in Figure 4.1.2. M.av-Ph were LAMP1 positive due to the presence of Ly in the dense fraction of the Percoll gradient. This was a relatively strong signal if compared to Ly alone (lane 7) and implies that very little of the LAMP1 in the M.av-Ph sample is on the Ph. The M.av-pellet (lane 8) was also LAMP1 positive. LAMP1 molecules were probably also tightly bound to the mycobacterial surface. mLB-Ph were positive for LAMP1, although only slightly. However, it is known that a small

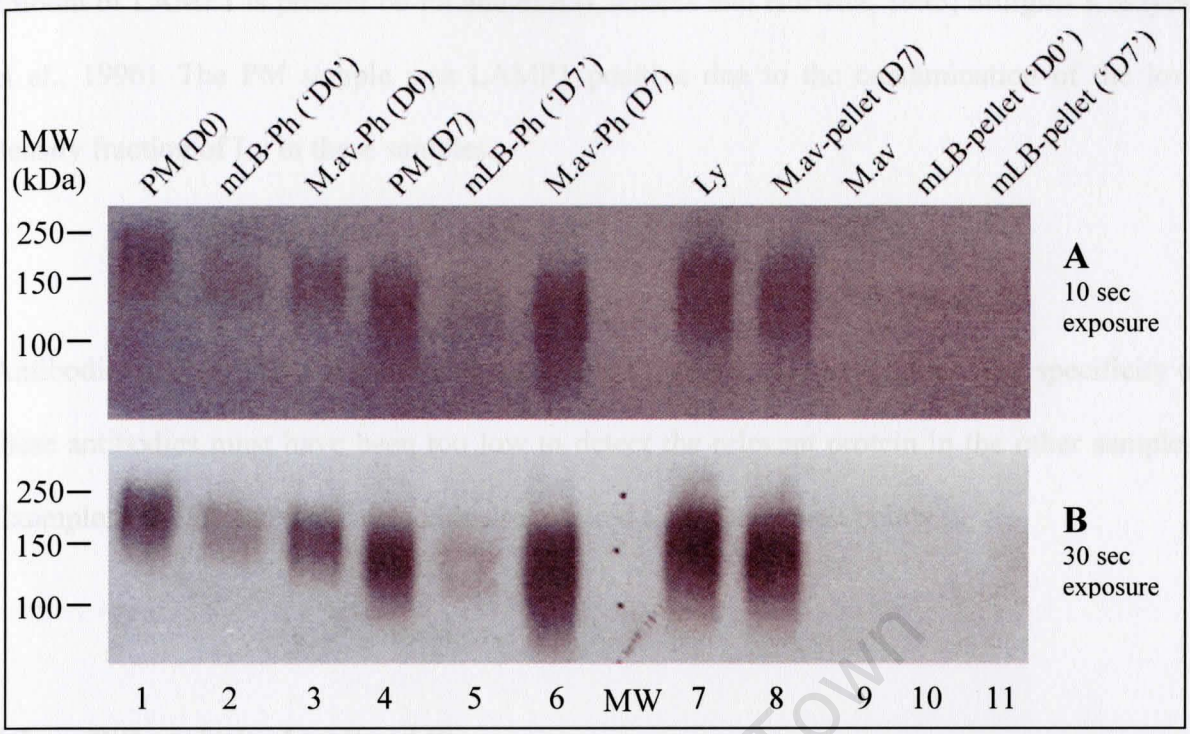

Figure 4.1.2: Presence of LAMP1 in M.av-Ph and mLB-Ph
The 1-D SDS-PAGE and Western blotting in Figure 4.1.1 was performed in duplicate. The second nitrocellulose membrane was treated with rat monoclonal anti-mouse LAMP1 antibody followed by peroxidase labelled anti-rat antibody. The exposure time was 10 sec for **A** and 30 sec for **B**. Lane **1:** PM, day 0 (D0); **2:** mLB-Ph, 'D0'; **3:** M.av-Ph, D0; **4:** PM, D7; **5:** mLB-Ph, 'D7'; **6:** M.av-Ph, D7; **7:** Lysosomes from uninfected cells; **8:** M.av-pellet (post extraction) to M.av-Ph, D7; **9:** M.av-pellet (mycobacteria directly from cold storage); **10:** bead-pellet to mLB-Ph, 'D0' and **11:** mLB-pellet to mLB-Ph, 'D7'. The entire LAMP1 signal for M.av-Ph (lanes 3 and 6) probably originated from the lysosomes because they had similar signal strengths. Differently to the PM and M.av-Ph, the mLB-Ph was not expected to be LAMP1 positive at all (because they bypassed the Percoll gradient and were washed several times before membrane extraction took place).

amount of LAMP1 is present on Ph and eEn (Clemens and Horwitz, 1995; Sturgill- Koszycki et al., 1996). The PM sample was LAMP1 positive due to the contamination of the low-density fraction of Ly in these samples.

Antibodies against TfR and Rab7 only showed a signal for the PM samples. The specificity of these antibodies must have been too low to detect the relevant protein in the other samples. Examples for TfR and Rab7 detection are referred to in the section below.

4.2 WB analysis of matured Ph

M.av-Ph, as immature Ph, have already been compared to other immature Ph, namely mLB-Ph. Now, for comparison, mature Ph are analysed by WB. In this regard, the best comparison was to have M.av-Ph that were in a matured state. *M. avium* blocks phagosome maturation by maintaining a close apposition between the phagosome membrane and its surface (de Chastellier and Thilo, 1997; de Chastellier and Thilo, 2006). The same authors proposed that M.av-Ph would mature if the close apposition was disrupted. Experimentally, the close apposition was disrupted by coupling 1 μm sized latex beads (LB, non-magnetic) to *M. avium* (de Chastellier et al., 2009).

BMDM were infected with mycobacteria to which LB had been coupled (M.av-LB) and the resulting Ph compared to M.av-Ph. Ph containing M.av-LB became matured and fused with Ly as shown in Figure 4.2. Figure 4.2A shows Ph containing either a single or two M.av-LB.

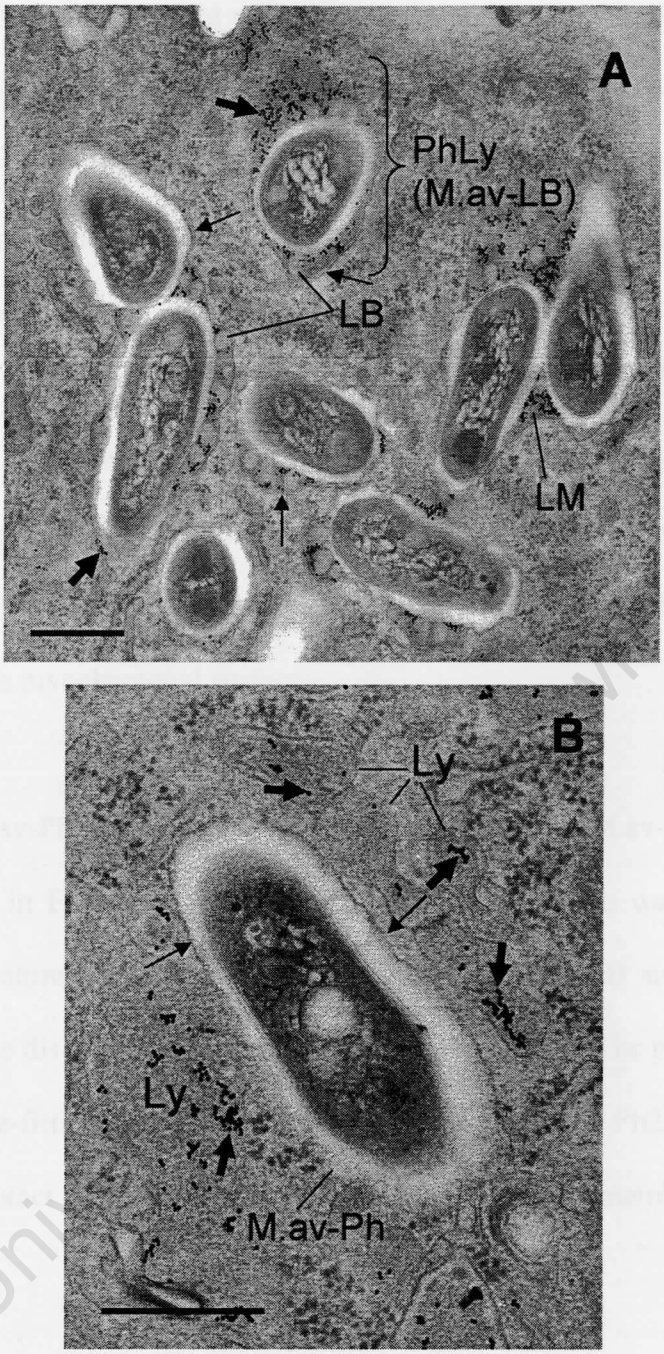

Figure 4.2: Electron micrographs comparing M.av-Ph to mLB-Ph
BMDM were infected with either *M. avium* to which latex beads (LB, non-magnetic) have been coupled (**A**) or with *M. avium* only (**B**). At 1 h p.i., the cells were fed medium containing BSA-gold which was chased to the Ly (as described in Methods). The cells were fixed and processed for EM. **A**: Thin section of a cell infected with *M. avium* coupled to latex beads (M.av-LB). The Ph, either having a single or several M.av-LB, have matured and fused with Ly – as evident by the presence of dense lysosomal material (LM) and gold particles (thick arrows) – to become phagolysosomes (PhLy). Thin arrows indicate the phagosome membrane which is loose-fitting around the M.av-LB. **B**: Thin section of a cell infected with *M. avium* not coupled to LB. Ly, containing BSA-gold, are in close vicinity of the immature phagosome but have not fused with it. Thin arrows indicate the phagosome membrane which is closely apposed to the mycobacterial surface. Bars = 0.5 μm. The Ph that contained mycobacteria coated with latex beads were mature Ph or PhLy. These pictures were kindly provided by Dr C de Chastellier, Marseille.

The LB are attached to the bacterial surface and the disruption of the close apposition is evident from the loose-fitting phagosome membrane (thin arrows). These Ph have matured and fused with Ly as can be seen by the BSA-gold particles (thick arrows) that were chased to Ly prior to phagocytic uptake. The bracket indicates a PhLy with a clearly loose-fitting phagosome membrane.

Figure 4.2B shows an immature M.av-Ph. Several Ly, containing gold particles, are surrounding the phagosome, but have not fused with it as is evident from the absence of gold particles and LM from the phagosome. The phagosome membrane (thin arrows) remained closely apposed to the mycobacterial surface.

As was done for M.av-Ph and mLB-Ph, enriched Ph containing M.av-LB are shown in the electron micrograph in Figure 4.3. The same procedure as before was followed to obtain enriched Ph. Two matured Ph (M.av-LB) can be observed. The LB are difficult to see and many of them become dislodged from the mycobacteria over time. The phagosome membrane (thin arrows) is loose-fitting around the mycobacteria for Ph1 and Ph2. Ly were part of the M.av-Ph samples. Intact Ph were present in the sample before membrane extraction was applied.

WB that were prepared with extracted membrane from M.av-Ph and Ph containing M.av-LB were treated with anti-Rab5B (Figure 4.4.1) and anti-LAMP1 (Figure 4.4.2) antibodies. In Figure 4.4.1 the PM sample was Rab5B positive. Matured Ph (M.av-LB) were Rab5 positive possibly due to the presence of Ly which have been consistently positive for Rab5.

In Figure 4.4.2 all the samples contained Ly and were therefore LAMP1 positive. However, the staining intensities were not all the same. Importantly, the M.av-Ph had much less

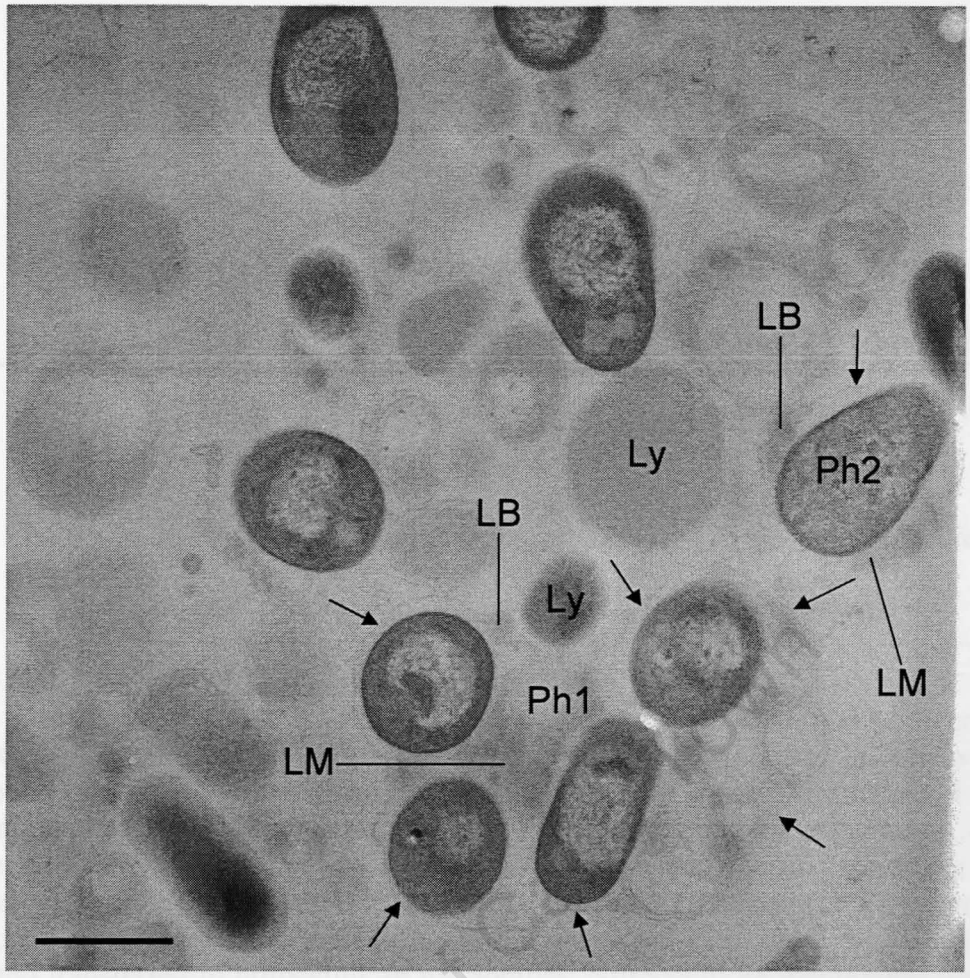

Figure 4.3: Electron micrograph showing enriched Ph containing Mav-LB
BMDM were infected with M.av-LB (as described). At seven days p.i., the cells were homogenised, a PNS was prepared and centrifuged on a 27% Percoll column. The Ph were isolated from the Percoll gradient in the same manner as M.av-Ph and centrifuged as described. The resultant pellet was fixed and processed for EM. **Ph1**: PhLy containing several M.av, some of which are coated with LB. LM can be seen in the Ph. **Ph2**: PhLy with only one M.av coated with LB. The phagosome membrane, indicated by the arrows, was loose-fitting for these matured Ph. Bar = 0.5 μm. It was still possible to isolate matured, intact Ph at the end of the phagosome purification procedure.

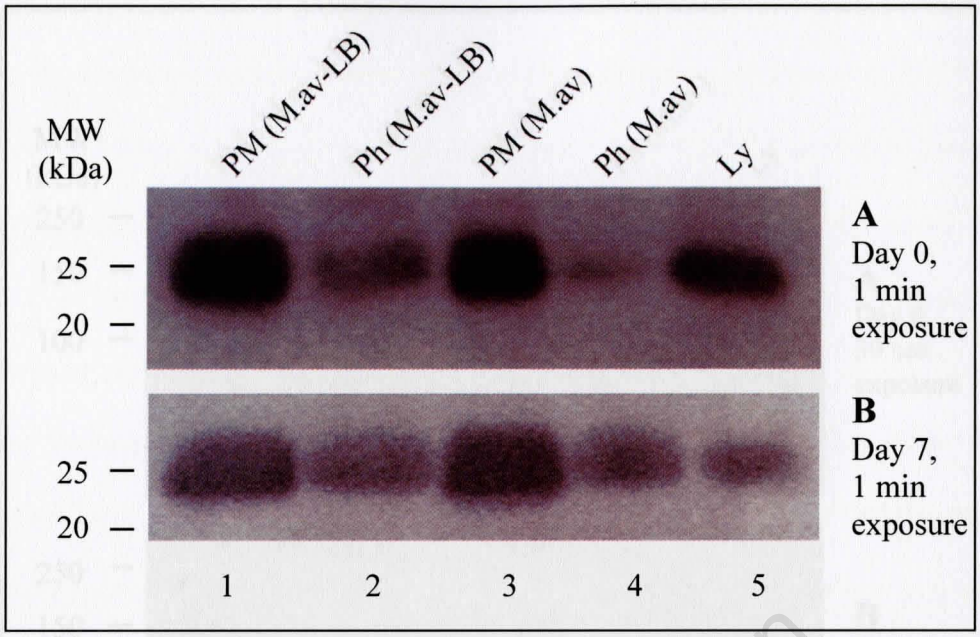

Figure 4.4.1: Presence of Rab5B in Ph containing M.av-LB or M.av
BMDM were infected with either M.av-LB or *M. avium* only. Phagosomes were isolated immediately after phagocytosis (day 0) or seven days after infection (day 7). The two types of Ph and corresponding PM (top Percoll-gradient band) were isolated from Percoll gradients. The membranes of the PM and phagosome samples were detergent extracted as described. Lysosomes (bottom Percoll-gradient band) from non-infected cells that were not detergent treated served as a negative control. SDS-PAGE and Western blotting was performed using equal protein amounts of the samples. Day 0 and day 7 samples were subjected to different PAGEs and transferred to nitrocellulose membranes. Nitrocellulose membranes were treated with rabbit polyclonal anti-human Rab5B antibody followed by peroxidase labelled anti-rabbit antibody. Panel **A:** Day 0 samples, panel **B:** Day 7 samples. Lane **1:** PM from M.av-LB infected cells; **2:** Ph from M.av-LB infected cells; **3:** PM from M.av-Ph; **4:** Ph membrane from M.av infected cells; **5:** Ly from non-infected cells. The positive signal for the mature phagosomes, which was expected to be Rab5B negative, could be from the lysosomes that consistently came up as positive for Rab5B.

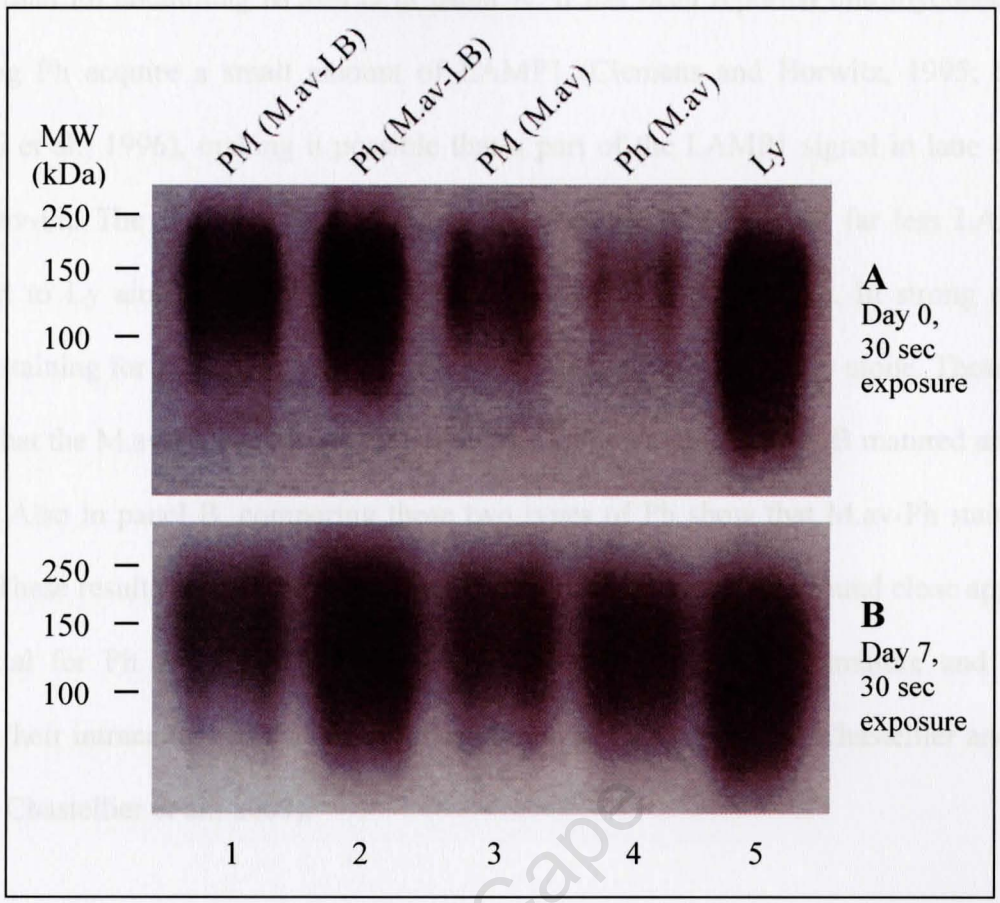

Figure 4.4.2: Presence of LAMP1 in Ph containing M.av-LB or M.av
The SDS-PAGE and Western blotting in Figure 4.4.1 was performed in duplicate. The duplicate nitrocellulose membranes were treated with rat monoclonal anti-mouse LAMP1 antibody followed by peroxidase labelled anti-rat antibody. Panel **A** and panel **B:** Day 0 and Day 7 samples respectively. Lane **1:** PM from M.av-LB infected cells; **2:** Ph from M.av-LB infected cells; **3:** PM from M.av-Ph; **4:** Ph membrane from M.av infected cells; **5:** Ly from non-infected cells. Although the mature phagosomes had a strong signal for LAMP1, this may have come from the lysosomal contamination. Immature Ph (M.av) had a stronger signal for LAMP1 at D7 than D0.

LAMP1 than Ph containing M.av-LB in panel A. It has been reported that mycobacterium-containing Ph acquire a small amount of LAMP1 (Clemens and Horwitz, 1995; Sturgill-Koszycki et al., 1996), making it possible that a part of the LAMP1 signal in lane 4 comes from M.av-Ph. The significance of this result is that the M.av-Ph had far less LAMP1 as compared to Ly alone, even though Ly form part of M.av-Ph sample. In strong contrast, LAMP1 staining for Ph containing M.av-Ph was of similar intensity to Ly alone. These results support that the M.av-Ph were immature while the Ph containing M.av-LB matured and fused with Ly. Also in panel B, comparing these two types of Ph show that M.av-Ph stained less intense. These results are in line with the published finding that an all-around close apposition is essential for Ph containing pathogenic mycobacteria to remain immature and thereby securing their intracellular survival (de Chastellier and Thilo, 1997; de Chastellier and Thilo, 2006; de Chastellier et al., 2009).

As mentioned, WB analysis for TfR and Rab7 were only partly successful. Examples are shown in Figure A14.

Two of the shortlist candidates (Table 3.1) were tested to confirm their presence on M.av-Ph. These are NPC1 and CD68. The antibodies against these proteins only bound to non-specific proteins. These results are not shown.

Discussion

This study was undertaken to identify the surface-derived glycoproteins on the phagosome membrane around *M. avium* that are changed in their abundance during infection as compared to En/PM and control Ph (containing magnetic latex beads with a hydrophobic surface, mLB-Ph). The proposal for this study is based on the observation that cell surface-derived glycoconjugates are found to be depleted about 3- to 4-fold in M.av-Ph as compared to early En, even though these Ph and early En exchange contents and intermingle membrane components continuously (de Chastellier et al., 1995; de Chastellier and Thilo, 2002). It might be that some of these surface-derived glycoproteins are involved in the maintenance of a close apposition with the mycobacterial surface and hence play a role in mycobacteria's intracellular survival.

The obtained results can be discussed under technical aspects that could have influenced its quality and the possible value the results bring to the relevant study field.

Technical aspects

Technical aspects include advantages and limitations of the approaches and / or techniques used, the reliability of results and what possible improvements can be made to overcome limitations. These aspects will be discussed for phagosome purification, PAGE analysis and protein identification.

Phagosome purification

Pure phagosomes were required to perform quantitative comparisons against other cellular organelles. Purification of M.av-Ph was based on their density. Sucrose gradients were the

first choice, but the required organelle separation was not obtained with them. Percoll, as an alternative to sucrose and used at 27% concentration, gave good separation between M.av-Ph and En/PM. This specific separation was important because surface-derived glycoprotein abundance needed to be compared between M.av-Ph and En/PM. Dense Ly, having close to or exactly the same density as M.av-Ph on 27 % Percoll (Figures 1.1 and A3) and sucrose gradients (Figures A1.1 and A1.2), could not be excluded from the phagosome sample. The presence of Ly in the phagosome samples is seen as the reason why Western Blot analysis of M.av-Ph showed a strong presence of LAMP1 (Figure 4.1.2). Mycobacterium-containing Ph do not fuse with Ly and have been reported to contain low amounts of LAMP1 (Clemens and Horwitz, 1995; Sturgill-Koszycki et al., 1996). EM analysis, however, showed that the majority or all the M.av-Ph were free from lysosomal material and always had an all-around close apposition between the phagosome membrane and bacterial surface (Figures 2.1 and 2.8). These characteristics are typical of immature Ph (de Chastellier and Thilo, 1997; de Chastellier and Thilo, 2002; de Chastellier and Thilo, 2006). Two research groups describe the contamination of other cellular material in their phagosome samples as 3 to 8% (calculated in terms of radioactivity associated with phagocytosed particles, i.e. beads and mycobacteria, Russell et al., 1996), but specifically 6 to 8% for mycobacterium-containing Ph (Sturgill-Koszycki et al., 1997), and $\leq$ 10% (also expressed in terms of radioactivity, Via et al., 1997). These reports indicate that mycobacterium-containing Ph overall do not contain the lysosomal markers Rab7 or LAMP molecules, except for a slight staining of LAMP1 (Sturgill-Koszycki et al., 1996). One group of authors (Russell et al., 1996) made use of a 5 µm pore filter to filter the PNS before using a sucrose gradient followed by a Ficoll gradient (10% low MW Ficoll) for phagosome isolation. The diameter of Ly are usually smaller than 0.5 µm (Callahan et al., 2009) or around 0.2 – 0.5 µm (Bright et al., 1997). All the Ly would therefore be expected to be present with the Ph in the flow through. No filtration of the PNS was applied in the current study. High molecular weight Ficoll can separate organelles on the

basis of density and size (www.gehealthcare.com), but low MW Ficoll was used (Russell et al., 1996) which is expected to separate only on the basis of density, i.e. similar to Percoll. However, WB analysis shows Ph only slightly positive for Ly (Russell et al., 1996). In this regard, Ficoll could be a better choice than Percoll or could be used in addition to Percoll. Although multiple gradients might result in a purer phagosome fraction, it was observed that an increase in centrifugation steps also increased the loss in radioactivity for samples and therefore discouraging this approach as a sufficient amount of labelled membrane was required for a successful experiment.

To decrease the amount of total lysosomal proteins in the final phagosome sample, luminal lysosomal proteins were decreased by sonication prior to the final centrifugation step for collecting membrane. This was primarily to decrease lysosomal proteins on the polyacrylamide gels. Ly contain numerous glycosylated proteins (Mellman, 1996) and although they contain minimal surface label (Haylett and Thilo, 1986), decreasing them was a precautionary step to minimize possible interference in protein identification. It was not ascertained how much luminal lysosomal protein was removed. Due to continuously expanding research into organelle proteomics, the identity of many related glycoproteins is known (Morelle et al., 2006; Callahan et al., 2009). This information makes it possible, to a certain extent, to ignore known lysosomal proteins in the phagosome membrane samples. The presence of Ly also meant that radioactivity other than associated with the Ph was present in the phagosome sample. The level of radioactivity on the Ly was expected to be negligible because for P388D_1 macrophages only 2 – 3% of total surface-derived label accumulates on dense Ly (Haylett and Thilo, 1986), but turned out to be about 6% for bone marrow macrophages (at steady state). In comparison, surface-derived label on Ph was calculated as about 11%. Therefore, about half of the radioactivity in the phagosome sample was associated with Ly. If this considerable percentage was due to mycobacterium-containing phagosomes

having fused with lysosomes, EM analysis would have revealed this. The more important consideration was how radioactivity from Ly possibly influenced the analysis/ construction of radioactivity profiles. Figure 2.4B shows a radioactivity profile for Ly. This profile had the purpose of correcting the phagosome profile for the contribution of radioactivity from Ly, but this specific approach was found to be unfeasible. However, the lysosomal profile was questioned because of the atypical profile shape observed for the phagosome membrane in this experiment, and it is uncertain if the lysosomal profile was similarly affected. The approach for doing a profile correction as attempted did not work and the idea for making such a correction was abandoned. A better approach would have been to use different isotopes for Ly and Ph and mixing the membranes on the same lane. This would have given a general result for which MW range(s) are definitely affected. PAGE analysis of dense Ly from $P388D_1$ revealed that the abundance of radioactive proteins are in the MW range of 66 to 116 kDa (Haylett and Thilo, 1986), which is of little importance for M.av-Ph in bone marrow macrophages, but the species difference makes such a comparison unreliable.

PAGE analysis

The approach to investigate differences (i.e. either non-specific or selective) that exist between different organelle membranes in terms of surface-derived glycoproteins was based on differential radiolabelling (with either ^{3}H- or ^{14}C-galactose) and PAGE analysis. Using either ^{3}H- or ^{14}C-galactose in conjunction with a Sample Oxidizer or in-gel trypsinisation combined with dual label liquid scintillation counting, made it possible to combine ^{3}H- and ^{14}C-galactose labelled membranes on the same PAGE for direct comparisons. Radioactivity profiles were constructed and gel fractions with differences were used to perform protein identification. Radioactivity is a sensitive method and especially suitable when differences between compared molecules are small. Although other methods exist for comparing protein or peptide abundance, the current approach was chosen to be in line with the basis of the

study, i.e. the abundance change in surface-derived glycoproteins. Other methods label certain amino acids or terminal groups, but would not reveal the difference in abundance of glycoproteins as seen in the original (de Chastellier et al., 1995) work. Other methods based on differential labelling of molecules, e.g. ICAT (isotope affinity-coded tag) (Baldwin, 2004), might serve as a follow-on step to verify the enrichment or depletion of molecules of interest.

Whereas 1-D electrophoresis resulted in many proteins per band, 2-D electrophoresis had to point out which individual surface-derived glycoproteins can be linked to a state of enrichment or depletion by analysing 2-D protein bands for radioactivity and performing protein identification. Autoradiography, performed with a Phosphor Imager, was used as a first approach to indicate the relative abundance in radioactivity for 2-D protein bands. The Phosphor Imager method did not produce usable results, possibly because the concentration of radioactivity on the PAGE was too low for detection by the Phosphor Imager, whereas the Sample Oxidizer results could be used. This clearly showed the Sample Oxidizer method to be more sensitive. An added advantage was that ^{3}H-label could also be detected when using the Sample Oxidizer and allowed the continuation of mixing the two isotopes (^{3}H and ^{14}C) for direct comparisons for the 2-D PAGEs. The preferred method of 2-D analysis was therefore through the use of the Sample Oxidizer. A problem of reproducibility was encountered for the radioactivity profiles from 2-D gel electrophoresis (Figures 2.15A and B). An investigation into the cause of the reproducibility problem revealed that a portion of the radioactive proteins remained on the IPG strip during transference (electrophoresis) from the first to second dimension (Figure 2.16). Most of the radioactivity peaks were on the acidic (low pI) side of the IPG strips for both the Control and Remnant. The incomplete transference of radioactive proteins between the polyacrylamide gels made it impossible to reproduce the 2-D electrophoresis results. This problem has been widely encountered (Santoni et al., 2000). The

literature reports that the most common problems with 2-D electrophoresis for membrane proteins are poor solubility in aqueous IEF buffers, which is especially problematic for integral membrane proteins. Membrane proteins are usually in low abundance in the sample and therefore difficult to detect on standard polyacrylamide gels, and generally have alkaline iso-electric points which can lead to exclusion from IEF strips (Santoni et al., 2000). The sample preparation in the current study could probably be improved with detergents better suited for very hydrophobic proteins. A popular choice is the detergent ASB-14 (amidosulfobetaine-14). However, it has been reported that the use of ASB-14 in the IEF sample buffer solubilised only 50% of a certain integral membrane protein as compared to SDS as analysed by PAGE, suggesting that SDS more efficiently solubilise proteins than cationic detergents (Rabilloud, 2009). Tributyl phosphine (TBP), as a substitute for DTT, has also been suggested as a solution to poor solubility and transfer between first and second dimension polyacrylamide gels (Molloy, 2000). With variable results for possible solutions to 2-D problems, many researchers have opted for 1-D PAGE separation combined with secondary separation techniques (like column chromatography) and / or powerful sequencing machines to analyse and identify proteins (Rabilloud, 2009).

Protein identifications

The mixing of membranes from the respective organelles that were to be compared, had the advantage of allowing direct comparisons. Specific gel fractions could be selected for protein identification based on the observed locations where the respective labelling profiles differed. A disadvantage of sequencing a mixture of proteins is that low abundance proteins can be missed altogether because in general not all peptides are sequenced and this can be worse for more complex mixtures (Andersen and Mann, 2006; Rabilloud, 2009). In the current study, identified glycoproteins could not be linked directly to their specific source, i.e. mycobacterium- or bead-containing phagosome. Because 2-D separation seemed unfeasible to

perform, identifications were based on 1-D separations after disappointment with 2-D electrophoresis. Many researchers have opted for more reliable 1-D separation, coupled with the use of powerful instruments (Rabilloud, 2009). Various instrument combinations are possible, each with its own advantages and disadvantages (Baldwin, 2004). One of the best choices for analysing a protein mixture is LC-MS/MS (liquid chromatography coupled with tandem mass spectrometry) because multiple fragmentation yields better quality data (Andersen and Mann, 2006). The current study used an ESI-Q-TOF (electrospray ionisation coupled to a quadrupole time of flight mass analyser), which can also perform MS/MS (Jonscher and Yates, 1997). MS/MS has become the norm for protein identification because of its greater reliability as compared to original MS (Baldwin, 2004).

The radioactivity profiles obtained in the current study show good reproducibility. Mascot is a popular and powerful search engine, incorporating several types of search algorithms that give good protection against obtaining false positive results (Perkins et al., 1999). The majority of the Mascot identifications fall within their expected MW ranges for the gel fractions. Also, most of the identifications listed as cell surface-derived glycoproteins, have relatively high ions/ total scores that are well above the threshold for a positive match.

Value of results

The search for cell surface-derived glycoproteins puts the focus on a unique subset of molecules, in the sense that out of all the proteins on the phagosomal membrane, these are glycosylated and derived from (localised to) the cell surface. Focussing on cell surface-derived glycoproteins, gives an advantage over studies having to consider all the molecules of the phagosomal membrane for possible significance towards mycobacteria's intracellular

survival. For example, a study which compared bead- and mycobacterium-containing phagosomes, found only minor differences (Sturgill-Koszycki et al., 1997).

The current study observed an abundance change for labelled glycoproteins at the cell surface after infection with *M. avium*. Specifically, glycoproteins in the region of 116 to 205 kDa were up regulated by *M. avium* (Figures 2.3B and C). The up regulation of certain surface-glycoproteins might form part of mycobacteria's intracellular survival. For instance, some of the up regulated molecules could have signalling functions that, in an in vivo setting, stimulate the immune system for a favourable outcome for mycobacteria, e.g. a Th2 instead of a Th1 response (see Tapasin and H-2D, p103).

One published study which investigated the intracellular distribution of cell surface-derived glycoconjugates (label) at steady state, found that phagosomes containing hydrophobic beads (Ph(beads)) obtained the same level of label as eEn, while phagosomes containing *M. avium* (Ph(M.av)) was depleted 4-fold of label as compared to eEn, despite the Ph(beads) and Ph(M.av) being both immature phagosomes (de Chastellier et al., 1995). Therefore, the comparison between Ph(M.av) and eEn could be substituted with comparing Ph(beads) to Ph(M.av), as was done in the current study. In the current study, comparing M.av-Ph to mLB-Ph (Figure 2.11) or PM (used as substitute for eEn, Figures 2.7 and A5), show up regulation (over about 40 to 66 kDa) and down regulation (over about 150 to 350 kDa) of cell surface-derived glycoproteins on M.av-Ph. Although depletion was expected (based on the published work), both enrichment and depletion are applicable, answering the question whether the observed depletion reported by de Chastellier et al. (1995) and de Chastellier and Thilo (2002) is limited to a state of depletion, as pointed out in the Introduction (p17, under Study question).

Enrichment, as seen in the radioactivity profiles, means that certain cell surface-derived glycoproteins are up regulated, while depletion means a down regulation of others during infection with *M. avium* (as compared to hydrophobic latex beads). Comparing live mycobacteria to inert particles implies that the molecule-abundance changed due to active processes by the mycobacteria, while the variety of molecules implicated in both up and down regulation implies that different mechanisms could be involved. Literature does propose and support that pathogenic mycobacteria use various mechanisms for their intracellular survival (see Introduction).

The contamination of the M.av-Ph by Ly, could have influenced the radioactivity profiles because Ly carried radioactivity. Observations of enrichment and depletion of surface-derived glycoproteins could therefore be larger or smaller than represented in this study. This means that some of the proteins of interest (Table 3.1) might be of greater significance than currently realised.

Individual cell surface-derived glycoproteins in context of mycobacterial survival

The cell surface-derived glycoproteins that are listed in Table 3.1 (p 72) can be discussed for their potential significance during mycobacteria's intracellular survival. Their identification can serve to probe directly whether they play a role in the maintenance of the *M. avium*-containing phagosome. Attention was drawn to identifications that have relatively high ion scores/ peptide abundance and can be linked to known or suspected strategies used by mycobacteria for their intracellular survival.

NPC1

NPC1 was found to be depleted on the membrane of M.av-Ph. Niemann Pick type C (NPC) disease is a neurodegenerative disorder that progresses to a fatal outcome, is marked by

cholesterol accumulation in late endocytic organelles and is caused by NPC1 and NPC2 gene mutations (95% and 5% of cases respectively) (Karten et al., 2009). NPC1 is located in late endocytic compartments according most reports, but have been found on the PM (Karten et al., 2009). In the current study, the analysed phagocytic compartment was contaminated with lysosomes, making NPC1 a possible contaminant in the phagosomal sample. NPC1 transports cholesterol and other lipids from late En and Ly, but its exact function and mechanism of action is currently unknown (Karten et al., 2009). NPC1's possible significance towards mycobacteria's intracellular survival can be linked to cholesterol, which was reported as essential for the maintenance of immature phagosomes (de Chastellier and Thilo, 2006). If NPC1 is part of the phagosome membrane, cholesterol would be pumped out of phagosomes. It is conceivable that mycobacteria could reduce the loss of cholesterol by reducing (down regulating) NPC1 on the phagosome membrane (Table 3.1).

Macrosialin (mouse CD68)

Macrosialin was found to be depleted on the membrane of M.av-Ph. Macrosialin is largely specific to macrophages (Jiang et al., 1998) where it is predominantly localised in early and late En, with up to 15% on the cell-surface and it "has been detected in all phagosomes analysed to date" (da Silva and Gordon, 1999; Holness et al., 1993). Macrosialin is characterised as heavily glycosylated, 87 to 115 kDa in size and it is an integral membrane protein (Holness et al., 1993). Macrosialin binds oxidised low density lipoprotein (oxLDL) at the cell surface, but its exact function is not known (Ng et al., 2009). If macrosialin causes a cholesterol decrease in phagosomes, mycobacteria could down regulate macrosialin.

Sialoadhesin

Sialoadhesin (Sn) was found to be depleted on the membrane of M.av-Ph. Sn is a siglec (sialic acid-binding Ig-like lectin), belongs to the Ig superfamily, expressed mostly by hematopoietic

cells and is located on the cell-surface (Crocker and Varki, 2001; Ducreux et al., 2009). Siglecs bind through sialic acid-recognition and play a regulatory role in the immune system and inflammatory responses (Crocker and Redelinghuys, 2008). Sn can mediate cell-cell interactions by recognising sialylated glycoconjugates (Crocker and Varki, 2001). Sialic acid-expression is important to different pathogens for infecting and surviving in the host (Crocker and Varki, 2001). Sialic acid, which is produced by some pathogens and obtained from the host by others, might be used for host mimicry and suppression of antibody production and complement activation (Crocker and Varki, 2001). Down regulating Sn might be one of the ways in which mycobacteria influence immune system responses.

Nogo B

Nogo B was found to be enriched on the membrane of M.av-Ph. Neurite outgrowth inhibitor protein (Nogo) exists in three splice forms, namely Nogo-A, -B and -C that are referred to as reticulons because they have the same C-terminal domain and occur abundantly in the ER (Teng and Tang, 2008). Nogo-A, -B and -C are also present on the cell-surface, but less abundant and can interact with each other to form multisubunit complexes that typically function as channels, pores and transporters (Dodd et al., 2005). Nogo-A and -B's N-terminal contains a putative calcium-ion binding site that could regulate Ca^{2+} and, as a channel, could be functional at the PM, in the ER or other intracellular organelles (Dodd et al., 2005). Such a calcium-ion regulation might be linked to the decreased Ca^{2+} fluxes for mycobacterial infections as proposed by (Malik et al., 2000; Malik et al., 2001) and (Vergne et al., 2003).

DC-HIL (Putative transmembrane glycoprotein)

DC-HIL was found to be enriched on the membrane of M.av-Ph. Although Mascot database searches from the two protein sequencing experiments (Chapter 3) gave different results, i.e. [AF322054]: Dendritic cell-associated transmembrane protein precursor, 63 634 Da (from

comparing Ph to PM) and [gi| 6688788]: Putative transmembrane glycoprotein, 64 439 Da (from comparing M.av-Ph to mLB-Ph) (Table 3.1), the identifications in question are linked to the same gene (Gene ID: 93695) and are also known as iris pigment dispersion (ipd), osteoactivin, glycoprotein transmembrane (Gpnmb) and DC-HIL (www.ncbi.nlm.nih.gov/gene/93695). DC-HIL's amino acid sequence is characteristic of a type I integral membrane protein with N- and O-glycosylation sites, contains a heparin and integrin binding motif and has a cytoplasmic tail with two lysosomal targeting motifs among other characteristics (Shikano et al., 2001). Antigen presenting cells, including macrophages, express DC-HIL on their surface. The binding of DC-HIL is probably through multiple sites (Shikano et al., 2001) and several roles have been proposed for DC-HIL (Table 3.1). The current study indicates that there may be a slight enrichment of DC-HIL on the *M. avium*-containing phagosome membrane. DC-HIL's inhibitory effect on the activation of T cells, a function that resides in DC-HIL's extracellular Ig-like domain, can lead to the suppression of immune system responses (Chung et al., 2007). Suppression of the immune system may favour mycobacteria's intracellular survival (Jozefowski et al., 2008).

Tapasin and H-2D

Tapasin and H-2D were found to be enriched on the membrane of M.av-Ph. Tapasin and H-2D play roles in MHC class I antigen presentation (Momburg and Tan, 2002; Raghavan et al., 2008). Tapasin is localised to the ER (Momburg and Tan, 2002), which can become a contaminant during phagosome purification (Huber et al., 2003). In the current study, however, Tapasin was identified from the comparison between M.av-Ph and mLB-Ph, but specifically in the PM sample from the comparison between M.av-Ph and PM (Table 3.1). Tapasin and H-2D's possible significance towards mycobacteria's intracellular survival relates to antigen cross-presentation, i.e. a process whereby extracellular antigens that are usually presented by MHC class II molecules are presented by MHC class I molecules

(Groothuis and Neefjes, 2005). Antigen presentation by MHC class II molecules activates a cell-mediated (type I T helper (Th1)) immune response which offers protection against intracellular pathogens, but MHC class I molecules activates a humoral (Th2) response which is effective against extracellular pathogens, but not intracellular ones, as they are inaccessible to antibodies (Jozefowski et al., 2008).

CD45/ leukocyte common antigen (L-CA)/ T200

CD45 was found to be depleted on the membrane of M.av-Ph. CD45 is heavily glycosylated with a MW ranging from 180 to 240 kDa (Thomas et al., 1985). CD45 is found on the PM, with the majority in the fluid portion and a small percentage in the lipid rafts where its presence is dependent on cholesterol (Saunders and Johnson, 2010). CD45 is described as a receptor-like protein tyrosine phosphatase (PTP) that exists as several alternative spliced isoforms (Saunders and Johnson, 2010). The threshold of antigen receptor signalling is lowered by CD45. This influences the activation and development of T and B cells. CD45 also affects the adhesion and migration of immune cells (Saunders and Johnson, 2010). The carbohydrate moieties of CD45 can interact with various lectin molecules (Saunders and Johnson, 2010). Reducing CD45 on the phagosome membrane might lead to a decreased recruitment or activation of other immune cells. CD45, through positive or negative regulation of Src family kinase activity, can regulate immune cell signalling either positively or negatively (Saunders and Johnson, 2010).

Protein tyrosine phosphatase (PTP)

PTP was found to be depleted on the membrane of M.av-Ph. PTPs are enzymes that play important roles in various physiological processes like cellular signalling, differentiation and immune responses (Mustelin et al., 2005). In humans, small changes in PTPs can lead to immune dysfunction and cause disease (Mustelin et al., 2005). As for CD45, a reduction in

PTPs might decrease important cellular signalling events and immune responses that might favour mycobacteria, because the host cell's (macrophage) normal response to the infection could be altered.

Tumor rejection antigen gp96

Tumor rejection antigen gp96 (gp96) was found to be depleted on the membrane of M.av-Ph. Gp96 has a central role in the innate and acquired immune systems. More specifically, gp96 mediates inflammation signals that selectively primes CD8-positive cells (Doody et al., 2004). These inflammatory signals can come directly from pathogens or are expressed in response to infection by the host cell (Doody et al., 2004). A lowered abundance of gp96 on the phagosome membrane could suppress activating signals that stimulate other immune cells. The obligate intracellular bacterium, *Orientia tsutsugamushi*, is reported to inhibit gp96 expression (transcripts and protein) in J774A.1 macrophages (Cho et al., 2004). The authors propose that gp96 is a target for intracellular bacteria to evade immune responses (Cho et al., 2004).

Sphingosine-1-phosphate lyase

Sphingosine-1-phosphate lyase (SPL) was found to be enriched on the membrane of M.av-Ph. SPL is an enzyme that breaks down sphingosine-1-phosphate (S-1-P) which plays a role in signal transduction pathways (Zhou and Saba, 1998). It has been reported that M.tb inhibits Ca^{2+} release from the endoplasmic reticulum, an event linked to phagosome-lysosome fusion, by suppressing sphingosine kinase from producing S-1-P, which is the second messenger (Malik et al., 2003; Kusner, 2005). The breakdown of S-1-P (by SPL), might have the same effect as suppressing its production (by sphingosine kinase), resulting in membrane fusion factors like EEA1 being excluded from mycobacterium-containing phagosomes (see Introduction). An up regulation of SPL, therefore, may help prevent mycobacterium-

containing phagosomes from fusing with late endocytic organelles or from fusion events in general.

Integrin alpha M

Integrin alpha M was found to be depleted on the membrane of M.av-Ph. Integrins regulate certain cellular behaviour, like attachment and migration, through signalling pathways (Harris et al., 2000). Interestingly, Integrin alpha M has been found to be up regulated on the cell surface (Itoe, Dissertation, 2007). Perhaps mycobacteria down regulate Integrin alpha M on the phagosome membrane because its signalling function might stimulate or enhance pathways with an undesirable effect for mycobacteria.

Alanyl aminopeptidase

Alanyl aminopeptidase, also known as aminopeptidase N (APN) (EC 3.4.11.2) or CD13, is an ectoenzyme located on the PM of various cell types, including monocytes and macrophages (reviewed in Mina-Osorio, 2008; Gabrilovac et al., 2010). APN plays roles in cholesterol absorption, endocytosis, signal transduction, antigen presentation and phagocytosis (Larsen et al., 1996; Kramer et al., 2005; Mina-Osorio, 2008). Although the level of APN is the same in M.av-Ph and mLB-Ph, it is included in Table 3.1 because it was identified from the highest peak, meaning it is one of the most abundant (considering area under the curve) or most glycosylated surface-derived glycoproteins on these phagosomes. Given that APN is in high abundance on immature phagosomes and partake in several important cellular processes, it might be important to *M. avium* intracellularly, e.g. APN might help maintain sufficient cholesterol in the phagosome membrane of immature phagosomes.

Conclusions

Radioactivity profiles showed good reproducibility. Both depletion and enrichment of cell surface-derived glycoproteins happens on *M. avium*-containing phagosomes as compared to mLB-Ph and PM, implying that *M. avium* actively and selectively influences the abundance of cell surface-derived glycoproteins at the phagosome it resides in. Protein identification through a 1-D separation approach was successful. Some of the selected proteins of interest can be coupled to lipid homeostasis and immune functions, both of which have been reported as critical in the intracellular survival of pathogenic mycobacteria.

The *M. avium*-containing phagosomes analysed in this study was well separated from endosomes and PM, but not Ly, which contained about half of the radioactivity in the phagosomal sample. Radioactivity contamination could have influenced the radioactivity profiles.

Future studies should first embark on refining the phagosome purification method, an issue that is often reported as a challenge, and then verify the presence of and comparative abundance of the 'proteins of interest'. It will be worthwhile to study the binding characteristics of a verified glycoprotein to ascertain if it possibly makes tight interactions with the mycobacterial surface and what the binding partner(s) is (are) on the mycobacterial surface. The binding partner may serve as a drug target and drug design can be towards interference with the close apposition between the cell surface-derived glycoprotein and mycobacterial surface.

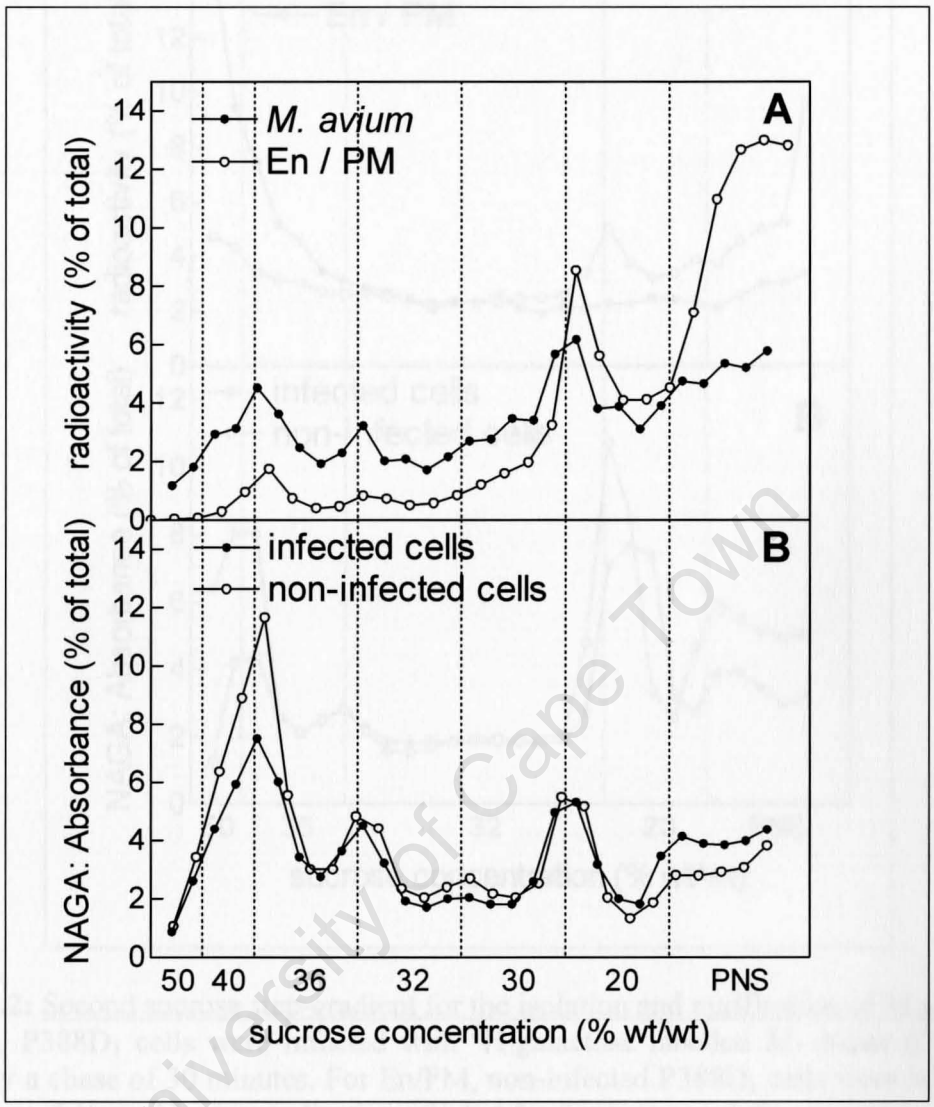

Figure A1.1: First sucrose step-gradient for the isolation and purification of *M. avium*-containing phagosomes (M.av-Ph) **A:** For Ph, P388D$_1$ cells were infected with ^{3}H-galactose labelled *M. avium* (Op) for 2 h followed by a chase of 3 h. For En/PM, non-infected P388D$_1$ cells were labelled with ^{14}C-galactose, followed by internalisation of label for 5 minutes and the enzymatic removal of uninternalised label. A post nuclear supernatant (PNS, 8% wt/wt throughout this study) was prepared for each of the two cell treatments, loaded on top of separate sucrose step-gradients and centrifuged (as described in Methods). The gradients were fractionated from the bottom and aliquots counted for radioactivity. **B:** Aliquots from the gradient fractions in A were analysed for the enzyme N- acetyl glucosaminidase (NAGA) which revealed the position of the lysosomes (Ly) (as described in Methods). It could not be concluded which one of the *M. avium* radioactivity peaks represented the Ph. Furthermore, Ly occurred in the same positions as the mycobacteria.

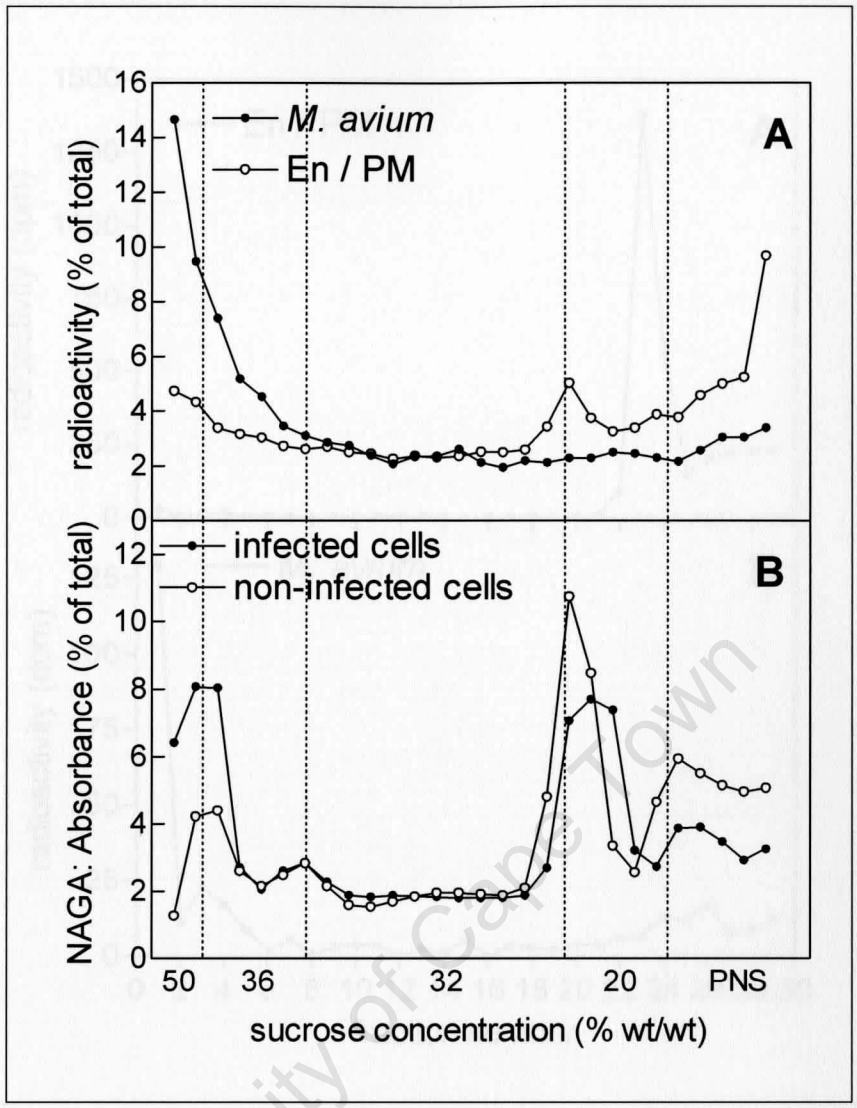

Figure A1.2: Second sucrose step-gradient for the isolation and purification of M.av-Ph
A: For Ph, P388D$_1$ cells were infected with ^{3}H-galactose labelled *M. avium* (Op) for 1 h followed by a chase of 30 minutes. For En/PM, non-infected P388D$_1$ cells were labelled with ^{14}C-galactose, followed by internalisation of label for 5 minutes and the enzymatic removal of uninternalised label. The respective PNS preparations were loaded on separate sucrose step-gradients and centrifuged. The gradients were fractionated from the bottom and aliquots counted for radioactivity. **B:** Aliquots from the gradient fractions were analysed for NAGA content. Only partial separation between Ph and En/PM could be achieved with this gradient.

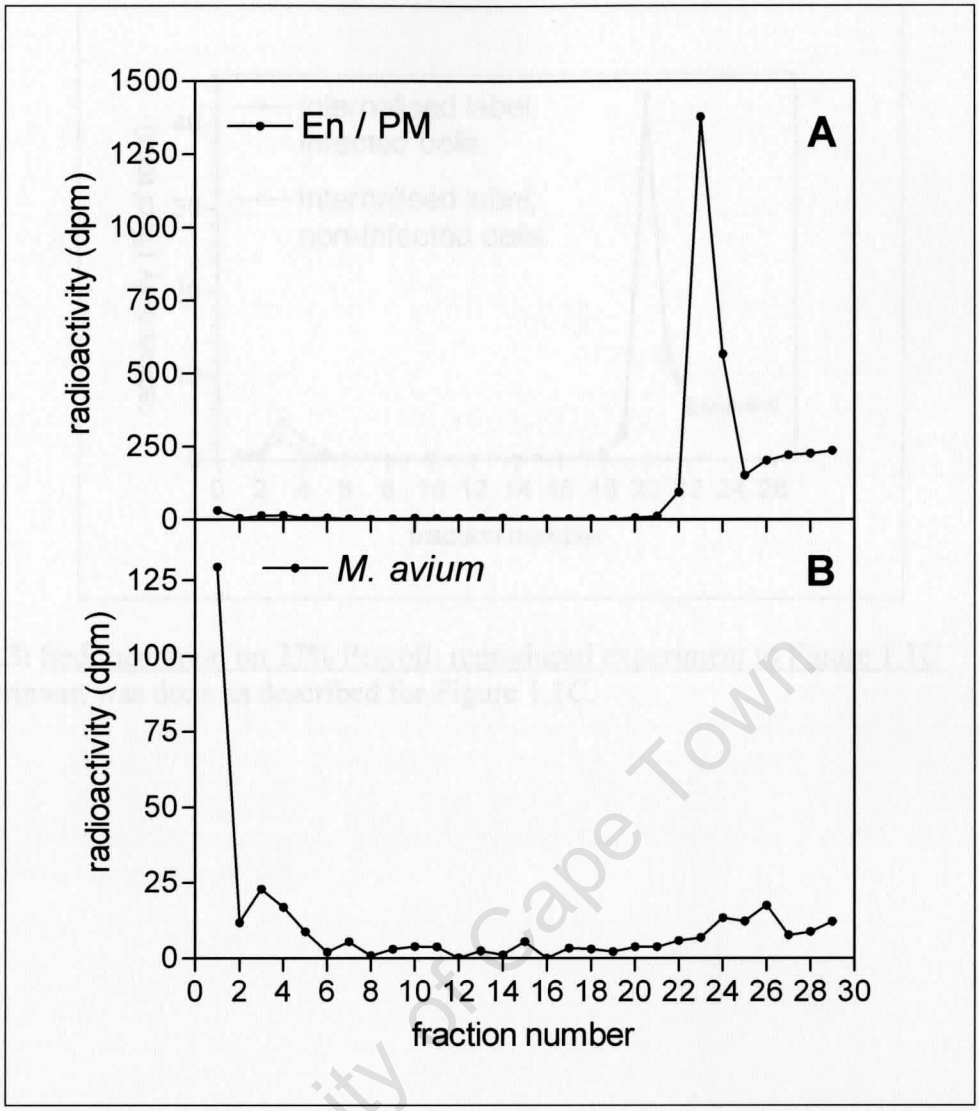

Figure A2: Sedimentation on 27% Percoll: reproduced experiments to Figures 1.1A and 1.1B
The experiment was done as described for Figure 1.1A and B. The different plotting scale of graph B is revealing the extent of the deviation in the counts which is less obvious in graph A.

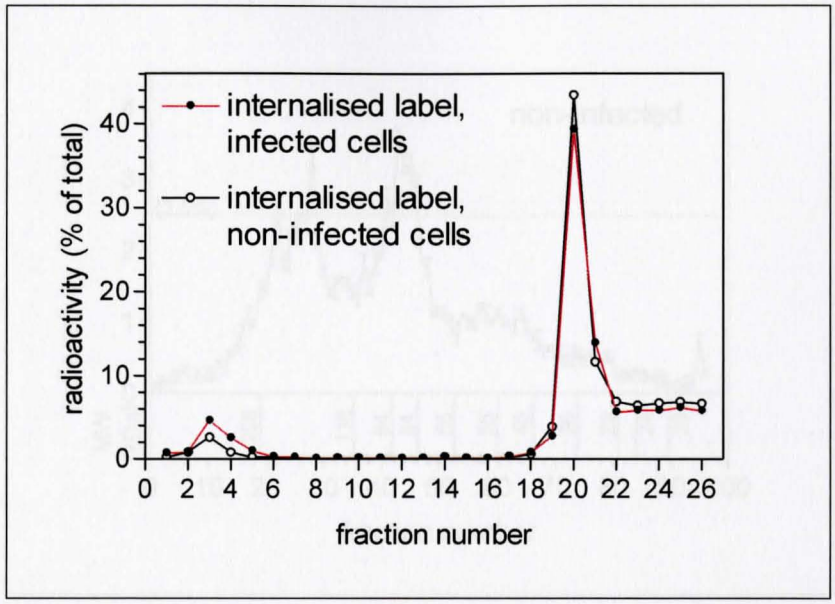

Figure A3: Sedimentation on 27% Percoll: reproduced experiment to Figure 1.1C
The experiment was done as described for Figure 1.1C.

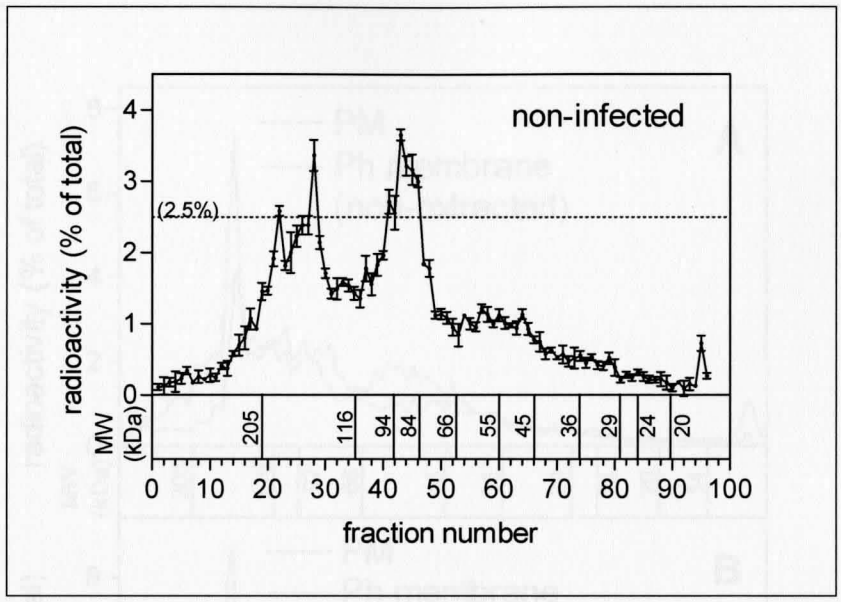

Figure A4: <u>En/PM profile for non-infected cells</u>
This experiment was a reproduction to Figure 2.3A, except that the label was internalised in this case but not removed afterwards. Non-infected BMDM were labelled with ^{14}C-galactose, followed by internalisation of label for 2 h. A PNS was prepared. The ^{14}C-En/PM was subjected to gel electrophoresis. Each data point was plotted as the mean and standard deviation of 3 scintillation counts. A similar profile was obtained for En/PM as compared to PM only from non-infected cells.

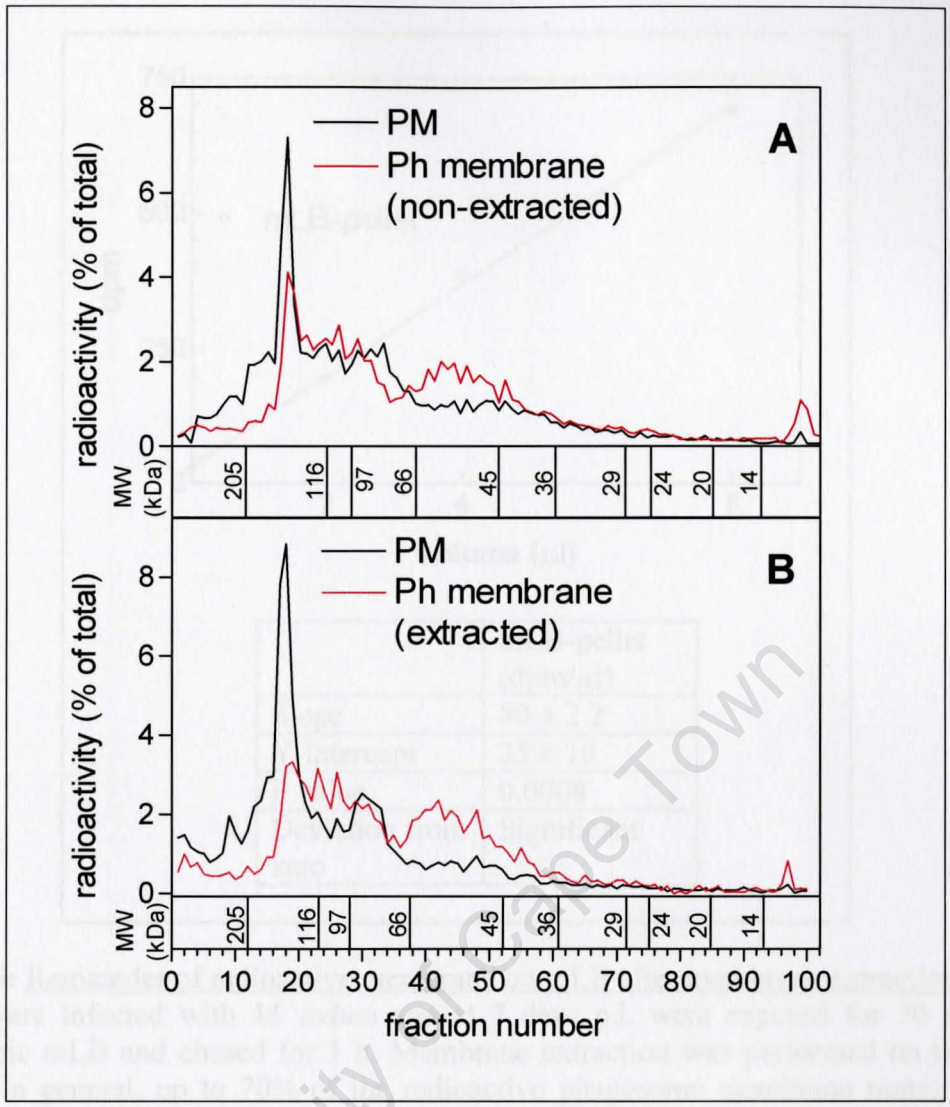

Figure A5: Comparison between PM and phagosome membrane profiles: reproduced experiments to Figure 2.7 Ph and PM were prepared, isolated and treated as described in Figure 2.7. It is clear that there are specific variations from profile to profile, but the overall result of depletion and enrichment of surface-derived glycoproteins in the phagosome membrane stayed constant.

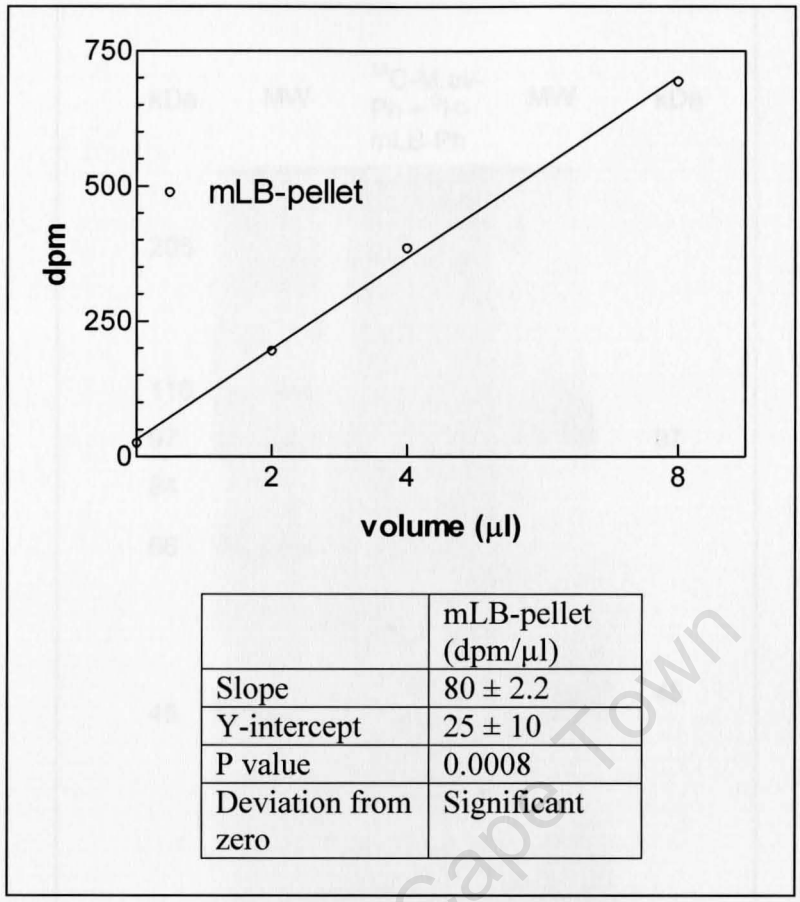

	mLB-pellet (dpm/µl)
Slope	80 ± 2.2
Y-intercept	25 ± 10
P value	0.0008
Deviation from zero	Significant

Figure A6: Remainder of radioactive membrane on mLB after membrane extraction
BMDM were infected with *M. avium* and at 7 days p.i. were exposed for 30 minutes to hydrophobic mLB and chased for 1 h. Membrane extraction was performed on the isolated mLB-Ph. In general, up to 70% of the radioactive phagosome membrane remained on the beads after one round of membrane extraction. The remaining membrane was removed by boiling the mLB-pellet in SDS sample buffer (10% glycerol, 2.3% SDS, 8.3% of 4-fold concentrated upper gel buffer, a trace of bromophenol blue, and 5% β-mercaptoethanol, Methods).

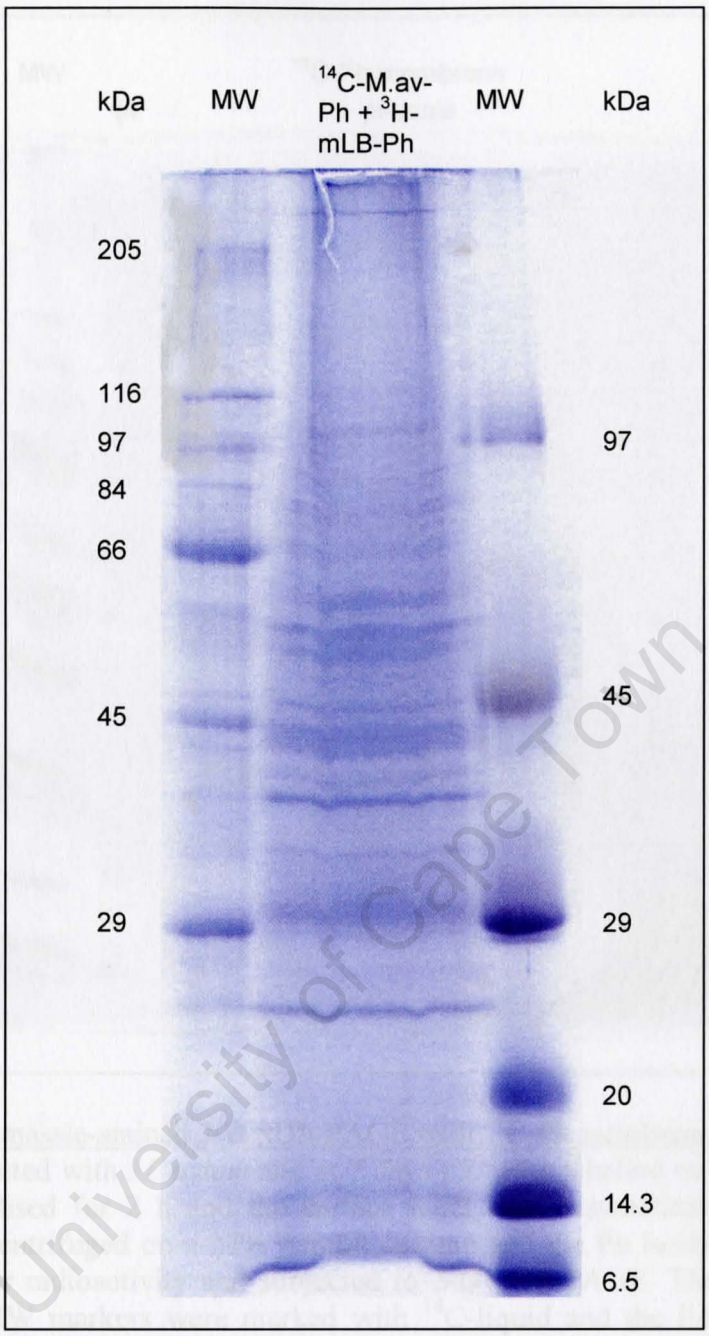

Figure A7: Coomassie stained 1-D SDS-PAGE showing bands for Ph membrane from M.av-Ph and mLB-Ph: reproduced experiment to Figure 2.10 For this PAGE Phagosome membrane from ^{14}C-M.av-Ph was mixed with phagosome membrane from ^{3}H-mLB-Ph. The profiles from this PAGE appear in Figure 2.11A.

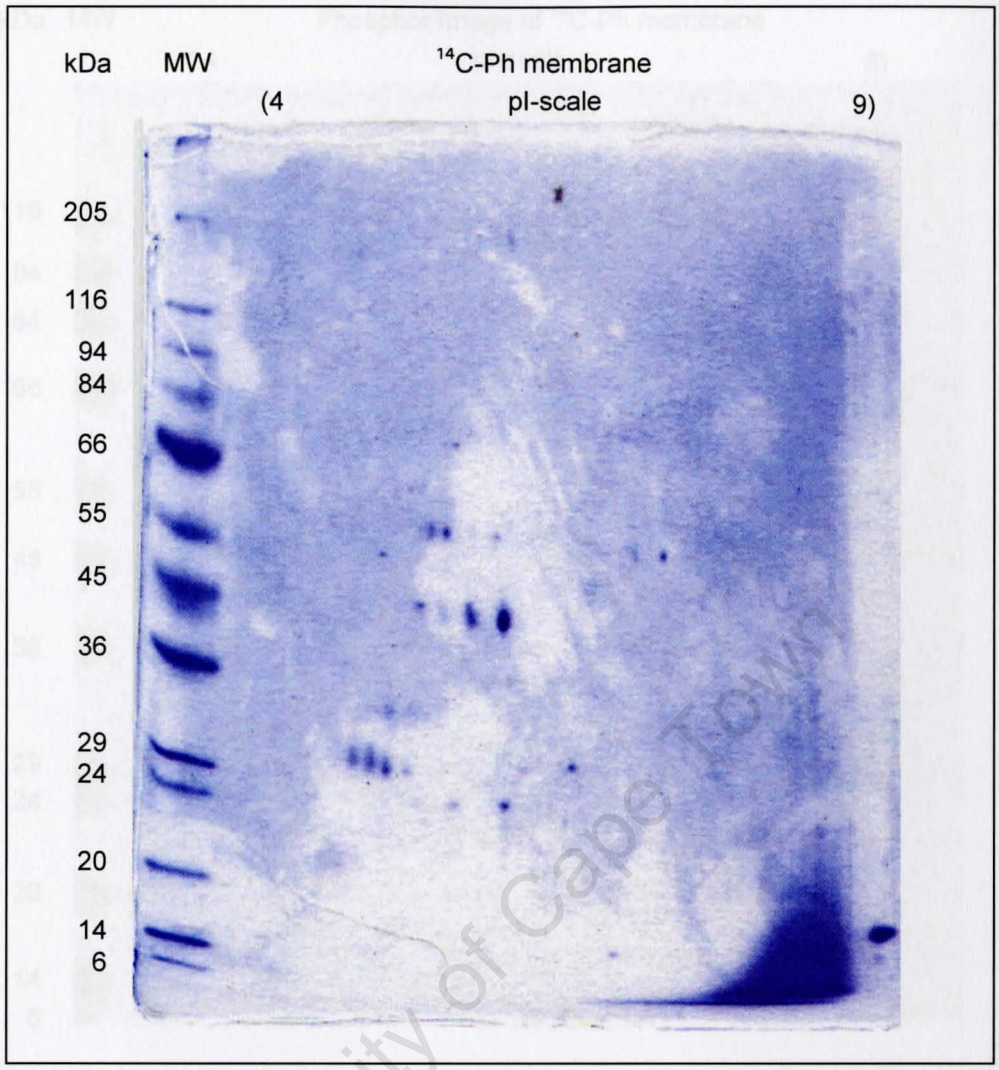

Figure A8.1: Coomassie-stained 2-D SDS-PAGE with ^{14}C-Ph membrane
BMDM were infected with *M. avium* and at 7 days p.i. were labelled with ^{14}C-galactose. The label was internalised for 2 h and the surface label was enzymatically removed. A PNS preparation was centrifuged on a 27% Percoll column and the Ph isolated. The phagosomes were measured for radioactivity and subjected to 2-D SDS-PAGE. The PAGE was stained and dried. The MW markers were marked with ^{14}C-liquid and the PAGE developed on a Phosphor Imager. The result is shown in Figure A8.2.

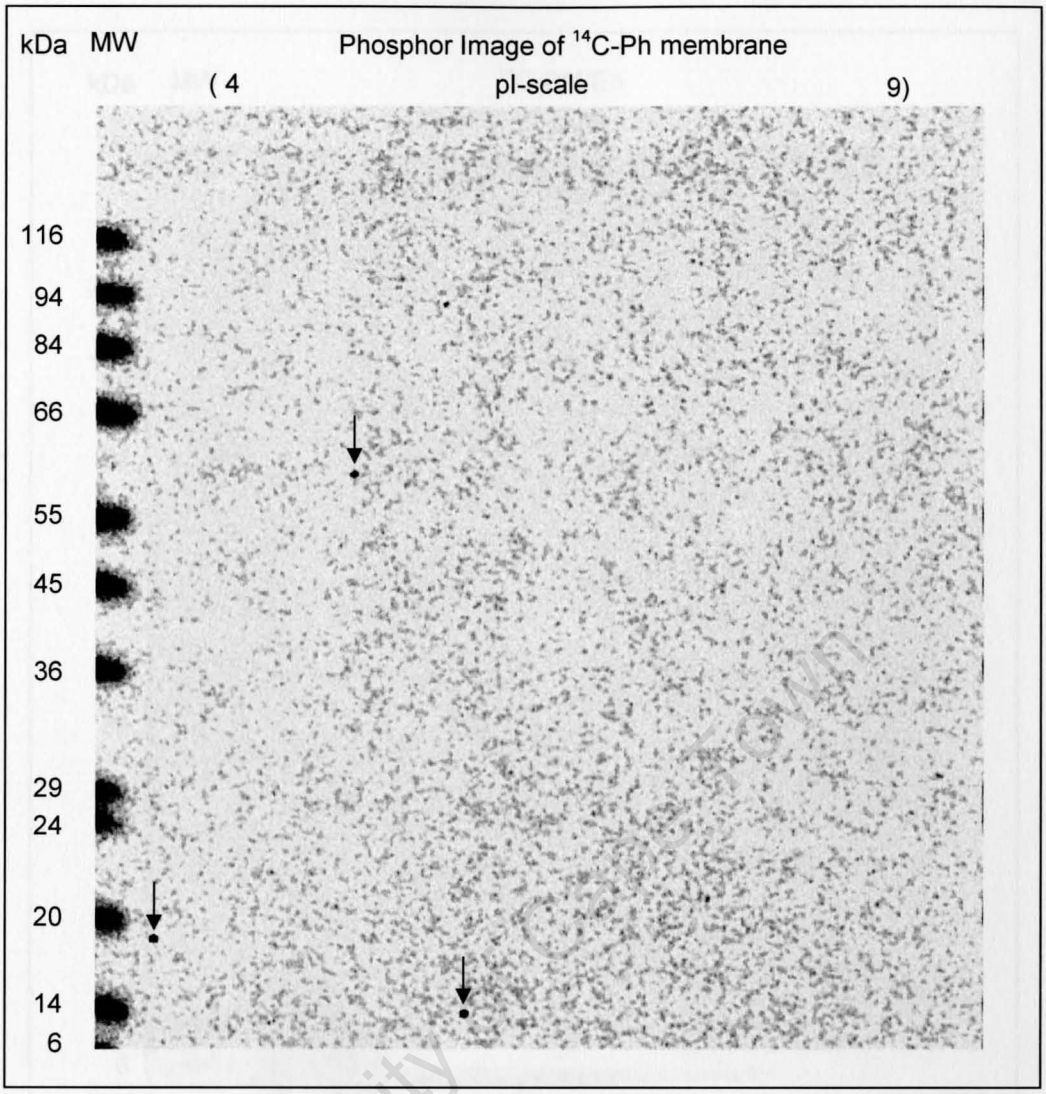

Figure A8.2: Phosphor Image of the 2-D SDS-PAGE with ^{14}C-Ph membrane (Figure A8.1)
The PAGE was developed in a Phosphor Imager for a week. Spots pointed to by the arrows were due to contamination. The MW markers showed up strongly, but no indication of labelled glycoproteins could be seen. The reason for this was most likely that only about 6 000 dpm of labelled proteins that was loaded on the IPG strip.

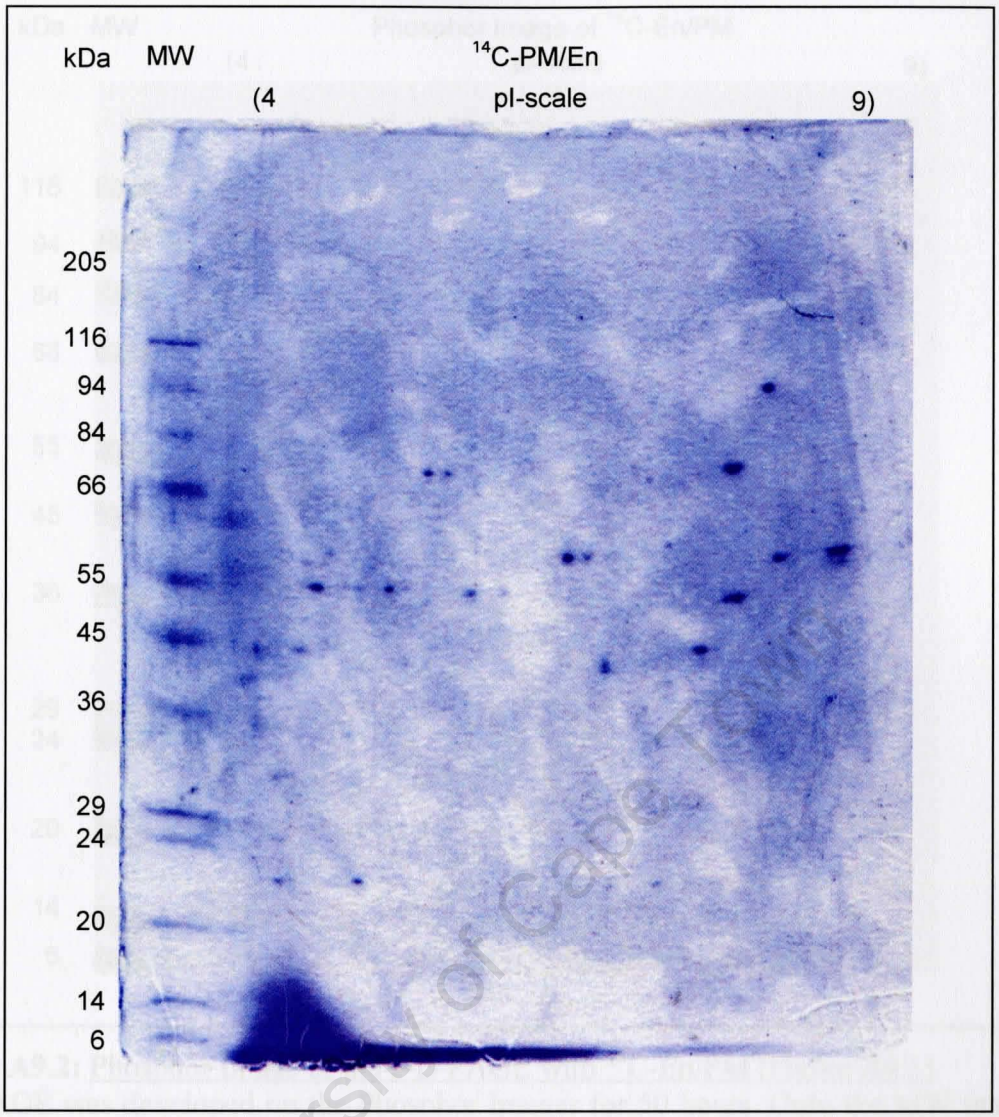

Figure A9.1: Coomassie-stained 2-D SDS-PAGE with ^{14}C-En/PM
BMDM were infected with *M. avium* and at 7 days p.i. were labelled with ^{14}C-galactose. The label was internalised for 2 h. A PNS was prepared, measured for radioactivity and subjected to 2-D SDS-PAGE. About 6 000 dpm of radioactivity was loaded. The PAGE was stained and dried. The MW markers were marked with ^{14}C-liquid and the PAGE developed on a Phosphor Imager. The result is shown in Figure A9.2.

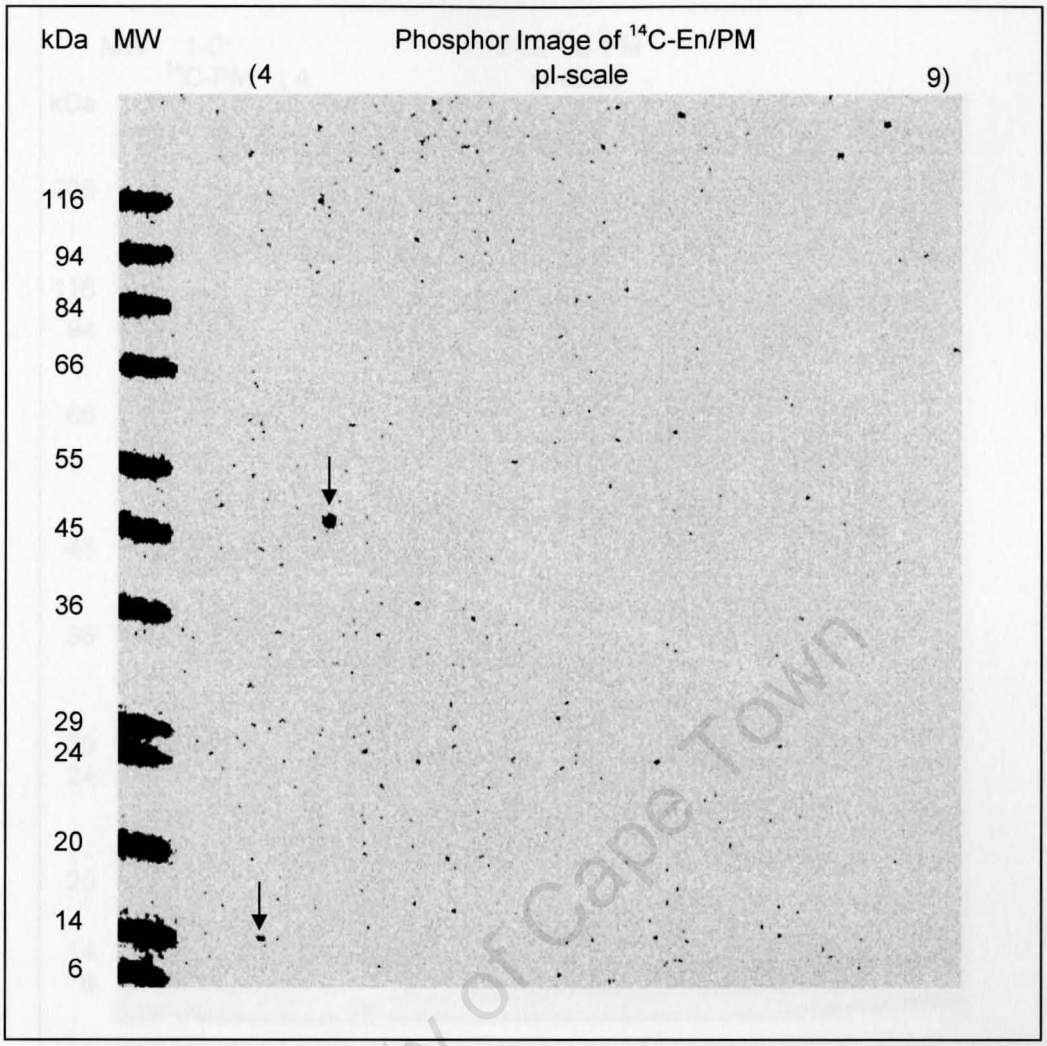

Figure A9.2: Phosphor Image of the 2-D PAGE with ^{14}C-En/PM (Figure A9.1)
The PAGE was developed on the Phosphor Imager for 50 hours. Only the MW markers and spots of contamination (arrows) showed up. The same amount of radioactivity as for the ^{14}C-Ph was used. It was accepted that the reason for no other bands appearing was due to the low concentration of radioactivity on the PAGE.

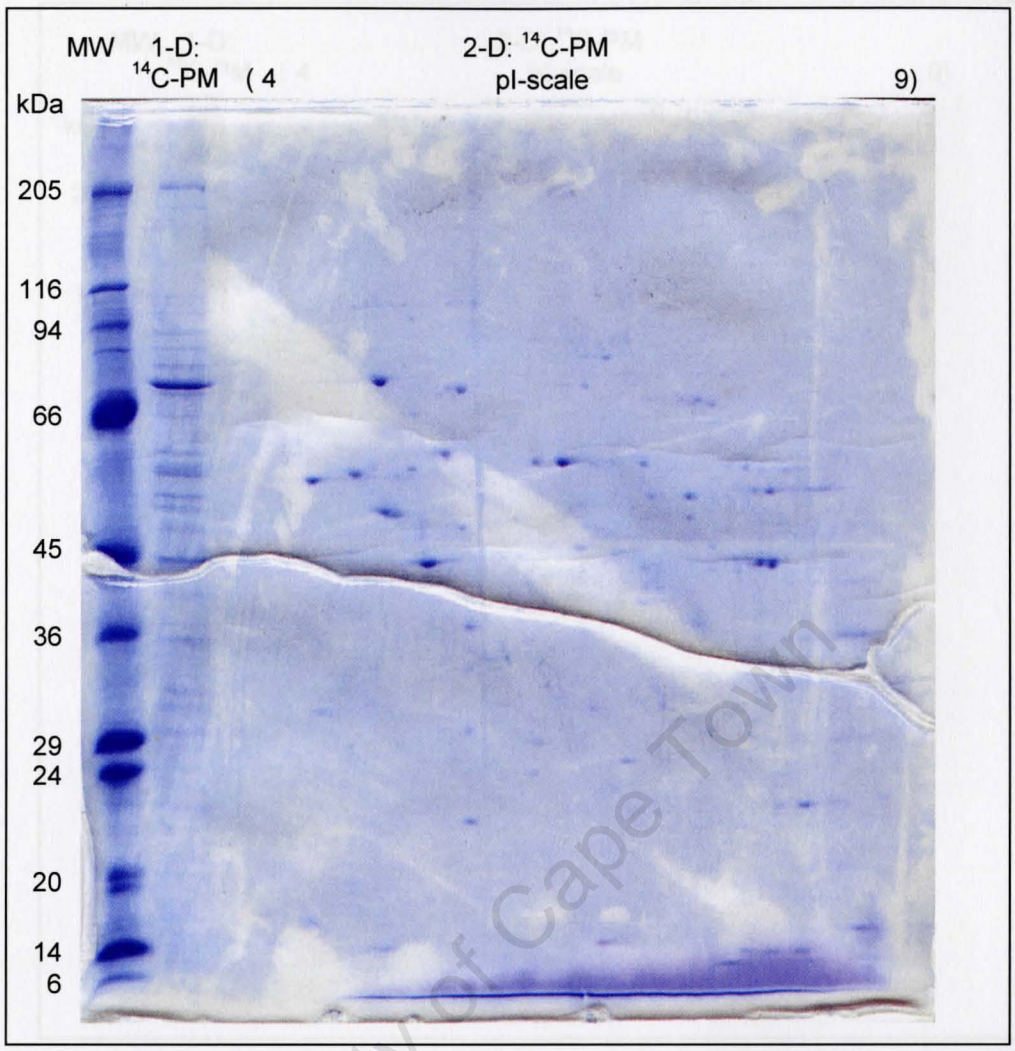

Figure A10.1: Coomassie-stained 2-D SDS-PAGE with P388D$_1$ ^{14}C-PM to test the detection limit of the Phosphor Imager with a specific amount of radioactivity P388D$_1$ macrophages were labelled with ^{14}C-galactose. A PNS preparation was centrifuged on a 27% Percoll column and the PM (light density fraction) isolated. Equal amounts (50 000 dpm) of radioactive membrane were subjected to 2-D and 1-D electrophoresis, using the same SDS-PAGE (as described). The SDS-PAGE was stained, dried and developed on a Phosphor Imager (as described). The autoradiograph is shown in Figure A10.2. For the P388D$_1$ cells most of the visibly stained proteins appeared in the region of 66 – 45 kDa. In the case of the BMDM this region was already focussed on.

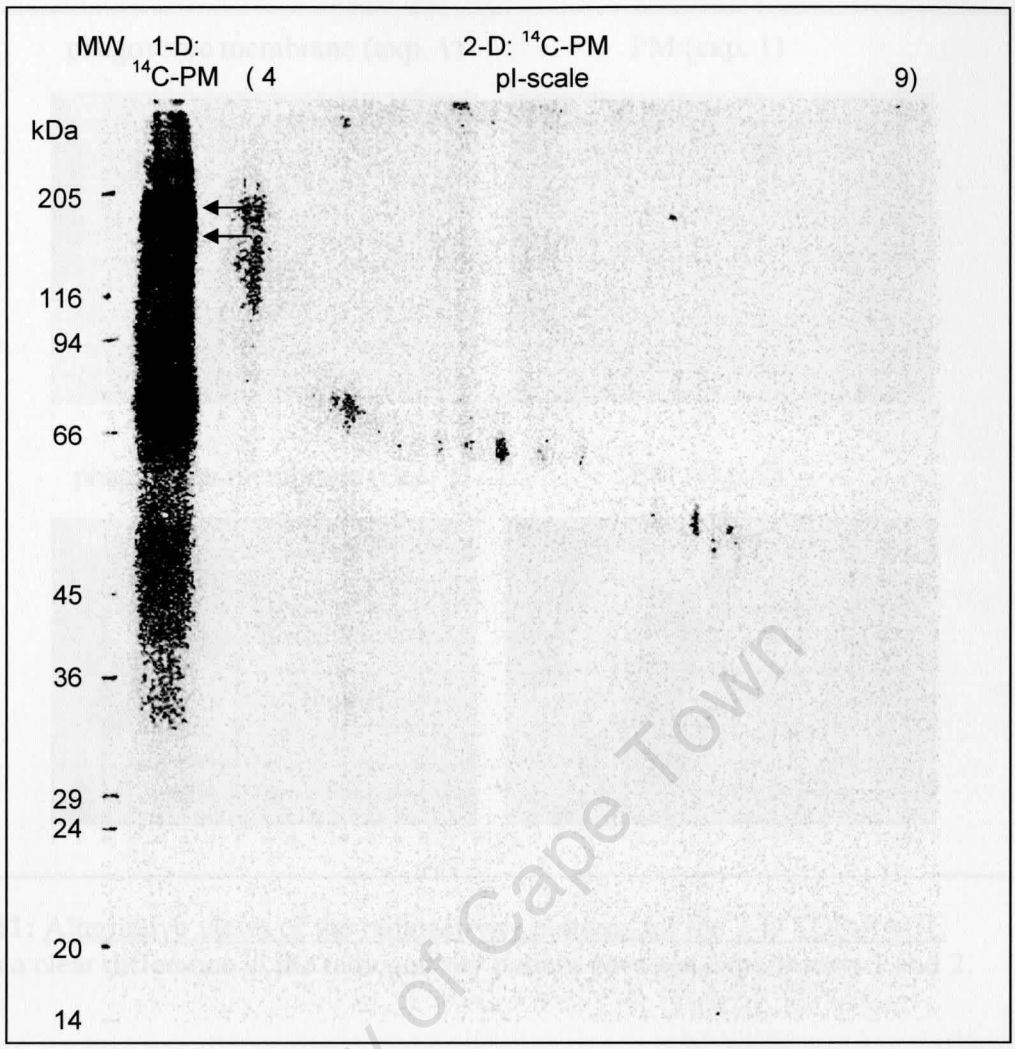

Figure A10.2: Autoradiograph of the 2-D SDS-PAGE in Figure A10.1
The PAGE was on the Phosphor Imager for 25 h. Intense bands developed from the 1-D lane. The arrows show the bands which might correspond to the bands in the same position on the PAGE in Figure 2.12B. Several bands can be seen on the 2-D area of the PAGE. These bands (spots) are streaky, indicating their glycocidic nature. It is interesting that these spots occur largely in the region on the PAGE where the enriched glycoproteins for the phagosome membrane can be found and also correspond to the area where most visible spots are on the PAGE. From experience it was predicted that a longer exposure time would most likely only increased the intensity of the signals already seen as well as the background, but unlikely produce signals not seen here. Probably more radioactivity must be used to detect low abundance or poorly labelled surface-derived glycoproteins for detection with the Phosphor Imager, making it an unfeasible approach.

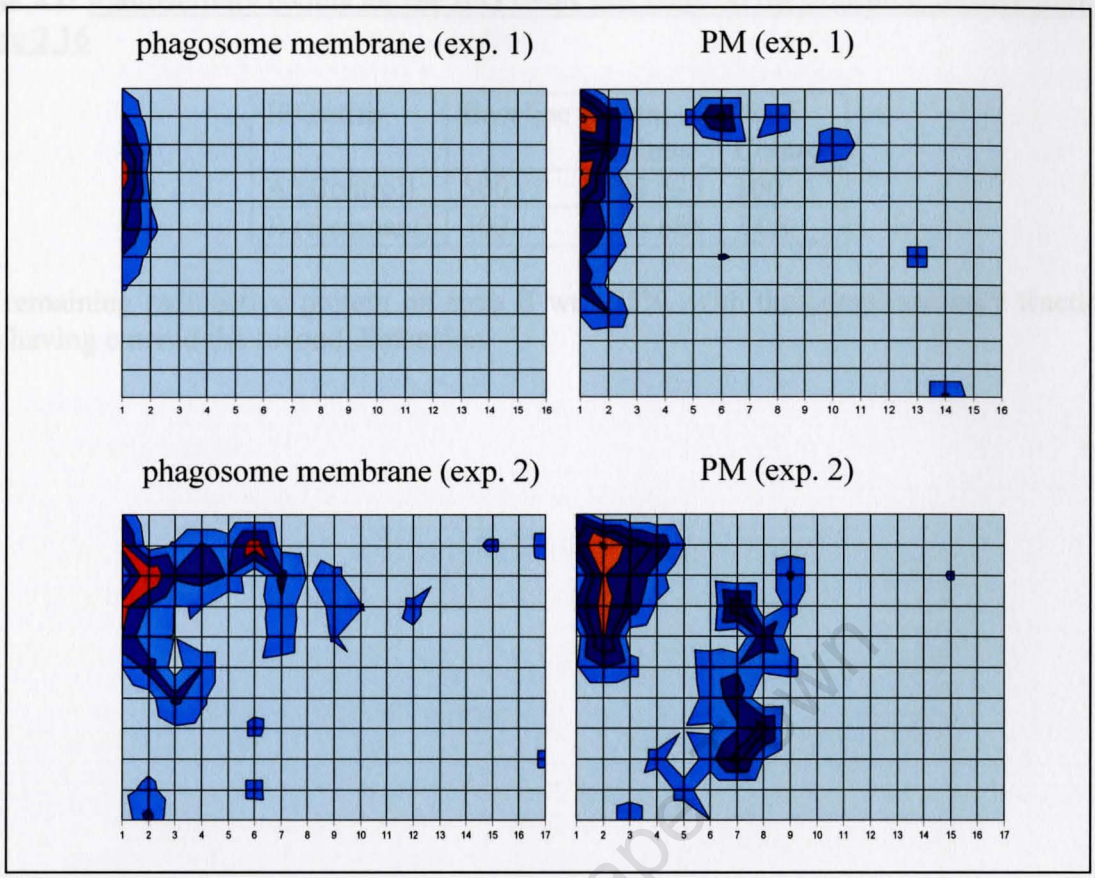

Figure A11: Alternative views of the radioactivity patterns for the 2-D SDS-PAGE
There was a clear difference in the radioactivity pattern between experiments 1 and 2.

Table A1: Radioactivity counts for the IPG strips that were on the Phosphor Imager from Figure 2.16

IPG strip	Baseline	Total Counts	% of Control
A (Control)	500	593 533	100
B (Remnant)	300	206 688	34.8

The remaining radioactive protein on strip B was 35%, with the complementary fraction of 65% having entered the second dimension.

Table A2: Complete list of identified proteins from the comparison between Ph membrane and PM in Figure 3.1 The protein identity search was performed using the Mascot search engine (Database NCBInr 20020719, http://www.matrixscience.com) with the following parameters: Type of search: MS/MS Ion Search, Enzyme: Trypsin, Variable modifications: Oxidation (M), Mass values: Monoisotopic, Protein Mass: Unrestricted, Peptide Mass Tolerance: ± 0.5 Da, Fragment Mass Tolerance: ± 0.8 Da, Maximum Missed Cleavages: 1 and Instrument type: ESI-QUAD-TOF. Figure A12 shows a portion of the results sheet from the database search for Gel strip Ph8. Obvious contaminants have been excluded from the list. From the total list of identified proteins, a selection of surface-derived glycoproteins is shown in Table 3.1. (All protein sequencing was kindly performed by Dr G Plum, Cologne.)

Gel strip Ph1

List No.	Protein name	MW (Da)	Pep-tides	Total score
5	**(U29947) alpha-D-mannosidase**	112 352	1	59
6	**(NM_020258) solute carrier family 37 (glycerol-3-phosphate transporter), member 1; cAMP inducible 2**	55 037	1	49
7	**(XM_131951) similar to hydroxyacyl-Coenzyme A dehydrogenase/3-ketoacyl-Coenzyme A thiolase/enoyl-Co**	51 353	1	47
9	**IgG Fc binding protein - mouse (fragment**	109 137	1	36
10	**(NM_019658) soc-2 (suppressor of clear) homolog (C elegans); suppressor of clear, C. elegans, homo**	64 909	1	30

Gel strip Ph3

List No.	Protein name	MW (Da)	Pep-tides	Total score
5	**(AF218253) vacuolar proton-translocating ATPase 100 kDa**	93 446	1	75
9	**IgG Fc binding protein - mouse (fragment**	109 137	1	44
10	**(AY061989) hypothetical protein [Mus musculus**	53 416	1	39
11	**(NM_020258) solute carrier family 37 (glycerol-3-phosphate transporter), member 1; cAMP inducible 2**	55 037	1	36

Gel strip Ph4

List No.	Protein name	MW (Da)	Pep-tides	Total score
6	**(XM_126698) expressed sequence AI626930**	52 834	2	95

Gel strip Ph5

List No.	Protein name	MW (Da)	Pep-tides	Total score
3	**(XM_126698) expressed sequence AI626930**	52 834	2	155
10	**(NM_033073) hypothetical protein D15Wsu77e**	50 678	2	36

Gel strip Ph6…

Gel strip Ph6

List No.	Protein name	MW (Da)	Pep-tides	Total score
2	**Beta hexosaminidase beta**	61 127	2	57
3	**(NM_031843) dipeptidyl peptidase 7; dipeptidyl peptidase II precursor**	56 234	2	56
4	**IgG Fc binding protein**	109 137	1	36
5	**(AF356520) axonemal dynein heavy chain 8 long form**	540 945	2	33

Gel strip Ph8

List No.	Protein name	MW (Da)	Pep-tides	Total score
1	**(AF079458) alpha-N-acetylgalactosaminidase**	47 204	4	184
2	**(NM_133792) lysophospholipase 3**	47 277	4	141
3	**(AF322054) dendritic cell-associated transmembrane protein precursor**	63 634	4	85
6	**MPS1 protein - mouse (fragment**	73 120	3	51
7	**(NM_013463) galactosidase, alpha; alpha-galactosidase**	47 611	1	50
9	**(NM_008720) Niemann Pick type C1**	142 795	1	38
11	**(AJ011912) putative tripeptidyl peptidase I**	58 667	2	32

Gel strip PM3

List No.	Protein name	MW (Da)	Pep-tides	Total score
1	**(NM_133933) expressed sequence AU018702**	68 486	11	409
2	**(XM_127743) similar to L-plastin (Lymphocyte cytosolic protein 1) (LCP-1) (65 kDa macrophage protei**	70 105	6	312
3	**(NM_133838) EH domain containing protein MPAST2**	61 453	6	270
4	**(NM_012019) programmed cell death 8 (apoptosis inducing factor); apoptosis-inducing factor**	66 724	3	173
5	**(AY044265) dihydrolipoamide S-acetyltransferase Precursor**	59 047	3	94
6	**(NM_007458) adaptor-related protein complex AP-2, alpha 1 subunit**	107 596	2	89
7	**(NM_019642) ribophorin II; ribophorin**	66 261	2	81
12	**(NM_015829) solute carrier family 25 (mitochondrial Carrier; adenine nucleotide translocator), memb**	74 420	1	52
14	**Chain A, Crystal Structure Of The Arf-Gap Domain And Ankyrin Repeats Of Papbeta**	30 827	1	32

Gel strip PM4…

Gel strip PM4

List No.	Protein name	MW (Da)	Pep-tides	Total score
1	**chaperonin groEL precursor**	60 903	9	309
2	**(NM_007591) calreticulin**	47 965	7	237
3	**Pyruvate kinase, M2 isozyme**	57 850	5	96
5	**(U14655) snoN2**	71 012	2	32

Gel strip PM5

List No.	Protein name	MW (Da)	Pep-tides	Total score
1	**Protein disulfide isomerase precursor (PDI) (Prolyl 4-hydroxylase beta subunit) (Cellular thyroid**	57 108	24	1106
4	**(NM_007861) dihydrolipoamide dehydrogenase**	54 178	7	282
8	**(NM_009163) sphingosine phosphate lyase 1**	63 666	4	143
9	**chaperonin groEL precursor**	60 903	5	121
10	**(NM_009898) coronin, actin binding protein 1A; Coronin-like actin binding protein; coronin 1a; coro**	50 957	4	119
12	**(NM_007807) cytochrome b-245, beta polypeptide**	65 262	4	95
14	**(NM_057213) ATPase, H+ transporting, lysosomal (vacuolar proton pump), beta 56/58 kDa, isoform 2**	56 515	2	73
17	**(XM_128952) lectin, mannose-binding, 1**	57 753	1	64
18	**(XM_125941) membrane bound C2 domain containing protein**	121 478	2	56
22	**(NM_008749) nucleobindin**	52 965	1	43
23	**(NM_008879) plastin 2, L**	70 157	1	42
24	**thromboxane-A synthase (EC 5.3.99.5)**	60 197	2	42
26	**(AK008830) evidence:NAS~hypothetical protein~putative**	18 500	1	38
27	**protein-tyrosine kinase (EC 2.7.1.112) lyn, long splice form**	58 774	1	36

Gel strip PM6

List No.	Protein name	MW (Da)	Pep-tides	Total score
3	**(NM_008133) glutamate dehydrogenase**	61 298	15	537
4	**IMMUNE-RESPONSIVE PROTEIN 1**	71 240	7	299
5	**(NM_007437) aldehyde dehydrogenase family 3, subfamily A2; alcohol dehydrogenase family 3, subfamily**	53 908	5	235
7	**(XM_131377) aldehyde dehydrogenase 1 family, member B1**	57 516	7	198
8	**(NM_057213) ATPase, H+ transporting, lysosomal (vacuolar proton pump), beta 56/58 kDa, isoform 2**	56 515	5	183
9	**serine C-palmitoyltransferase (EC 2.3.1.50) Lcb2 chain**	63 013	2	118

Continued…

Gel strip PM6

List No.	Protein name	MW (Da)	Pep-tides	Total score
10	**(AF362571) aldehyde dehydrogenase ALDH3B1**	49 908	3	97
11	**(NM_133826) expressed sequence AU022349**	55 805	2	76
13	**protein-tyrosine kinase (EC 2.7.1.112) lyn, long splice form**	58 774	1	63
14	**(M57696) lyn A protein tyrosine kinase**	58 835	1	63
15	**(NM_016773) nucleobindin 2; DNA-binding protein NEFA precursor**	50 243	2	59
21	**(NM_009841) CD14 antigen**	39 179	1	34
22	**(J03302) lipoprotein lipase precursor**	52 207	1	32

Gel strip PM8

List No.	Protein name	MW (Da)	Pep-tides	Total score
1	**(XM_131951) similar to hydroxyacyl-Coenzyme A dehydrogenase/3-ketoacyl-Coenzyme A thiolase/enoyl-Co**	51 353	12	423
4	**(AK002379) data source:MGD, source key: MGI: 95530, evidence:ISS~fumarate hydratase 1~putative**	50 078	4	206
6	**MHC class I histocompatibility antigen H-2D(b) alpha chain**	38 378	4	192
7	**(NM_133838) EH domain containing protein MPAST2**	61 453	3	187
9	**(NM_007838) dolichyl-di-phosphooligosaccharide-protein glycotransferase**	48 983	5	183
10	**H-2 CLASS I HISTOCOMPATIBILITY ANTIGEN, D-D ALPHA CHAIN PRECURSOR (H-2D(D))**	41 084	4	163
11	**(AF043943) tapasin**	49 725	4	160
12	**(NM_029572) ERp44**	46 823	5	125
13	**(NM_009898) coronin, actin binding protein 1A; coronin-like actin binding protein; coronin 1a; coro**	50 957	3	115
15	**(NM_145367) similar to thioredoxin related protein**	36 092	3	102

Table A3: List of identified proteins of significance from the comparison between M.av-Ph and mLB-Ph in Figure 3.2 The protein identity search was performed using the Mascot search engine (Database NCBInr 20050416, http://www.matrixscience.com) with the same parameters stated for Table A2. Figure A13 shows a portion of the results sheet from the database search for Gel strip 8. Obvious contaminants have been excluded. From this list a selection of surface-derived glycoproteins was made which is shown in Table 3.1.

Gel strip 3 (MW region of 350 kDa)

List No.	Protein name	MW (Da)	Pep-tides	Total score
1	**osteoclast-specific 116-kDa V-ATPase subunit**	94 084	14	451
2	**Unknown (protein for MGC:116262)**	59 555	4	231
4	**Niemann Pick type C1**	145 475	8	192
5	**Na,K-ATPase alpha-1 subunit**	114 504	4	180
7	**GLUT4 vesicle protein**	121 369	4	166
21	**nogo-B**	38 543	5	79
30	**lysosomal membrane glycoprotein A**	41 936	3	57
32	**Low density lipoprotein receptor-related protein 1**	523 309	2	54

Gel strip 4 (MW region of 320 kDa)

List No.	Protein name	MW (Da)	Pep-tides	Total score
1	**osteoclast-specific 116-kDa V-ATPase subunit**	94 084	10	405
2	**Niemann Pick type C1**	145 475	12	318
3	**Na,K-ATPase alpha-1 subunit**	114 504	6	181
5	**tumor rejection antigen gp96**	92 703	3	153
7	**mKIAA0886 protein**	135 859	8	141
14	**GLUT4 vesicle protein**	121 369	3	114
34	**unnamed protein product**	142 716	1	64
35	**Low density lipoprotein receptor-related protein 1**	523 309	3	61
38	**Macrosialin**	35 322	2	59
46	**lysosomal membrane glycoprotein A**	41 936	1	48
47	**NPC1 (Niemann-Pick disease, type C1, gene)-like 1**	149 318	1	48

Gel strip 5 (MW region of 300 kDa)

List No.	Protein name	MW (Da)	Pep-tides	Total score
1	**Niemann Pick type C1**	145 475	8	230
2	**ATPase alpha1,Na/K**	114 132	8	201
4	**osteoclast-specific 116-kDa V-ATPase subunit**	94 084	8	173
6	**tumor rejection antigen gp96 (predicted)**	74 390	4	152
9	**unnamed protein product**	142 716	3	93
11	**Macrosialin**	35 322	2	90
14	**lysosomal membrane glycoprotein A**	41 936	3	85
18	**nogo-B**	38 543	6	80

Continued…

Gel strip 5 (MW region of 300 kDa)

List No.	Protein name	MW (Da)	Pep-tides	Total score
31	**leukocyte common antigen**	152 410	2	58
39	**NPC1 (Niemann-Pick disease, type C1, gene)-like 1**	149 318	1	43
45	**mFLJ00021 protein**	51 805	1	40
46	**PREDICTED: similar to lipoprotein receptor-related Protein**	523 489	3	40

Gel strip 6 (MW region of 280 kDa)

List No.	Protein name	MW (Da)	Pep-tides	Total score
2	**osteoclast-specific 116-kDa V-ATPase subunit**	94 084	11	261
3	**Niemann Pick type C1**	145 475	9	257
4	**tumor rejection antigen gp96**	92 703	6	181
19	**Na,K-ATPase alpha-1 subunit**	114 504	4	85
25	**GLUT4 vesicle protein**	121 369	2	75
26	**unnamed protein product**	142 716	2	74
29	**Sialoadhesin**	175 051	4	69
33	**nogo-B**	38 543	3	67
37	**lysosomal membrane glycoprotein A**	41 936	3	62
42	**Macrosialin**	35 322	2	55

Gel strip 7 (MW region of 260 kDa)

List No.	Protein name	MW (Da)	Pep-tides	Total score
2	**Niemann Pick type C1**	145 475	8	194
3	**unnamed protein product**	65 481	6	169
4	**osteoclast-specific 116-kDa V-ATPase subunit**	94 084	6	165
12	**Sialoadhesin**	175 051	5	111
17	**GLUT4 vesicle protein**	121 369	2	102
18	**Macrosialin**	35 322	3	96
20	**Endoplasmin**	15 234	2	89
26	**Atp1a1 protein**	109 650	5	71
34	**nogo-B**	38 543	2	56
35	**unnamed protein product**	142 716	1	52
37	**NPC1 (Niemann-Pick disease, type C1, gene)-like 1**	149 318	1	47

Gel strip 8 (MW region of 250 kDa)

List No.	Protein name	MW (Da)	Pep-tides	Total score
1	**Niemann Pick type C1**	145 475	4	111
2	**Macrosialin**	35 322	2	94
3	**osteoclast-specific 116-kDa V-ATPase subunit**	94 084	3	82
6	**mKIAA1207 protein**	237 934	2	69
11	**tumor rejection antigen gp96**	92 703	2	37

Gel strip 9...

Gel strip 9 (MW region of 240 kDa)

List No.	Protein name	MW (Da)	Pep-tides	Total score
1	**Sialoadhesin**	185 255	27	883
5	**Niemann Pick type C1**	145 475	5	156
8	**osteoclast-specific 116-kDa V-ATPase subunit**	94 084	5	121
9	**GLUT4 vesicle protein**	121 369	4	118
13	**Macrosialin**	35 322	2	99
14	**Na,K-ATPase alpha-1 subunit**	114 504	3	93
23	**lysosomal membrane glycoprotein A**	41 936	2	55
27	**unnamed protein product**	142 716	1	51

Gel strip 10 (MW region of 230 kDa)

List No.	Protein name	MW (Da)	Pep-tides	Total score
1	**Sialoadhesin**	185 331	19	648
3	**Macrosialin**	35 322	2	98
4	**protein-tyrosine-phosphatase (EC 3.1.3.48) Ly-5 precursor (B-cell variant)**	146 224	2	70
9	**osteoclast-specific 116-kDa V-ATPase subunit**	94 084	2	51
10	**similar to osmotic stress protein**	148 900	3	49
12	**Niemann Pick type C1**	145 475	1	39

Gel strip 11 (MW region of 220 kDa)

List No.	Protein name	MW (Da)	Pep-tides	Total score
1	**Sialoadhesin**	185 255	8	228
3	**L-CA variant 3**	134 114	1	55
5	**osteoclast-specific 116-kDa V-ATPase subunit**	94 084	2	47

Gel strip 12 (MW region of 200 kDa)

List No.	Protein name	MW (Da)	Pep-tides	Total score
1	**lymphocyte common antigen**	146 180	4	117
5	**Sialoadhesin**	185 255	3	78

Gel strip 13 (MW region of 190 kDa)

List No.	Protein name	MW (Da)	Pep-tides	Total score
1	**IQ motif containing GTPase activating protein 1**	189 437	8	194
2	**alanyl (membrane) aminopeptidase**	110 022	4	92
3	**lymphocyte common antigen**	146 180	5	71
8	**Lysosome-associated membrane glycoprotein 2 precursor (LAMP-2) (Lysosomal membrane glycoprotein-typ**	46 131	2	48
13	**Macrosialin**	35 322	1	37

Gel strip 14...

Gel strip 14 (MW region of 180 kDa)

List No.	Protein name	MW (Da)	Pep-tides	Total score
1	**Integrin alpha M**	128 541	5	199
8	**L-CA variant 3**	134 114	1	39

Gel strip 15 (MW region of 170 kDa)

List No.	Protein name	MW (Da)	Pep-tides	Total score
1	**integrin alpha M**	128 541	10	237
2	**Alanyl (membrane) aminopeptidase**	110 038	8	197

Gel strip 18 (MW region of 140 kDa)

List No.	Protein name	MW (Da)	Pep-tides	Total score
1	**Alanyl (membrane) aminopeptidase**	110 038	16	501
2	**Integrin alpha M**	128 541	5	151
3	**lysosomal membrane glycoprotein A**	41 936	3	136

Gel strip 25 (MW region of 105 kDa)

List No.	Protein name	MW (Da)	Pep-tides	Total score
1	**osteoclast-specific 116-kDa V-ATPase subunit**	94 084	8	282
2	**lysosomal membrane glycoprotein A**	41 936	6	194
5	**alpha glucosidase 2 alpha neutral subunit**	109 791	7	134
6	**similar to oxysterol-binding protein-like protein 8; oxysterol-binding protein-related protein 8;**	131 944	3	121
11	**Ogdh protein**	117 572	2	86
12	**tumor rejection antigen gp96**	92 703	4	65
13	**MALA-2**	59 520	2	64
14	**mKIAA0253 protein**	80 479	3	64
16	**Inhibitory receptor SHPS-1 short isoform**	32 057	1	60
19	**Macrosialin**	35 322	2	57

Gel strip 28 (MW region of 90 kDa)

List No.	Protein name	MW (Da)	Pep-tides	Total score
1	**Tumor rejection antigen gp96**	92 703	29	809
2	**CD18 antigen preprotein**	88 031	18	577
4	**Murine valosin-containing protein**	89 936	4	176
5	**Platelet glycoprotein IV (GPIV) (GPIIIB) (CD36 antigen) (PAS IV) (PAS-4 protein)**	53 234	4	140
6	**lysosomal membrane glycoprotein 2 precursor**	46 131	5	138
7	**lysosomal membrane glycoprotein A**	41 936	3	133
8	**CD98 heavy chain**	58 899	3	97

Continued…

Gel strip 28 (MW region of 90 kDa)

List No.	Protein name	MW (Da)	Pep-tides	Total score
9	**Macrosialin**	35 322	2	89
12	**beta5A integrin**	91 273	1	52
15	**GLUT4 vesicle protein**	78 708	1	42
16	**Toll-like receptor 2**	90 590	1	40
17	**solute carrier family 3, member 2**	58 150	2	40

Gel strip 30 (MW region of 85 kDa)

List No.	Protein name	MW (Da)	Pep-tides	Total score
2	**Platelet glycoprotein IV (GPIV) (GPIIIB) (CD36 antigen) (PAS IV) (PAS-4 protein)**	53 234	7	262
4	**protein kinase C substrate 80K-H**	59 725	5	193
6	**lysosomal membrane glycoprotein 2 precursor**	46 131	4	151
7	**Cell surface protein CD36**	53 268	5	148
8	**CD98 heavy chain**	58 899	3	143
10	**lysosomal membrane glycoprotein A**	41 936	3	137
12	**CD18 antigen preprotein**	88 031	4	119
17	**Macrosialin**	35 322	2	78
19	**scavenger receptor class B, member 2**	54 466	2	61
20	**solute carrier family 3, member 2**	58 150	2	60

Gel strip 34 (MW region of 70 kDa)

List No.	Protein name	MW (Da)	Pep-tides	Total score
5	**Long-chain-fatty-acid--CoA ligase 1 (Long-chain acyl-CoA synthetase 1) (LACS 1)**	78 900	2	77

Gel strip 35 (MW region of 68 kDa)

List No.	Protein name	MW (Da)	Pep-tides	Total score
4	**unnamed protein product**	65 481	11	376
8	**similar to grp75**	52 213	5	249
11	**vacuolar adenosine triphosphatase subunit A**	68 567	7	173
14	**Long-chain-fatty-acid--CoA ligase 1 (Long-chain acyl-CoA synthetase 1) (LACS 1)**	78 900	3	109

Gel strip 35 (MW region of 68 kDa)

List No.	Protein name	MW (Da)	Pep-tides	Total score
15	**similar to ATPase, H+ transporting, V1 subunit A, Isoform 1**	72 884	5	108
20	**lysosomal membrane glycoprotein 2 precursor**	46 131	2	72

Gel strip 39...

Gel strip 39 (MW region of 58 kDa)

List No.	Protein name	MW (Da)	Pep-tides	Total score
4	**ATP receptor P2X4 subunit**	44 262	4	97
10	**EH-domain containing 1**	62 980	3	76
20	**putative transmembrane glycoprotein**	64 439	2	54

Gel strip 43 (MW region of 52 kDa)

List No.	Protein name	MW (Da)	Pep-tides	Total score
7	**Vacuolar adenosine triphosphatase subunit B**	56 948	3	56
8	**Putative transmembrane glycoprotein**	64 439	3	46

Gel strip 44 (MW region of 50 kDa)

List No.	Protein name	MW (Da)	Pep-tides	Total score
3	**unnamed protein product**	53 998	15	400
4	**ATPase, H+ transporting, V1 subunit B, isoform 2**	56 857	12	299
11	**ATPase, H+ transporting, V1 subunit B, isoform 1**	57 154	6	105
16	**sphingosine-1-phosphate lyase; pyridoxal-phosphate protein; SPL**	64 293	2	71
18	**putative transmembrane glycoprotein**	64 439	3	49

Gel strip 49 (MW region of 45 kDa)

List No.	Protein name	MW (Da)	Pep-tides	Total score
1	**H-2D cell surface glycoprotein**	38 606	9	261
3	**H-2 class I histocompatibility antigen, K-B alpha chain precursor (H-2K(B))**	41 675	4	142
4	**class I histocompatibility antigen H-2D-r alpha chain Precursor**	41 002	3	126
6	**class I histocompatibility antigen H-2D-s alpha chain Precursor**	40 799	3	117
7	**MHC class I heavy chain precursor**	40 894	3	113
10	**nogo-A**	127 126	3	106
12	**Tapasin**	50 010	2	87
15	**putative transmembrane glycoprotein**	64 439	3	75

Gel strip 51 (MW region of 43 kDa)

List No.	Protein name	MW (Da)	Pep-tides	Total score
8	**nogo-B**	38 543	5	167
17	**putative transmembrane glycoprotein**	64 439	3	61

Gel strip 55...

Gel strip 55 (MW region of 37 kDa)

List No.	Protein name	MW (Da)	Pep-tides	Total score
5	**putative transmembrane glycoprotein**	64 439	4	115

Gel strip 56 (MW region of 36 kDa)

List No.	Protein name	MW (Da)	Pep-tides	Total score
4	**putative transmembrane glycoprotein**	64 439	5	100

MATRIX SCIENCE **Mascot Search Results**

Search title : Ph8
MS data file : 1584.pkl
Database : NCBInr 20020719 (1028309 sequences; 324619532 residues)
Taxonomy : Mus musculus (house mouse) (42752 sequences)
Timestamp : 12 Nov 2003 at 18:52:52 GMT
Significant hits:

gi|3396057 (AF079458) alpha-N-acetylgalactosaminidase
gi|19527008 (NM_133792) lysophospholipase 3 [Mus
gi|13172897 (AF322054) dendritic cell-associated
gi|6678647 (NM_008476) keratin complex 2, gene 6a; 60-
gi|71527 keratin, 59K type I cytoskeletal - mouse
gi|2137564 MPS1 protein - mouse (fragment)
gi|7305089 (NM_013463) galactosidase, alpha; alpha-
gi|6753556 (NM_009983) cathepsin D [Mus musculus]
gi|6679104 (NM_008720) Niemann Pick type C1 [Mus
gi|16716569 (NM_053243) trypsinogen 16 [Mus musculus]
gi|3766471 (AJ011912) putative tripeptidyl peptidase I [Mus musculus]

Probability Based Mowse Score

Score is -10*Log(P), where P is the probability that the observed match is a random event.
Individual ions scores > 29 indicate identity or extensive homology (p<0.05).

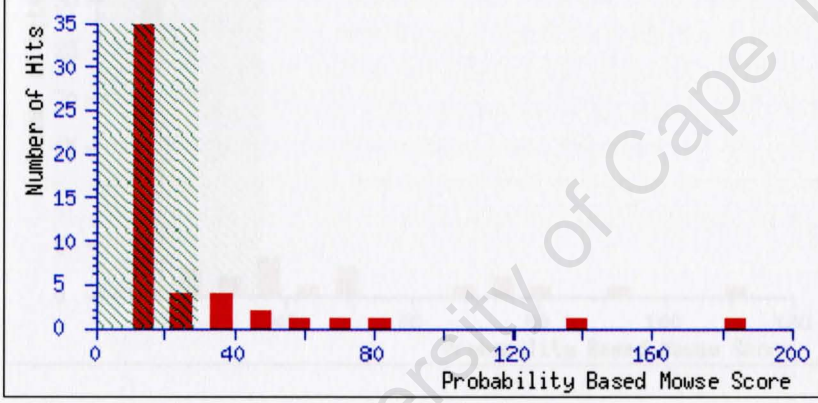

Figure A12: Example of the database search results showing the "Probability Based Mowse Score" for the proteins in Table A2 Displayed here is part of the results sheet for the fraction Ph8 in Figure 3.1.

Mascot Search Results

Search title : zba
MS data file : \\Uc212\PKL\F100\3594b.pkl
Database : NCBInr 20050416 (2440549 sequences; 825977590 residues)
Taxonomy : Rodentia (Rodents) (125777 sequences)
Timestamp : 9 Jun 2005 at 15:03:10 GMT
Significant hits: gi|6679104 Niemann Pick type C1 [Mus musculus]

gi|3098526	macrosialin [Mus musculus]
gi|7140942	osteoclast-specific 116-kDa V-ATPase subunit [Mus musculus]
gi|71537	keratin, type II cytoskeletal - mouse (fragment)
gi|9910294	keratin complex 2, basic, gene 6g [Mus musculus]
gi|50510847	mKIAA1207 protein [Mus musculus]
gi|52789	unnamed protein product [Mus musculus]
gi|47086911	keratin Kb40 [Mus musculus]
gi|71527	keratin, 59K type I cytoskeletal - mouse
gi|554464	keratin K6
gi|6755863	tumor rejection antigen gp96 [Mus musculus]

Probability Based Mowse Score

Score is -10*Log(P), where P is the probability that the observed match is a random event.
Individual ions scores > 36 indicate identity or extensive homology (p<0.05).

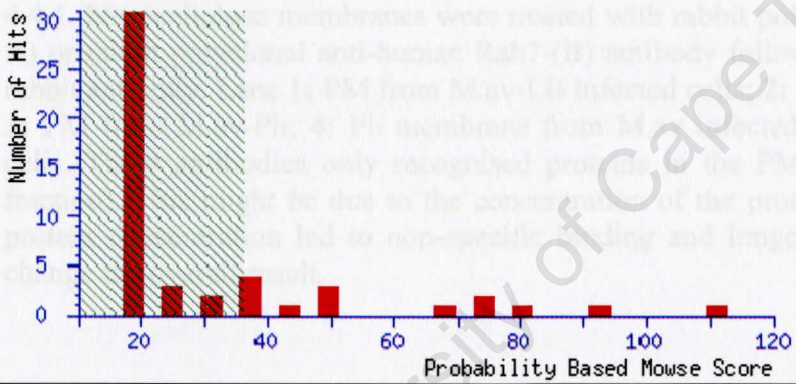

Figure A13: Example of the database search results showing the "Probability Based Mowse Score" for the proteins in Table A3 Part of the results sheet for the fraction number 8 in Figure 3.1.

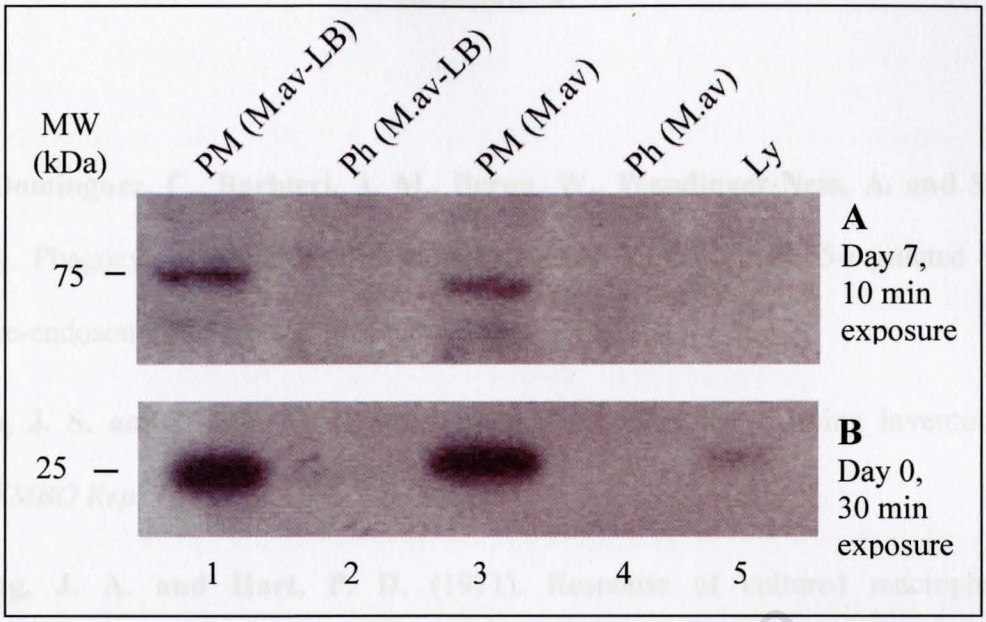

Figure A14: Inconclusive WB results for the analysis of TfR and Rab7 in Ph containing M.av-LB or M.av SDS-PAGE and Western blotting was performed as described in Figure 4.4.1. Nitrocellulose membranes were treated with rabbit polyclonal anti-human CD71 (TfR, **A**) or rabbit polyclonal anti-human Rab7 (**B**) antibody followed by peroxidase labelled anti-rabbit antibody. Lane **1:** PM from M.av-LB infected cells; **2:** Ph from M.av-LB infected cells; **3:** PM from M.av-Ph; **4:** Ph membrane from M.av infected cells; **5:** Ly from non-infected cells. These antibodies only recognised proteins in the PM samples (light density Percoll fraction). This might be due to the concentration of the proteins in the PM samples. Higher protein concentration led to non-specific binding and longer (overnight) exposures did not change the overall result.

References

Alvarez-Dominguez, C., Barbieri, A. M., Beron, W., Wandinger-Ness, A. and Stahl, P. D. (1996). Phagocytosed live listeria monocytogenes influences Rab5-regulated in vitro phagosome-endosome fusion. *J. Biol. Chem.* **271,** 13834-13843.

Andersen, J. S. and Mann, M. (2006). Organellar proteomics: Turning inventories into insights. *EMBO Rep.* **7,** 874-879.

Armstrong, J. A. and Hart, P. D. (1971). Response of cultured macrophages to mycobacterium tuberculosis, with observations on fusion of lysosomes with phagosomes. *J. Exp. Med.* **134,** 713-740.

Armstrong, J. A. and Hart, P. D. (1975). Phagosome-lysosome interactions in cultured macrophages infected with virulent tubercle bacilli. reversal of the usual nonfusion pattern and observations on bacterial survival. *J. Exp. Med.* **142,** 1-16.

Bachner, D., Schroder, D. and Gross, G. (2002). mRNA expression of the murine glycoprotein (transmembrane) nmb (gpnmb) gene is linked to the developing retinal pigment epithelium and iris. *Brain Res. Gene Expr. Patterns* **1,** 159-165.

Baldwin, M. A. (2004). Protein identification by mass spectrometry: Issues to be considered. *Mol. Cell. Proteomics* **3,** 1-9.

Bandhuvula, P. and Saba, J. D. (2007). Sphingosine-1-phosphate lyase in immunity and cancer: Silencing the siren. *Trends Mol. Med.* **13,** 210-217.

Beatty, W. L., Rhoades, E. R., Ullrich, H. J., Chatterjee, D., Heuser, J. E. and Russell, D. G. (2000). Trafficking and release of mycobacterial lipids from infected macrophages. *Traffic* **1,** 235-247.

Beharka, A. A., Gaynor, C. D., Kang, B. K., Voelker, D. R., McCormack, F. X. and Schlesinger, L. S. (2002). Pulmonary surfactant protein A up-regulates activity of the mannose receptor, a pattern recognition receptor expressed on human macrophages. *J. Immunol.* **169,** 3565-3573.

Blitzer, B. L. and Donovan, C. B. (1984). A new method for the rapid isolation of basolateral plasma membrane vesicles from rat liver. characterization, validation, and bile acid transport studies. *J. Biol. Chem.* **259,** 9295-9301.

Blocker, A., Severin, F. F., Burkhardt, J. K., Bingham, J. B., Yu, H., Olivo, J. C., Schroer, T. A., Hyman, A. A. and Griffiths, G. (1997). Molecular requirements for bi-directional movement of phagosomes along microtubules. *J. Cell Biol.* **137,** 113-129.

Blocker, A., Severin, F. F., Habermann, A., Hyman, A. A., Griffiths, G. and Burkhardt, J. K. (1996). Microtubule-associated protein-dependent binding of phagosomes to microtubules. *J. Biol. Chem.* **271,** 3803-3811.

Brennan, P. J. (2003). Structure, function, and biogenesis of the cell wall of mycobacterium tuberculosis. *Tuberculosis (Edinb)* **83,** 91-97.

Bright, N. A., Reaves, B. J., Mullock, B. M. and Luzio, J. P. (1997). Dense core lysosomes can fuse with late endosomes and are re-formed from the resultant hybrid organelles. *J. Cell. Sci.* **110 (Pt 17),** 2027-2040.

Callaghan, J., Nixon, S., Bucci, C., Toh, B. H. and Stenmark, H. (1999). Direct interaction of EEA1 with Rab5b. *Eur. J. Biochem.* **265,** 361-366.

Callahan, J. W., Bagshaw, R. D. and Mahuran, D. J. (2009). The integral membrane of lysosomes: Its proteins and their roles in disease. *J. Proteomics* **72,** 23-33.

Cambi, A., Koopman, M. and Figdor, C. G. (2005). How C-type lectins detect pathogens. *Cell. Microbiol.* **7,** 481-488.

Chatterjee, D., Lowell, K., Rivoire, B., McNeil, M. R. and Brennan, P. J. (1992). Lipoarabinomannan of mycobacterium tuberculosis. capping with mannosyl residues in some strains. *J. Biol. Chem.* **267,** 6234-6239.

Cho, N. H., Choi, C. Y. and Seong, S. Y. (2004). Down-regulation of gp96 by orientia tsutsugamushi. *Microbiol. Immunol.* **48,** 297-305.

Christoforidis, S., McBride, H. M., Burgoyne, R. D. and Zerial, M. (1999). The Rab5 effector EEA1 is a core component of endosome docking. *Nature* **397,** 621-625.

Chua, J., Vergne, I., Master, S. and Deretic, V. (2004). A tale of two lipids: Mycobacterium tuberculosis phagosome maturation arrest. *Curr. Opin. Microbiol.* **7,** 71-77.

Chung, J. S., Sato, K., Dougherty, I. I., Cruz, P. D.,Jr and Ariizumi, K. (2007). DC-HIL is a negative regulator of T lymphocyte activation. *Blood* **109,** 4320-4327.

Clemens, D. L. and Horwitz, M. A. (1995). Characterization of the mycobacterium tuberculosis phagosome and evidence that phagosomal maturation is inhibited. *J. Exp. Med.* **181,** 257-270.

Collins, F. M. (1989). Mycobacterial disease, immunosuppression, and acquired immunodeficiency syndrome. *Clin. Microbiol. Rev.* **2,** 360-377.

Crocker, P. R. and Redelinghuys, P. (2008). Siglecs as positive and negative regulators of the immune system. *Biochem. Soc. Trans.* **36,** 1467-1471.

Crocker, P. R. and Varki, A. (2001). Siglecs, sialic acids and innate immunity. *Trends Immunol.* **22,** 337-342.

Crouch, E. and Wright, J. R. (2001). Surfactant proteins a and d and pulmonary host defense. *Annu. Rev. Physiol.* **63,** 521-554.

Cywes, C., Hoppe, H. C., Daffe, M. and Ehlers, M. R. (1997). Nonopsonic binding of mycobacterium tuberculosis to complement receptor type 3 is mediated by capsular polysaccharides and is strain dependent. *Infect. Immun.* **65,** 4258-4266.

da Silva, R. P. and Gordon, S. (1999). Phagocytosis stimulates alternative glycosylation of macrosialin (mouse CD68), a macrophage-specific endosomal protein. *Biochem. J.* **338 (Pt 3),** 687-694.

de Chastellier, C. and Thilo, L. (1997). Phagosome maturation and fusion with lysosomes in relation to surface property and size of the phagocytic particle. *Eur. J. Cell Biol.* **1,** 49-62.

de Chastellier, C. and Thilo, L. (1999). Mycobacteria and the endocytic pathway. In *Advances in Cell and Molecular Biology of Membranes and Organelles*, pp. 107-- 135: JAI Press Inc.

de Chastellier, C. and Thilo, L. (2002). Pathogenic mycobacterium avium remodels the phagosome membrane in macrophages within days after infection. *Eur. J. Cell Biol.* **81,** 17-25.

de Chastellier, C. and Thilo, L. (2006). Cholesterol depletion in mycobacterium avium-infected macrophages overcomes the block in phagosome maturation and leads to the reversible sequestration of viable mycobacteria in phagolysosome-derived autophagic vacuoles. *Cell. Microbiol.* **8,** 242-256.

de Chastellier, C., Forquet, F., Gordon, A. and Thilo, L. (2009). Mycobacterium requires an all-around closely apposing phagosome membrane to maintain the maturation block and this apposition is re-established when it rescues itself from phagolysosomes. *Cell. Microbiol.* **11,** 1190-1207.

de Chastellier, C., Lang, T. and Thilo, L. (1995). Phagocytic processing of the macrophage endoparasite, mycobacterium avium, in comparison to phagosomes which contain bacillus subtilis or latex beads. *Eur. J. Cell Biol.* **68,** 167-182.

de Figueiredo, P., Doody, A., Polizotto, R. S., Drecktrah, D., Wood, S., Banta, M., Strang, M. S. and Brown, W. J. (2001). Inhibition of transferrin recycling and endosome tubulation by phospholipase A2 antagonists. *J. Biol. Chem.* **276,** 47361-47370.

Defacque, H., Egeberg, M., Habermann, A., Diakonova, M., Roy, C., Mangeat, P., Voelter, W., Marriott, G., Pfannstiel, J., Faulstich, H. et al. (2000). Involvement of ezrin/moesin in de novo actin assembly on phagosomal membranes. *EMBO J.* **19,** 199-212.

DePina, A. S. and Langford, G. M. (1999). Vesicle transport: The role of actin filaments and myosin motors. *Microsc. Res. Tech.* **47,** 93-106.

Deretic, V. and Fratti, R. A. (1999). Mycobacterium tuberculosis phagosome. *Mol. Microbiol.* **31,** 1603-1609.

Deretic, V., Singh, S., Master, S., Harris, J., Roberts, E., Kyei, G., Davis, A., de Haro, S., Naylor, J., Lee, H. H. et al. (2006). Mycobacterium tuberculosis inhibition of phagolysosome biogenesis and autophagy as a host defence mechanism. *Cell. Microbiol.* **8,** 719-727.

Deretic, V., Vergne, I., Chua, J., Master, S., Singh, S. B., Fazio, J. A. and Kyei, G. (2004). Endosomal membrane traffic: Convergence point targeted by mycobacterium tuberculosis and HIV. *Cell. Microbiol.* **6,** 999-1009.

Desjardins, M., Huber, L. A., Parton, R. G. and Griffiths, G. (1994a). Biogenesis of phagolysosomes proceeds through a sequential series of interactions with the endocytic apparatus. *J. Cell Biol.* **124,** 677-688.

Desjardins, M., Huber, L. A., Parton, R. G. and Griffiths, G. (1994b). Biogenesis of phagolysosomes proceeds through a sequential series of interactions with the endocytic apparatus. *J. Cell Biol.* **124,** 677-688.

Dodd, D. A., Niederoest, B., Bloechlinger, S., Dupuis, L., Loeffler, J. P. and Schwab, M. E. (2005). Nogo-A, -B, and -C are found on the cell surface and interact together in many different cell types. *J. Biol. Chem.* **280,** 12494-12502.

Dongre, A. R., Eng, J. K. and Yates, J. R.,3rd. (1997). Emerging tandem-mass-spectrometry techniques for the rapid identification of proteins. *Trends Biotechnol.* **15,** 418-425.

Doody, A. D., Kovalchin, J. T., Mihalyo, M. A., Hagymasi, A. T., Drake, C. G. and Adler, A. J. (2004). Glycoprotein 96 can chaperone both MHC class I- and class II-restricted epitopes for in vivo presentation, but selectively primes CD8+ T cell effector function. *J. Immunol.* **172,** 6087-6092.

Dramsi, S. and Cossart, P. (1998). Intracellular pathogens and the actin cytoskeleton. *Annu. Rev. Cell Dev. Biol.* **14,** 137-166.

Ducreux, J., Crocker, P. R. and Vanbever, R. (2009). Analysis of sialoadhesin expression on mouse alveolar macrophages. *Immunol. Lett.* **124,** 77-80.

Dye, C. and Williams, B. G. (2008). Eliminating human tuberculosis in the twenty-first century. *J. R. Soc. Interface* **5,** 653-662.

Ernst, J. D. (1998). Macrophage receptors for mycobacterium tuberculosis. *Infect. Immun.* **66,** 1277-1281.

Erwig, L. P., McPhilips, K. A., Wynes, M. W., Ivetic, A., Ridley, A. J. and Henson, P. M. (2006). Differential regulation of phagosome maturation in macrophages and dendritic cells mediated by rho GTPases and ezrin-radixin-moesin (ERM) proteins. *Proc. Natl. Acad. Sci. U. S. A.* **103,** 12825-12830.

Falkinham, J. O. (2003). The changing pattern of nontuberculous mycobacterial disease. *Can. J. Infect. Dis.* **14,** 281-286.

Ferguson, J. S., Voelker, D. R., McCormack, F. X. and Schlesinger, L. S. (1999). Surfactant protein D binds to mycobacterium tuberculosis bacilli and lipoarabinomannan via carbohydrate-lectin interactions resulting in reduced phagocytosis of the bacteria by macrophages. *J. Immunol.* **163,** 312-321.

Ferguson, J. S., Voelker, D. R., Ufnar, J. A., Dawson, A. J. and Schlesinger, L. S. (2002). Surfactant protein D inhibition of human macrophage uptake of mycobacterium tuberculosis is independent of bacterial agglutination. *J. Immunol.* **168,** 1309-1314.

Ferrari, G., Langen, H., Naito, M. and Pieters, J. (1999). A coat protein on phagosomes involved in the intracellular survival of mycobacteria. *Cell* **97,** 435-447.

Fontoura, P. and Steinman, L. (2006). Nogo in multiple sclerosis: Growing roles of a growth inhibitor. *J. Neurol. Sci.* **245,** 201-210.

Fratti, R. A., Backer, J. M., Gruenberg, J., Corvera, S. and Deretic, V. (2001). Role of phosphatidylinositol 3-kinase and Rab5 effectors in phagosomal biogenesis and mycobacterial phagosome maturation arrest. *J. Cell Biol.* **154,** 631-644.

Fratti, R. A., Chua, J. and Deretic, V. (2003a). Induction of p38 mitogen-activated protein kinase reduces early endosome autoantigen 1 (EEA1) recruitment to phagosomal membranes. *J. Biol. Chem.* **278,** 46961-46967.

Fratti, R. A., Chua, J., Vergne, I. and Deretic, V. (2003b). Mycobacterium tuberculosis glycosylated phosphatidylinositol causes phagosome maturation arrest. *Proc. Natl. Acad. Sci. U. S. A.* **100,** 5437-5442.

Frehel, C., de Chastellier, C., Lang, T. and Rastogi, N. (1986). Evidence for inhibition of fusion of lysosomal and prelysosomal compartments with phagosomes in macrophages infected with pathogenic mycobacterium avium. *Infect. Immun.* **52,** 252-262.

Frehel, C., Canonne-Hergaux, F., Gros, P. and De Chastellier, C. (2002). Effect of Nramp1 on bacterial replication and on maturation of mycobacterium avium-containing phagosomes in bone marrow-derived mouse macrophages. *Cell. Microbiol.* **4,** 541-556.

Gabrilovac, J., Cupic, B., Zivkovic, E., Horvat, L. and Majhen, D. (2010). Expression, regulation and functional activities of aminopeptidase N (EC 3.4.11.2; APN; CD13) on murine macrophage J774 cell line. *Immunobiology*.

Garg, S. K., Volpe, E., Palmieri, G., Mattei, M., Galati, D., Martino, A., Piccioni, M. S., Valente, E., Bonanno, E., De Vito, P. et al. (2004). Sphingosine 1-phosphate induces antimicrobial activity both in vitro and in vivo. *J. Infect. Dis.* **189,** 2129-2138.

Gharahdaghi, F., Weinberg, C. R., Meagher, D. A., Imai, B. S. and Mische, S. M. (1999). Mass spectrometric identification of proteins from silver-stained polyacrylamide gel: A method for the removal of silver ions to enhance sensitivity. *Electrophoresis* **20,** 601-605.

Gillooly, D. J., Simonsen, A. and Stenmark, H. (2001). Phosphoinositides and phagocytosis. *J. Cell Biol.* **155,** 15-17.

Glickman, M. S. and Jacobs, W. R.,Jr. (2001). Microbial pathogenesis of mycobacterium tuberculosis: Dawn of a discipline. *Cell* **104,** 477-485.

Groothuis, T. A. and Neefjes, J. (2005). The many roads to cross-presentation. *J. Exp. Med.* **202,** 1313-1318.

Gruenberg, J. and Maxfield, F. R. (1995). Membrane transport in the endocytic pathway. *Curr. Opin. Cell Biol.* **7,** 552-563.

Guerin, I. and de Chastellier, C. (2000a). Pathogenic mycobacteria disrupt the macrophage actin filament network. *Infect. Immun.* **68,** 2655-2662.

Guerin, I. and de Chastellier, C. (2000b). Disruption of the actin filament network affects delivery of endocytic contents marker to phagosomes with early endosome characteristics: The case of phagosomes with pathogenic mycobacteria. *Eur. J. Cell Biol.* **79,** 735-749.

Harries, A. D. and Dye, C. (2006). Tuberculosis. *Ann. Trop. Med. Parasitol.* **100,** 415-431.

Harris, E. S., McIntyre, T. M., Prescott, S. M. and Zimmerman, G. A. (2000). The leukocyte integrins. *J. Biol. Chem.* **275,** 23409-23412.

Haylett, T. and Thilo, L. (1986). Limited and selective transfer of plasma membrane glycoproteins to membrane of secondary lysosomes. *J. Cell Biol.* **103,** 1249-1256.

Hirsch, C. S., Ellner, J. J., Russell, D. G. and Rich, E. A. (1994). Complement receptor-mediated uptake and tumor necrosis factor-alpha-mediated growth inhibition of mycobacterium tuberculosis by human alveolar macrophages. *J. Immunol.* **152,** 743-753.

Holness, C. L., da Silva, R. P., Fawcett, J., Gordon, S. and Simmons, D. L. (1993). Macrosialin, a mouse macrophage-restricted glycoprotein, is a member of the lamp/lgp family. *J. Biol. Chem.* **268,** 9661-9666.

Hopkins, C. R., Gibson, A., Shipman, M., Strickland, D. K. and Trowbridge, I. S. (1994). In migrating fibroblasts, recycling receptors are concentrated in narrow tubules in the pericentriolar area, and then routed to the plasma membrane of the leading lamella. *J. Cell Biol.* **125,** 1265-1274.

Huang, L., Baldwin, M. A., Maltby, D. A., Medzihradszky, K. F., Baker, P. R., Allen, N., Rexach, M., Edmondson, R. D., Campbell, J., Juhasz, P. et al. (2002). The identification of protein-protein interactions of the nuclear pore complex of saccharomyces cerevisiae using high throughput matrix-assisted laser desorption ionization time-of-flight tandem mass spectrometry. *Mol. Cell. Proteomics* **1,** 434-450.

Huber, L. A., Pfaller, K. and Vietor, I. (2003). Organelle proteomics: Implications for subcellular fractionation in proteomics. *Circ. Res.* **92,** 962-968.

Huynh, K. K. and Grinstein, S. (2007). Regulation of vacuolar pH and its modulation by some microbial species. *Microbiol. Mol. Biol. Rev.* **71,** 452-462.

Indik, Z. K., Park, J. G., Hunter, S. and Schreiber, A. D. (1995). The molecular dissection of fc gamma receptor mediated phagocytosis. *Blood* **86,** 4389-4399.

Itoe, M. (2007). Regulation of integrin-alpha M and -beta 2 expression on the surface of macrophages in response to infection with *mycobacterium avium.*

Ivetic, A. and Ridley, A. J. (2004). Ezrin/radixin/moesin proteins and rho GTPase signalling in leucocytes. *Immunology* **112,** 165-176.

Jiang, Z., Shih, D. M., Xia, Y. R., Lusis, A. J., de Beer, F. C., de Villiers, W. J., van der Westhuyzen, D. R. and de Beer, M. C. (1998). Structure, organization, and chromosomal mapping of the gene encoding macrosialin, a macrophage-restricted protein. *Genomics* **50,** 199-205.

Jo, E. K., Yang, C. S., Choi, C. H. and Harding, C. V. (2007). Intracellular signalling cascades regulating innate immune responses to mycobacteria: Branching out from toll-like receptors. *Cell. Microbiol.* **9,** 1087-1098.

Jonscher, K. R. and Yates, J. R.,3rd. (1997). The quadrupole ion trap mass spectrometer--a small solution to a big challenge. *Anal. Biochem.* **244,** 1-15.

Jozefowski, S., Sobota, A. and Kwiatkowska, K. (2008). How mycobacterium tuberculosis subverts host immune responses. *Bioessays* **30,** 943-954.

Julian, E., Matas, L., Ausina, V. and Luquin, M. (1997). Detection of lipoarabinomannan antibodies in patients with newly acquired tuberculosis and patients with relapse tuberculosis. *J. Clin. Microbiol.* **35,** 2663-2664.

Karten, B., Peake, K. B. and Vance, J. E. (2009). Mechanisms and consequences of impaired lipid trafficking in niemann-pick type C1-deficient mammalian cells. *Biochim. Biophys. Acta* **1791,** 659-670.

Kramer, W., Girbig, F., Corsiero, D., Pfenninger, A., Frick, W., Jahne, G., Rhein, M., Wendler, W., Lottspeich, F., Hochleitner, E. O. et al. (2005). Aminopeptidase N (CD13) is a molecular target of the cholesterol absorption inhibitor ezetimibe in the enterocyte brush border membrane. *J. Biol. Chem.* **280,** 1306-1320.

Kuehnel, M. P., Goethe, R., Habermann, A., Mueller, E., Rohde, M., Griffiths, G. and Valentin-Weigand, P. (2001). Characterization of the intracellular survival of mycobacterium avium ssp. paratuberculosis: Phagosomal pH and fusogenicity in J774 macrophages compared with other mycobacteria. *Cell. Microbiol.* **3,** 551-566.

Kusner, D. J. (2005). Mechanisms of mycobacterial persistence in tuberculosis. *Clin. Immunol.* **114,** 239-247.

Larsen, S. L., Pedersen, L. O., Buus, S. and Stryhn, A. (1996). T cell responses affected by aminopeptidase N (CD13)-mediated trimming of major histocompatibility complex class II-bound peptides. *J. Exp. Med.* **184,** 183-189.

Lawe, D. C., Patki, V., Heller-Harrison, R., Lambright, D. and Corvera, S. (2000). The FYVE domain of early endosome antigen 1 is required for both phosphatidylinositol 3-phosphate and Rab5 binding. critical role of this dual interaction for endosomal localization. *J. Biol. Chem.* **275,** 3699-3705.

Lindmo, K. and Stenmark, H. (2006). Regulation of membrane traffic by phosphoinositide 3-kinases. *J. Cell. Sci.* **119,** 605-614.

Lopez, J. P., Clark, E. and Shepherd, V. L. (2003). Surfactant protein A enhances mycobacterium avium ingestion but not killing by rat macrophages. *J. Leukoc. Biol.* **74,** 523-530.

Low, T. Y., Seow, T. K. and Chung, M. C. (2002). Separation of human erythrocyte membrane associated proteins with one-dimensional and two-dimensional gel electrophoresis followed by identification with matrix-assisted laser desorption/ionization-time of flight mass spectrometry. *Proteomics* **2,** 1229-1239.

Lukacs, G. L., Rotstein, O. D. and Grinstein, S. (1990). Phagosomal acidification is mediated by a vacuolar-type H(+)-ATPase in murine macrophages. *J. Biol. Chem.* **265,** 21099-21107.

Malik, Z. A., Denning, G. M. and Kusner, D. J. (2000). Inhibition of ca(2+) signaling by mycobacterium tuberculosis is associated with reduced phagosome-lysosome fusion and increased survival within human macrophages. *J. Exp. Med.* **191,** 287-302.

Malik, Z. A., Iyer, S. S. and Kusner, D. J. (2001). Mycobacterium tuberculosis phagosomes exhibit altered calmodulin-dependent signal transduction: Contribution to inhibition of phagosome-lysosome fusion and intracellular survival in human macrophages. *J. Immunol.* **166,** 3392-3401.

Malik, Z. A., Thompson, C. R., Hashimi, S., Porter, B., Iyer, S. S. and Kusner, D. J. (2003). Cutting edge: Mycobacterium tuberculosis blocks Ca2+ signaling and phagosome maturation in human macrophages via specific inhibition of sphingosine kinase. *J. Immunol.* **170,** 2811-2815.

Maloy WL, Nathenson SG, Coligan JE. (1981). Primary structure of murine major histocompatibility complex alloantigens. amino acid sequence of the NH2-terminal ninety-eight residues of the H-2Db glycoprotein. *J. Biol. Chem.* **256,** 2863-2872.

Matteoni, R. and Kreis, T. E. (1987). Translocation and clustering of endosomes and lysosomes depends on microtubules. *J. Cell Biol.* **105,** 1253-1265.

May, R. C. (2001). The Arp2/3 complex: A central regulator of the actin cytoskeleton. *Cell Mol. Life Sci.* **58,** 1607-1626.

Mellman, I. (1996). Endocytosis and molecular sorting. *Annu. Rev. Cell Dev. Biol.* **12,** 575-625.

Melo, M. D., Catchpole, I. R., Haggar, G. and Stokes, R. W. (2000). Utilization of CD11b knockout mice to characterize the role of complement receptor 3 (CR3, CD11b/CD18) in the growth of mycobacterium tuberculosis in macrophages. *Cell. Immunol.* **205,** 13-23.

Mills, I. G., Urbe, S. and Clague, M. J. (2001). Relationships between EEA1 binding partners and their role in endosome fusion. *J. Cell. Sci.* **114,** 1959-1965.

Mina-Osorio, P. (2008). The moonlighting enzyme CD13: Old and new functions to target. *Trends Mol. Med.* **14,** 361-371.

Molloy, M. P. (2000). Two-dimensional electrophoresis of membrane proteins using immobilized pH gradients. *Anal. Biochem.* **280,** 1-10.

Momburg, F. and Tan, P. (2002). Tapasin-the keystone of the loading complex optimizing peptide binding by MHC class I molecules in the endoplasmic reticulum. *Mol. Immunol.* **39,** 217-233.

Moreira, A. L., Wang, J., Tsenova-Berkova, L., Hellmann, W., Freedman, V. H. and Kaplan, G. (1997). Sequestration of mycobacterium tuberculosis in tight vacuoles in vivo in lung macrophages of mice infected by the respiratory route. *Infect. Immun.* **65,** 305-308.

Morelle, W., Canis, K., Chirat, F., Faid, V. and Michalski, J. C. (2006). The use of mass spectrometry for the proteomic analysis of glycosylation. *Proteomics* **6,** 3993-4015.

Mu, F. T., Callaghan, J. M., Steele-Mortimer, O., Stenmark, H., Parton, R. G., Campbell, P. L., McCluskey, J., Yeo, J. P., Tock, E. P. and Toh, B. H. (1995). EEA1, an early endosome-associated protein. EEA1 is a conserved alpha-helical peripheral membrane protein flanked by cysteine "fingers" and contains a calmodulin-binding IQ motif. *J. Biol. Chem.* **270,** 13503-13511.

Mullin, N. P., Hitchen, P. G. and Taylor, M. E. (1997). Mechanism of Ca2+ and monosaccharide binding to a C-type carbohydrate-recognition domain of the macrophage mannose receptor. *J. Biol. Chem.* **272,** 5668-5681.

Mullins, R. D., Heuser, J. A. and Pollard, T. D. (1998). The interaction of Arp2/3 complex with actin: Nucleation, high affinity pointed end capping, and formation of branching networks of filaments. *Proc. Natl. Acad. Sci. U. S. A.* **95,** 6181-6186.

Mustelin, T., Vang, T. and Bottini, N. (2005). Protein tyrosine phosphatases and the immune response. *Nat. Rev. Immunol.* **5,** 43-57.

Mwandumba, H. C., Russell, D. G., Nyirenda, M. H., Anderson, J., White, S. A., Molyneux, M. E. and Squire, S. B. (2004). Mycobacterium tuberculosis resides in nonacidified vacuoles in endocytically competent alveolar macrophages from patients with tuberculosis and HIV infection. *J. Immunol.* **172,** 4592-4598.

Niemann, S., Rusch-Gerdes, S., Joloba, M. L., Whalen, C. C., Guwatudde, D., Ellner, J. J., Eisenach, K., Fumokong, N., Johnson, J. L., Aisu, T. et al. (2002). Mycobacterium africanum subtype II is associated with two distinct genotypes and is a major cause of human tuberculosis in kampala, uganda. *J. Clin. Microbiol.* **40,** 3398-3405.

Oh, Y. K. and Straubinger, R. M. (1996). Intracellular fate of mycobacterium avium: Use of dual-label spectrofluorometry to investigate the influence of bacterial viability and opsonization on phagosomal pH and phagosome-lysosome interaction. *Infect. Immun.* **64,** 319-325.

Oh, Y. K. and Swanson, J. A. (1996). Different fates of phagocytosed particles after delivery into macrophage lysosomes. *J. Cell Biol.* **132,** 585-593.

Perkins, D. N., Pappin, D. J., Creasy, D. M. and Cottrell, J. S. (1999). Probability-based protein identification by searching sequence databases using mass spectrometry data. *Electrophoresis* **20,** 3551-3567.

Pertoft, H. (2000). Fractionation of cells and subcellular particles with percoll. *J. Biochem. Biophys. Methods* **44,** 1-30.

Pfeffer, S. R. (1996). Transport vesicle docking: SNAREs and associates. *Annu. Rev. Cell Dev. Biol.* **12,** 441-461.

Pfeffer, S. R. (2007). Unsolved mysteries in membrane traffic. *Annu. Rev. Biochem.* **76,** 629-645.

Pietersen, R., Thilo, L. and de Chastellier, C. (2004). Mycobacterium tuberculosis and mycobacterium avium modify the composition of the phagosomal membrane in infected macrophages by selective depletion of cell surface-derived glycoconjugates. *Eur. J. Cell Biol.* **83,** 153-158.

Pitt, A., Mayorga, L. S., Stahl, P. D. and Schwartz, A. L. (1992). Alterations in the protein composition of maturing phagosomes. *J. Clin. Invest.* **90,** 1978-1983.

Rabilloud, T. (2009). Membrane proteins and proteomics: Love is possible, but so difficult. *Electrophoresis* **30 Suppl 1,** S174-80.

Raghavan, M., Del Cid, N., Rizvi, S. M. and Peters, L. R. (2008). MHC class I assembly: Out and about. *Trends Immunol.* **29,** 436-443.

Raposo, G., Cordonnier, M. N., Tenza, D., Menichi, B., Durrbach, A., Louvard, D. and Coudrier, E. (1999). Association of myosin I alpha with endosomes and lysosomes in mammalian cells. *Mol. Biol. Cell* **10,** 1477-1494.

Rivers, E. C. and Mancera, R. L. (2008). New anti-tuberculosis drugs in clinical trials with novel mechanisms of action. *Drug Discov. Today* **13,** 1090-1098.

Rooyakkers, A. W. and Stokes, R. W. (2005). Absence of complement receptor 3 results in reduced binding and ingestion of mycobacterium tuberculosis but has no significant effect on the induction of reactive oxygen and nitrogen intermediates or on the survival of the bacteria in resident and interferon-gamma activated macrophages. *Microb. Pathog.* **39,** 57-67.

Russell, D. G., Dant, J. and Sturgill-Koszycki, S. (1996). Mycobacterium avium- and mycobacterium tuberculosis-containing vacuoles are dynamic, fusion-competent vesicles that are accessible to glycosphingolipids from the host cell plasmalemma. *J. Immunol.* **156,** 4764-4773.

Russell, D. G., Mwandumba, H. C. and Rhoades, E. E. (2002). Mycobacterium and the coat of many lipids. *J. Cell Biol.* **158,** 421-426.

Saleh, M. T. and Belisle, J. T. (2000). Secretion of an acid phosphatase (SapM) by mycobacterium tuberculosis that is similar to eukaryotic acid phosphatases. *J. Bacteriol.* **182,** 6850-6853.

Santoni, V., Molloy, M. and Rabilloud, T. (2000). Membrane proteins and proteomics: Un amour impossible? *Electrophoresis* **21,** 1054-1070.

Saunders, A. E. and Johnson, P. (2010). Modulation of immune cell signalling by the leukocyte common tyrosine phosphatase, CD45. *Cell. Signal.* **22,** 339-348.

Sawicki, M. W., Dimasi, N., Natarajan, K., Wang, J., Margulies, D. H. and Mariuzza, R. A. (2001). Structural basis of MHC class I recognition by natural killer cell receptors. *Immunol. Rev.* **181,** 52-65.

Schaible, U. E., Sturgill-Koszycki, S., Schlesinger, P. H. and Russell, D. G. (1998). Cytokine activation leads to acidification and increases maturation of mycobacterium avium-containing phagosomes in murine macrophages. *J. Immunol.* **160,** 1290-1296.

Schaub, B. E., Nair, P. and Rohrer, J. (2005). Analysis of protein transport to lysosomes. *Curr. Protoc. Cell. Biol.* **Chapter 15,** Unit 15.8.

Schlesinger, L. S. (1993). Macrophage phagocytosis of virulent but not attenuated strains of mycobacterium tuberculosis is mediated by mannose receptors in addition to complement receptors. *J. Immunol.* **150,** 2920-2930.

Schlesinger, L. S., Bellinger-Kawahara, C. G., Payne, N. R. and Horwitz, M. A. (1990). Phagocytosis of mycobacterium tuberculosis is mediated by human monocyte complement receptors and complement component C3. *J. Immunol.* **144,** 2771-2780.

Schlesinger, L. S., Hull, S. R. and Kaufman, T. M. (1994). Binding of the terminal mannosyl units of lipoarabinomannan from a virulent strain of mycobacterium tuberculosis to human macrophages. *J. Immunol.* **152,** 4070-4079.

Sharma, S. K., Mohan, A., Sharma, A. and Mitra, D. K. (2005). Miliary tuberculosis: New insights into an old disease. *Lancet Infect. Dis.* **5,** 415-430.

Shikano, S., Bonkobara, M., Zukas, P. K. and Ariizumi, K. (2001). Molecular cloning of a dendritic cell-associated transmembrane protein, DC-HIL, that promotes RGD-dependent adhesion of endothelial cells through recognition of heparan sulfate proteoglycans. *J. Biol. Chem.* **276,** 8125-8134.

Sidobre, S., Puzo, G. and Riviere, M. (2002). Lipid-restricted recognition of mycobacterial lipoglycans by human pulmonary surfactant protein A: A surface-plasmon-resonance study. *Biochem. J.* **365,** 89-97.

Simonsen, A., Gaullier, J. M., D'Arrigo, A. and Stenmark, H. (1999). The Rab5 effector EEA1 interacts directly with syntaxin-6. *J. Biol. Chem.* **274,** 28857-28860.

Simonsen, A., Lippe, R., Christoforidis, S., Gaullier, J. M., Brech, A., Callaghan, J., Toh, B. H., Murphy, C., Zerial, M. and Stenmark, H. (1998). EEA1 links PI(3)K function to Rab5 regulation of endosome fusion. *Nature* **394,** 494-498.

Stahl, P. D. and Ezekowitz, R. A. (1998). The mannose receptor is a pattern recognition receptor involved in host defense. *Curr. Opin. Immunol.* **10,** 50-55.

Stenmark, H., Aasland, R., Toh, B. H. and D'Arrigo, A. (1996). Endosomal localization of the autoantigen EEA1 is mediated by a zinc-binding FYVE finger. *J. Biol. Chem.* **271,** 24048-24054.

Strohmeier, G. R. and Fenton, M. J. (1999). Roles of lipoarabinomannan in the pathogenesis of tuberculosis. *Microbes Infect.* **1,** 709-717.

Sturgill-Koszycki, S., Haddix, P. L. and Russell, D. G. (1997). The interaction between mycobacterium and the macrophage analyzed by two-dimensional polyacrylamide gel electrophoresis. *Electrophoresis* **18,** 2558-2565.

Sturgill-Koszycki, S., Schaible, U. E. and Russell, D. G. (1996). Mycobacterium-containing phagosomes are accessible to early endosomes and reflect a transitional state in normal phagosome biogenesis. *EMBO J.* **15,** 6960-6968.

Sturgill-Koszycki, S., Schlesinger, P. H., Chakraborty, P., Haddix, P. L., Collins, H. L., Fok, A. K., Allen, R. D., Gluck, S. L., Heuser, J. and Russell, D. G. (1994). Lack of acidification in mycobacterium phagosomes produced by exclusion of the vesicular proton-ATPase. *Science* **263,** 678-681.

Taunton, J., Rowning, B. A., Coughlin, M. L., Wu, M., Moon, R. T., Mitchison, T. J. and Larabell, C. A. (2000). Actin-dependent propulsion of endosomes and lysosomes by recruitment of N-WASP. *J. Cell Biol.* **148,** 519-530.

Teng, F. Y. and Tang, B. L. (2008). Cell autonomous function of nogo and reticulons: The emerging story at the endoplasmic reticulum. *J. Cell. Physiol.* **216,** 303-308.

Thilo, L. (1983). Labeling of plasma membrane glycoconjugates by terminal glycosylation (galactosyltransferase and glycosidase). *Methods Enzymol.* **98,** 415-421.

Thilo, L. and de Chastellier, C. (2004). Phagosome biogenesis in relation to intracellular survival mechanisms. In *Intracellular Pathogens in Membrane Interactions and Vacuole Biogenesis* (ed. J. Gorvel), pp. 153-169: Eurekah.com and Kluwer Academic / Plenum Publishers.

Thomas, M. L., Barclay, A. N., Gagnon, J. and Williams, A. F. (1985). Evidence from cDNA clones that the rat leukocyte-common antigen (T200) spans the lipid bilayer and contains a cytoplasmic domain of 80,000 mr. *Cell* **41,** 83-93.

Tino, M. J. and Wright, J. R. (1996). Surfactant protein A stimulates phagocytosis of specific pulmonary pathogens by alveolar macrophages. *Am. J. Physiol.* **270,** L677-88.

Toyohara, A. and Inaba, K. (1989). Transport of phagosomes in mouse peritoneal macrophages. *J. Cell. Sci.* **94 (Pt 1),** 143-153.

Valdivia-Arenas, M., Amer, A., Henning, L., Wewers, M. and Schlesinger, L. (2007). Lung infections and innate host defense. *Drug Discov. Today Dis. Mech.* **4,** 73-81.

van de Wetering, J. K., van Golde, L. M. and Batenburg, J. J. (2004). Collectins: Players of the innate immune system. *Eur. J. Biochem.* **271,** 1229-1249.

Vergne, I., Chua, J. and Deretic, V. (2003). Tuberculosis toxin blocking phagosome maturation inhibits a novel Ca2+/calmodulin-PI3K hVPS34 cascade. *J. Exp. Med.* **198,** 653-659.

Vergne, I., Chua, J., Lee, H. H., Lucas, M., Belisle, J. and Deretic, V. (2005). Mechanism of phagolysosome biogenesis block by viable mycobacterium tuberculosis. *Proc. Natl. Acad. Sci. U. S. A.* **102,** 4033-4038.

Vergne, I., Chua, J., Singh, S. B. and Deretic, V. (2004a). Cell biology of mycobacterium tuberculosis phagosome. *Annu. Rev. Cell Dev. Biol.* **20,** 367-394.

Vergne, I., Fratti, R. A., Hill, P. J., Chua, J., Belisle, J. and Deretic, V. (2004b). Mycobacterium tuberculosis phagosome maturation arrest: Mycobacterial phosphatidylinositol analog phosphatidylinositol mannoside stimulates early endosomal fusion. *Mol. Biol. Cell* **15,** 751-760.

Via, L. E., Deretic, D., Ulmer, R. J., Hibler, N. S., Huber, L. A. and Deretic, V. (1997). Arrest of mycobacterial phagosome maturation is caused by a block in vesicle fusion between stages controlled by rab5 and rab7. *J. Biol. Chem.* **272,** 13326-13331.

Vieira, O. V., Botelho, R. J. and Grinstein, S. (2002). Phagosome maturation: Aging gracefully. *Biochem. J.* **366,** 689-704.

Wilson, D. B. and Wilson, M. P. (1992). Identification and subcellular localization of human rab5b, a new member of the ras-related superfamily of GTPases. *J. Clin. Invest.* **89,** 996-1005.

Woodman, P. G. and Futter, C. E. (2008). Multivesicular bodies: Co-ordinated progression to maturity. *Curr. Opin. Cell Biol.* **20,** 408-414.

Zhou, J. and Saba, J. D. (1998). Identification of the first mammalian sphingosine phosphate lyase gene and its functional expression in yeast. *Biochem. Biophys. Res. Commun.* **242,** 502-507.

Zimmerli, S., Edwards, S. and Ernst, J. D. (1996). Selective receptor blockade during phagocytosis does not alter the survival and growth of mycobacterium tuberculosis in human macrophages. *Am. J. Respir. Cell Mol. Biol.* **15,** 760-770.

Methods

Mycobacterium avium cultures and stocks

Mycobacterium avium (virulent transparent strain), prepared from homogenised organs (liver and spleen) of infected C57BL/6 mice and grown for one passage on Middlebrook 7H10 agar (Difco Laboratories, Becton Dickinson, USA), was a kind gift from Dr C de Chastellier (Centre d'Immunologie de Marseille, France). The bacteria were expanded on Middlebrook 7H10 agar enriched with 0.05% glycerol and 10% oleic acid albumin-dextrose-catalase (OADC, Highveld Biological, South Africa) before final collection in Middlebrook 7H9 broth (Difco Laboratories). Homogenous aliquots were prepared and frozen at -80°C as stocks for experiments. Bacterial concentrations were ascertained by colony forming unit (CFU) counts for several aliquots from frozen stocks. All colonies were confirmed as transparent in appearance.

Conditioned medium preparation

Conditioned medium (source of colony stimulating factor (CSF-1)) was prepared from L-929 cells (kind gifts from Drs Gordon Brown and Muazzam Jacobs, Division of Immunology, University of Cape Town, South Africa) grown in RPMI-1640 medium with glutamine (Highveld Biological) supplemented with 10% heat-inactivated foetal calf serum (FCS, Highveld Biological) under high bicarbonate (3.7g/L) and 5% CO_2. The supernatant (medium) was collected off the L-929 cells (passaged nine or less times) when the cells were at maximum confluency, immediately filtered through a 0.2 μm filter, aliquoted and frozen at -20°C. Individual aliquots were thawed not more than two times for cell growth.

Culturing bone marrow macrophages

Bone marrow derived macrophages (BMDM) were cultured essentially as described by Frehel et al., (1986). Precursor cells (stem cells) were obtained from the bone marrow of femurs excised from female C57BL/6 mice that were 6 to 8 weeks old. Precursor cells were seeded in Lumox (50 mm diameter, Greiner bio-one, Germany) or Nunclon (60 mm diameter, Thermo Fisher Scientific Inc.) culture dishes at one million cells per dish in the presence of growth medium: RPMI-1640 medium supplemented with 10% FCS and 10% L-929 conditioned medium. Cells were incubated at 37°C in 5% CO_2 for 5 days to differentiate into macrophages and become adherent to the dish surface. Undifferentiated cells and cell debris were removed by washing twice with RPMI-1640 medium containing HEPES (4-(2-Hydroxyethyl)-1-piperazine-ethanesulfonic acid, Merck, Germany) and the growth medium replaced. Growth medium was replaced every second day afterwards.

Infecting the bone marrow macrophages

Depending on the experiment, BMDM were infected with *M. avium*, magnetic latex beads or *M. avium* to which latex beads have been coupled, as described below.

Mycobacterium avium

BMDM were infected according a modified version described by Frehel et al., (1986). After 7 days of growth (since seeding), the cell number (per dish) was established by lysing the cells in one dish with 0.1% Triton-X100 (Merck, Germany) and counting the nuclei on a haemocytometer (Neubauer counting chamber, Superior, Germany). The infection ratio for *M. avium* was 1:20 (cells:bacteria). Stocks of frozen *M. avium* were thawed and briefly vortexed. Bacteria were first placed in 2 – 3 ml of growth medium and vortexed for 20 seconds to break up bacterial clumps before adding and mixing the rest of the growth medium for the desired titre. A 2 ml bacterial suspension was added on top of the cells and incubated at 37°C in a 5%

CO_2 incubator. After 4 hours, non-ingested bacteria were removed by washing the cells four times with ice-cold phosphate buffered saline (PBS), pH7.4 and re-fed with complete culture medium. The cells were incubated for 7 days, unless stated otherwise, and the medium changed after every second day.

Magnetic latex beads (mLB):

Magnetic latex beads (0.82µm diameter, Prolab), pigmented (brown) for pellet visualisation, were diluted 150 fold from the original bead solution. The beads were first washed twice with 1.5 ml HEPES-saline (10 mM HEPES, 140 mM NaCl, pH 7.4, Merck), twice with 70% ethanol and three times with HEPES-saline. A microcentrifuge tube magnetic particle concentrator was used to separate the beads from the wash media. One ml of cell culture medium devoid of FCS was added to the beads, followed by vortexing and sonication (in a sonicator bath) until all clumps were dispersed, as observed for a 10µl aliquot under a light microscope. The 1 ml of beads was made up to the final volume with cell culture medium devoid of FCS. A 2 ml bead suspension was added on top of the cells (previously infected with *M. avium*) followed by incubation at 37°C for 30 minutes. Culture dishes were transferred to ice and the cells washed four times with ice-cold HEPES-saline. Cells were then either labelled radioactively (as described below) or re-incubated immediately for 1 hour, before collected.

M. avium to which latex beads have been coupled (M.av-LB):

BMDM were infected with M.av-LB according de Chastellier et al., 2009. A multiplicity of infection (MOI) of 20 was used, but the amount of bacteria taken at the start from frozen stocks was adjusted for a 30% loss during preparations. The bacteria were washed twice with PBS and oxidized in 1 ml of 4 mM Na-periodate that was prepared in 0.1 M Na-acetate buffer (pH 5.5) and filter (0.22µm) sterilised. The bacteria were protected from light while

incubating for 30 minutes at room temperature (RT) on a slow moving rotating shaker followed by the addition of 200µl of 0.1 M sterile glycerol to stop the oxidation reaction. The bacteria were washed 3 times with PBS. Bacteria were pelleted at 13000 rpm for 6 minutes. The pellet was gently re-suspended with PBS containing 0.1µm hydrazide-modified latex beads (Bangs laboratories, USA) in a ratio of 1000 beads to one bacterium. The bacteria and beads were incubated at 4°C overnight on a slow moving rotating shaker followed by 3 washes with PBS to remove non-attached beads and re-suspended in culture medium. A 2 ml M.av-LB suspension was added on top of the cells and incubated at 37°C for 4 hours. Cells were washed four times with ice-cold (PBS) and re-fed with complete culture medium. The cells were incubated for 7 days, unless stated otherwise, and the medium changed after every second day.

Radioactive labelling of surface glycoconjugates

Cells (infected or non-infected) were labelled with radio-isotopes by the method of exo-galactosylation described by Thilo (1983). Labelling was carried out on ice to prevent membrane internalisation. Culture medium was removed and the cells washed twice with HEPES-saline. The bottoms of the Lumox dishes were cut out with a scalpel and placed cell-side down on a 200µl drop of 0.2 Units/ml of a cocktail of β-galactosidase and neuraminidase (prepared from *Streptococcus pneumoniae*) for 10 minutes to remove N-terminal neuraminic acid and galactose from glycosylated plasma-membrane molecules including glycoproteins. (Pre-treatment with the β-galactosidase cocktail allow for a subsequent ten fold stronger labelling of radioactive galactose.) The Lumox-dish bottoms were transferred to 90 mm petri dishes containing ice-cold HEPES-saline (cells against medium) and the cells washed three times to stop the enzymes from reacting. Cells were labelled for 30 minutes on ice on a 200µl drop of labelling mix containing 10% (v/v) galactosyltransferase (0.5 Units/ml, Sigma-Aldrich, USA), 10% $MnCl_2$ (5 mM, Merck), HEPES-saline (up to final volume) and 5 µCi of

either ^{14}C-UDP-galactose or ^{3}H-UDP-galactose (AEC Amersham). The cells were washed four times with HEPES-saline to remove unbound label and when label-internalisation was required, incubated at 37°C for 2 hours (when infected with *M. avium* only) or one hour (when infected with *M. avium* and mLB). Radioactive label, covalently attached to glycoconjugates, distributes along the endocytic pathway to steady state during these incubation periods (de Chastellier et al., 1995; de Chastellier and Thilo, 2002).

Isolation of phagosomes, plasma membrane (PM), endosomes and lysosomes

For organelle isolation, done on ice and/ or with pre-cooled materials, infected cells (labelled or unlabelled) were washed twice in homogenisation buffer (HB: 0.25 M sucrose, 2 mM EDTA (ethylenediaminetetraacetic acid), 10 mM HEPES, pH 7.4). Cells were scraped with a rubber policeman in about 250µl per dish of HB containing protease inhibitors (Complete Protease Inhibitor Cocktail Tablets, Roche Pharmaceuticals, Switzerland) at 1 mM final concentration. Cells were homogenised by making 8-10 passes through a ball-bearing cell cracker. If the cells were infected with mLB and *M. avium*, phagosomes containing mLB (mLB-Ph) were separated from the homogenate in a microcentrifuge tube magnetic particle concentrator, thus effectively separating the two types of phagosomes. The homogenate was centrifuged at 200xg for 12 minutes to obtain a postnuclear supernatant (PNS). PNS preparations were layered on top of appropriate volumes of 27% Percoll columns in 12.5 ml Polyallomer Beckman centrifuge tubes (14 X 95 mm, Beckman Coulter, Inc., USA). 27% Percoll consisted of 27% (v/v) Percoll (Sigma-Aldrich) and 73% HB_{27} (27 times concentrated HB: 340 mM sucrose, 2.7 mM EDTA, 13.7 mM HEPES). A volume of 0.5 ml sucrose (80%, w/v) was placed at the bottom of the centrifuge tube to prevent the organelles from pelleting. Percoll columns, forming density gradients under centrifugation, were centrifuged in an L8-55M Beckman Ultracentrifuge using a SW40 Ti swing-out rotor at 15000xg for 90 minutes at 4°C. Phagosomes and dense lysosomes always banded near the bottom and PM, endosomes

and light lysosomes near the top of the centrifuge tube. To fractionate the gradients, tubes were immediately punctured at the bottom with a syringe that was connected to a fraction collector (model LKB2112 RediRac, LKB-Produkter, Sweden). Fractions were 10 drops (about 0.5 ml) in size. The fractions of interest (containing the desired organelles), were identified by an opaque appearance and determined as radioactive by liquid scintillation counting a 10 µl aliquot of all fractions in a model 1900CA Liquid scintillation Counter (Packard Instrument Company, Inc.). Fractions containing the same organelles were pooled, mixed with HB in a 12.5 ml Polyallomer Beckman centrifuge tube and centrifuged for 2 hours at 100000xg at 4°C to concentrate the organelles and membranes and remove excess Percoll. Organelles and membranes were sonicated 30 times for 5-second pulses in 0.5 M KCl in HB containing protease inhibitors with a probe sonicator (model W-10 Cell Disruptor, Scientific Associates, South Africa) to exclude luminal proteins from the samples. Samples were centrifuged at 100000xg for one hour in a fixed angled 70.1 Ti rotor (Beckman Coulter, Inc.) followed by 30 minutes at 28 psi (pressure per square inches) in an Airfuge centrifuge (Beckman Coulter, Inc.) at 4°C using 5 X 20 mm Polyallomer tubes. Samples were stored at -20°C or immediately subjected to membrane extraction (see below) if required.

NAGA assay

NAGA content was determined by the Oxford glucose method. A 3 mM p-nitrophenyl acetyl glucosaminade (pNAG) substrate containing 0.2% Triton-X100 was prepared in disodium hydrogen phosphate- (Na_2HPO_4) citric acid (Merck) buffer, pH 5.5. Na_2HPO_4 and citric acid stock concentration solutions were both 100 mM and mixed in a 2:1 (Na_2HPO_4:citric acid) ratio. A 5 – 20 µl aliquot of all density gradient fractions was mixed with 200 µl of pNAG substrate and kept on ice until all samples were prepared. Samples were incubated for 20

minutes at 37°C (water bath), immediate transferred to watery ice and mixed with 0.8 ml of 50 mM NaOH (Merck) to stop the reaction. Absorbances were read at 405 nm.

Membrane Extraction

Separating the phagosome membrane from the mycobacteria (referred to here as membrane extraction) was to lessen or remove bacterial proteins which could interfere with the analyses of membrane proteins. A slightly modified procedure described by Sturgill-Koszycki et al., (Electrophoresis 1997, 18, 2558-2565) was followed. The phagosomes were treated with the detergent n-octyl β-$_D$-glucopyranoside (O-β-G, Sigma-Aldrich) and high salt concentrations to solubilise the phagosome membrane after which the bacteria were spun out of suspension. Specifically, phagosomes were incubated with O-β-G at 0.5 times the critical micellar concentration (CMC) in HB without sucrose but containing protease inhibitors for 5 minutes on ice followed by two washes with 0.6 M KCl containing 0.5 times the CMC O-β-G. The supernatants were collected and pooled. Sonication (in a sonicator bath) was added to the described method to aid the solubilisation of the membrane. High salt concentrations which are incompatible with isoelectric focussing were decreased to less than 50 mM by washing in the membrane extraction buffer (excluding salt) and centrifuging through a 10 kDa MW cut off membrane (Vivaspin columns, Sigma-Aldrich) several times, which also concentrated the sample to a small volume. For radioactive samples, aliquots were taken before and after membrane extraction and counted in a scintillation counter to ascertain the yield of extracted membrane. Repeating the membrane extraction removed all radioactive membrane from *M. avium*-containing phagosomes, but was much less effective for mLB-Ph. Boiling mLB-Ph in sample buffer removed the remaining membrane.

Determining radioactivity or protein concentration for samples

In general, samples were expressed and used according radioactivity or protein concentration.

Radioactivity

Before the final preparation of samples for PAGE, 2, 4 and 8 µl aliquots were analysed in a scintillation counter. From the slope of straight line regression analysis, the radioactivity concentration (dpm/ µl) was determined.

Protein quantification

The protein concentration of samples was determined with the Bicinchoninic acid (BCA) protein assay, performed according the Pierce protocol. For the microplate method, protein standards ranging from 5 to 250 µg/ml of bovine serum albumin were prepared. BCA working reagent was prepared from reagent A and reagent B in a 50:1 ratio. Samples and standards, 25 µl each in duplicate, were pipetted into a 96-well plate, followed by the addition of 200 µl/ well of working reagent into the same wells. The plate was gently shaken to mix the contents of the wells. The plate was covered with foil, incubated at 37°C for 30 minutes, cooled to RT and the absorbances measured at 560 nm (ELISA plate reader, Labsystem, Finland). Protein concentrations of unknown samples were determined from the standard curve.

Two dimensional (2-D) gel electrophoresis

Depending on the nature of the experiment, ^{14}C-labelled and ^{3}H-labelled membrane from two different organelles or types that were being compared (obtained from the same batch of cells) were mixed (in either equal proportions of radioactivity or 3-fold more ^{3}H-label, depending on the equipment used for subsequent analysis) and divided into two portions when applicable. One portion was subjected to 1-D separation and the other to 2-D separation in such a manner as to have the separation by MW on the same SDS-PAGE in order to make direct comparisons. For the first dimension separation of two dimensional (2-D) separation, mixed membranes were mixed with 300 µl of rehydration buffer (8 M Urea, 2 M Thiourea, 4% CHAPS, 20 mM Tris (all from Merck), 30mM dithiothreitol (DTT) and a trace amount of

bromophenol blue from Sigma-Aldrich and 2% pH 3-10 carrier ampholytes from AEC Amersham), incubated at RT for 30 minutes, vortexed and centrifuged for 15 minutes at 300xg to pellet insoluble matter. Rehydrated samples were added to wells of an Immobiline DryStrip Reswelling Tray (Amersham Pharmacia Biotech Inc.) and Immobiline DryStrip (18cm, pH 3-10, non-linear (NL), AEC Amersham) applied on top of the samples, covered with silicon oil and left at RT overnight. Immobiline DryStrips were applied to an Isoelectric focussing (IEF) apparatus (Multiphor™ II Electrophoresis System, Amersham Pharmacia Biotech Inc.) and electrophoresed for 60 – 80 kVh. IPG strips were incubated in equilibration buffer (10% (v/v) Tris-HCl stock at 1 M and pH 6.8, 36% (w/v) Urea, 30% (v/v) glycerol and 2% (w/v) sodium dodecyl sulphate, SDS) containing 1% (w/v) DTT for 10 minutes while shaking, rinsed with water, then incubated in equilibration buffer containing 2.5% (w/v) iodoacetamide (IAA) (Sigma-Aldrich). The IPG strips were then applied to an SDS-PAGE.

SDS-PAGE

In general, an 8 - 15% continuous gradient PAGE was prepared by mixing separate 8% and 15% polyacrylamide solutions prepared by diluting a stock solution of 30% acrylamide and 0.8% bisacrylamide (Merck) with 4-fold lower gel buffer (1.5 M Tris, 0.4% SDS, pH 8.8). TEMED (N,N,N,N-tetramethylethlyendiamine) and ammonium persulphate (AMPS) were added to a final concentration of 0.039% and 0.02%, respectively, to each separate solution. With the aid of a gradient maker and peristaltic pump, the lower gel solutions were poured between glass plates which were assembled as a mould. PAGE dimensions were 18 X 28 cm (width X length) for 2-D application or 15 X 28 cm 1-D gels. The gel was left to polymerize overnight. The upper gel solution was prepared by diluting the acrylamide stock to 4% with upper gel buffer (0.5 M Tris, 0.4% SDS, pH 6.3) and adding AMPS (0.085%) and TEMED (0.426%). An appropriate comb was used for making wells in the upper gel to accommodate an IPG strip or/ and liquid samples. Polymerization of the acrylamide was allowed up to 30

minutes. When SDS-PAGE was prepared as the second dimension run for 2-D electrophoresis, the IPG strip was trimmed 1.5 cm off from the low pH (acidic) side and 2.5 cm from the high pH (alkaline) side to fit the gel pocket. MW markers and membrane (1-D) samples were prepared by adding SB (10% glycerol, 2.3% SDS, 8.3% of 4-fold concentrated upper gel buffer, a trace of bromophenol blue, and 5% β-mercaptoethanol) to the samples and boiling for 5 minutes before applying to the PAGE. Electrophoresis, aided by running buffer (0.25 mM Tris, 192 mM glycine, 0.1% SDS, pH 8.3), was under denaturing conditions. A current of 25 mA was applied until the proteins entered the upper gel followed by 20 mA for about 15 hours. Power was supplied by a model EPS 500/400 (Hoefer Scientific Instruments, USA) power pack.

Visualisation of protein bands by Coomassie and Silver staining

For Coomassie staining, the PAGE was soaked in stain solution (46% methanol, 8% acetic acid, and 0.1% Coomassie Brilliant Blue R, Sigma-Aldrich) for 30 minutes while shaking. The stain solution was replaced with destain solution (20% methanol and 8% acetic acid), left on a shaker for up to one hour and repeated until the protein bands were visible against a clear to slightly blue background. PAGEs were soaked in 3% acetic acid, 2% glycerol for 1 hour before drying in a slab gel drier (Hoefer Scientific Instruments, USA).

For Silver staining, a PAGE was soaked in 12% TCA (trichloroacetic acid), 2% $Cu(II)Cl_2$ and 50% methanol for 2-3 hours. Gels were sequentially soaked for 20 minutes in 10% ethanol, 5% acetic acid, for 10 minutes in 0.01% $KMnO_4$, again for 20 minutes in 10% ethanol, 5% acetic acid, for 40 minutes in 10% ethanol, for 30 minutes in deionised water, for 20 minutes in 0.1% $AgNO_3$, for 1 minute in deionised water, for 1½ minutes in 10% K_2CO_3, in 2% K_2CO_3, 0.01% formaldehyde until bands became visible. The gel was then washed for ½

minute with deionised water followed by 1 hour in 3% acetic acid, 2% glycerol before drying in a slab gel drier.

Fractionation of PAGEs and Oxidation/trypsinisation of fractions

A 1-D lane or 2-D area on a SDS-PAGE was divided into fractions by cutting along drawn lines according to the width of the protein bands and a height of 2.5 mm for 1-D lanes and 5 mm height, 10 mm width for a 2-D area. Fractions were combusted in a Packard Model C306 Tri-Carb Sample Oxidizer (that splits ^{14}C and ^{3}H in mixed samples, Packard Instruments, USA) with scintillation liquid volumes set at 10 ml for Monophase, 8 ml Carbasorb and 12 ml for Permaflour (PerkinElmer Inc., USA). The alternative to the Sample Oxidizer was trypsin ingel digestion for which the results were found to be comparable to the Sample Oxidizer method. Gel fractions were incubated twice in 0.05% trypsin at 37°C for 4 hours, the digestion products for individual fractions were pooled and analysed in a liquid scintillation counter. Radioactivity, expressed as dpm, was plotted against fraction number.

Preparation of cells for electron microscopy

The method by de Chastellier et al. (1995) was followed. At indicated times (Results), cells were fixed with 2.5% glutaraldehyde in 0.1 M sodium cacodylate (Sigma-Aldrich) buffer, pH 7.2, containing 5 mM $CaCl_2$ and $MgCl_2$ as well as 0.1 M sucrose at RT for 1 hour. Cells were washed twice with cacodylate buffer containing 0.1 M sucrose for 15 minutes while shaking then fixed with 1% Osmium tetroxide (OsO_4, Sigma-Aldrich) in 0.1 M sodium cacodylate buffer without sucrose for 1 hour at RT. Cells were washed twice with cacodylate buffer without sucrose for 30 seconds and scraped off gently from the culture dishes in the presence of sodium cacodylate buffer without sucrose. Cells were couriered to Dr C de Chastellier (Centre d'Immunologie de Marseille, France). Further processing included incubation with

1% Uranyl acetate in Veronal buffer for 1 hour (RT), dehydration in acetone and embedding in Epon. Thin sections were stained with uranyl acetate (2%) and lead citrate.

Western blotting

SDS-PAGE

SDS-PAGE preparation was essentially performed as described above. For gel casting and electrophoresis, the Mini-PROTEAN II Electrophoresis Cell system (Bio-Rad Laboratories, Inc., USA) was used according to the manufacturer's instructions. For Western blotting, an 8 or 10% SDS-PAGE was prepared. Equal amounts (ranging from 2 to 4 μg) in protein content was prepared for each sample per Western blot experiment. Precision Plus Protein Prestained Standards (dual colour) molecular weight markers (Bio-Rad Laboratories, Inc.) were used. Electrophoresis, under denaturing conditions, was for 45 minutes at 60 mA and constant voltage of 200 volts.

Western blotting (transfer to nitrocellulose membrane)

The gel was equilibrated for 15 - 20 minutes in protein transfer buffer (19.8 mM Tris, 14.9 mM glycine). Hybond ™ ECL ™ nitrocellulose membrane (Amersham Pharmacia Biotech) and two pieces of Whattman paper, cut to an appropriate size, was pre-wet with distilled water and equilibrated together with the gel in protein transfer buffer. The gel and nitrocellulose membrane was sandwiched in the assembly cassette of the Mini-PROTEAN II Electrophoresis Cell system and electrophoresed for 1 - 2 hours at 100 volts to effect protein transfer to the nitrocellulose membrane. The nitrocellulose membrane was rinsed with Tris-buffered saline (TBS, 10 mM Tris, 150 mM NaCl, pH 7.6) and incubated in 5% fat-free milk powder dissolved in TBS containing 0.1% Tween 20 (TBS-T, Merck) for 1 hour at RT while shaking.

Antibody treatment

Nitrocellulose membranes were incubated in TBS-T containing 5% fat-free milk powder and the relevant antibody followed by an HRP-conjugated secondary antibody at pre-tested dilutions for 1 hour each at RT. Specific antibodies used: rabbit polyclonal anti-human Rab5B antibody (Santa Cruz Biotechnology, Santa Cruz, USA), followed by peroxidase labelled polyclonal anti-rabbit antibody (GE Healthcare, UK); rat monoclonal anti-mouse LAMP1 antibody (ID4B-TCM), followed by HRP-linked goat anti-rat antibody (GE Healthcare); rabbit polyclonal anti-human Rab7 antibody (Santa Cruz), followed by peroxidase labelled polyclonal anti-rabbit antibody (GE Healthcare); rabbit polyclonal anti-human CD71 (transferrin receptor, Santa Cruz), followed by peroxidase labelled polyclonal anti-rabbit antibody (GE Healthcare). After each antibody treatment, the nitrocellulose membranes were twice briefly rinsed with TBS-T, washed for 15 minutes while shaking and washed again twice for 5 minutes with TBS-T. Nitrocellulose membranes were air-dried and exposed to X-ray film (ECL Hyperfilm™) after treatment with KPL LumiGlo detection reagent (KPL, Inc., USA) to visualise antibody signals.